NON-DESTRUCTIVE QUALITY ASSESSMENT OF HENS' EGGS AND SWEET CORNS USING NEAR INFRARED SPECTROSCOPY TECHNIQUES

SINEENART SUKTANARAK

A THESIS SUBMITTED IN PARTIAL FULFILLMENT

OF THE REQUIREMENT FOR THE DRGREE OF

DOCTOR OF PHILOSOPHY IN FOOD SCIENCE

FACULTY OF AGRO-INDUSTRY

KING MONGKUT'S INSTITUTE OF TECHNOLOGY LADKRABANG

2018

KMITL-2018-AI-D-051-308

NON-DESTRUCTIVE QUALITY ASSESSMENT OF HENS' EGGS AND SWEET CORNS USING NEAR INFRARED SPECTROSCOPY TECHNIQUES

SINEENART SUKTANARAK

A THESIS SUBMITTED IN PARTIAL FULFILLMENT

OF THE REQUIMENT FOR THE DRGREE OF

DOCTOR OF PHILOSOPHY IN FOOD SCIENCE

FACULTY OF AGRO-INDUSTRY

KING MONGKUT'S INSTITUTE OF TECHNOLOGY LADKRABANG

2018

KMITL-2018-AI-D-051-308

This material is reserved for educational use only, not allowed for commercial use.
Forbidden to modify the content, and cite the document when use

COPYRIGHT 2018

FACULTY OF AGRO – INDUSTRY

KING MONGKUT'S INSTITUTE OF TECHNOLOGY LADKRABANG

This material is reserved for educational use only, not allowed for commercial use.

Forbidden to modify the content, and cite the document when use

Thesis Certification

Faculty of Agro-Industry

King Mongkut's Institute of Technology Ladkrabang

Thesis Title NON-DESTRUCTIVE QUALITY ASSESSMENT OF HENS' EGGS AND SWEET CORNS USING NEAR INFRARED SPECTROSCOPY TECHNIQUES

Student MISS SINEENART SUKTANARAK

Student ID 56608002

Degree Doctor of Philosophy

Program Food Science

Major Advisor Associate Professor Dr.Sontisuk Teerachaichayut

Co-Advisor Dr. Panuwat Supprung

EXAMINERS	SIGNATURES
Assoc. Prof. Dr.Sontisuk Teerachaichayut	
Assist. Prof. Dr. Aphacha Jindaprasert	
Assist. Prof. Dr. Soraya Kerdpiboon	
Dr. Panuwat Supprung	
Assoc. Prof. Dr. Anupun Terdwongworakul	

Defense Date: July 17 , 2018 **Time** : Between 1.00 p.m.- 4.00 p.m.

Venue: A 303 Chaokhunthaharn Building, KMITL

(Assoc. Prof. Dr. Praphan Pinsirodom)

Dean

Faculty of Agro-Industry

Date : July 25 2018

This material is reserved for educational use only, not allowed for commercial use.
Forbidden to modify the content, and cite the document when use

Thesis	Non-destructive quality assessment of hens' eggs and sweet corns using near infrared spectroscopy techniques
Student	Miss Sineenart Suktanarak
Student ID	56608002
Degree	Doctor of Philosophy
Program	Food Science
Year	2018
Thesis Advisor	Assoc. Prof. Dr. Sontisuk Teerachaichayut

ABSTRACT

The freshness of agricultural products is important for consumers and food producers. In this research, near infrared (NIR) spectroscopy was used as a non-destructive method to predict eggs freshness and sweet corns freshness. The quality parameter for eggs freshness was Haugh unit. Quality parameters of sweet corns were total soluble solids content (TSS), moisture content and hardness value.

For prediction of Haugh unit, interactance mode (588-1091 nm), reflectance mode (1000-2500 nm) and hyperspectral imaging in reflectance mode (900-1700 nm) were investigated in this research. Hen eggs were taken for measurements at different days of storage. Calibration models were established and cross-validated using partial least squares regression (PLSR). The combination of smoothing and first derivative spectral pretreatment in the interactance mode (588-1091 nm) by FQA- NIR GUN obtained R of 0.91 and RMSEP of 5.64. The MSC spectral pretreatment in the reflectance mode (1000-2500 nm) by FT-NIR spectrophotometer obtained R of 0.83 and RMSEP of 7.11. The SNV spectral pretreatment in the reflectance mode (900-1700 nm) by NIR hyperspectral image obtained R of 0.92 and RMSEP of 6.29.

For predicting quality of sweet corns, interactance mode (588-1091 nm) and reflectance mode (1000-2500 nm) were investigated in this research. Comparisons accuracy between sweet corns with/without husk, it was found that the sweet corns without husk obtained better accuracy. The thickness of the husk had an effect on the accuracy of predicting quality of sweet corns.

This material is reserved for educational use only, not allowed for commercial use.
Forbidden to modify the content, and cite the document when use

ACKNOWLEDGEMENTS

I would like to express my sincere thanks to my thesis advisor, Associate Professor Dr.Sontisuk Teerachaichayut for his invaluable help and constant encouragement throughout the course of this research. I am most grateful for his teaching and advices.

I would like to thank my co-advisor, Dr. Panuwat Supprung for the suggestions, encouragement, insightful comments and all his help.

I would like to thank my committee members, Associate Professor Dr. Anupun Terdwongworakul, Assistant Professor Dr. Aphacha Jindaprasert and Assistant Professor Dr. Soraya Kerdpiboon for being good committee members even at hard times. I also would like to say thanks for their encouragement, brilliant ideas, comments and suggestions.

I would like to thank the technical staffs in the faculty of Agro-Industry at King Mongkut's University of Technology Ladkrabang and staffs in the faculty of Engineering at Rajamangala University of Technology Isan Khon Kaen Campus for help, their encouragement and their wishes for success in the completion of this dissertation.

Finally, I am most grateful to acknowledge my parents and my friends for all their support throughout the period of this dissertation.

Sineenart Suktanarak

2018

This material is reserved for educational use only, not allowed for commercial use.

Forbidden to modify the content, and cite the document when use

CONTENTS

Page

This material is reserved for educational use only, not allowed for commercial use.
Forbidden to modify the content, and cite the document when use

CONTENTS (continuous)

Page

This material is reserved for educational use only, not allowed for commercial use.
Forbidden to modify the content, and cite the document when use

CONTENTS (continuous)

Page

This material is reserved for educational use only, not allowed for commercial use.

Forbidden to modify the content, and cite the document when use

LIST OF TABLE

Table **Page**

This material is reserved for educational use only, not allowed for commercial use.
Forbidden to modify the content, and cite the document when use

LIST OF TABLE (continuous)

This material is reserved for educational use only, not allowed for commercial use.
Forbidden to modify the content, and cite the document when use

LIST OF TABLE (continuous)

Table **Page**

This material is reserved for educational use only, not allowed for commercial use.
Forbidden to modify the content, a[illegible]ite the document when use

LIST OF FIGURES

This material is reserved for educational use only, not allowed for commercial use.
Forbidden to modify the content, and cite the document when use

LIST OF FIGURES (continuous)

Figure **Page**

This material is reserved for educational use only, not allowed for commercial use.
Forbidden to modify the content, and cite the document when use

LIST OF ABBREVIATION

NIRS	near infrared spectroscopy
PLSR	partial least square regression
N	number of sample
F	Factors
Smoothing	Savitzky-Golay smoothing
1st derivative	Savitzky-Golay first derivative
2nd derivative	Savitzky-Golay second derivative
MSC	multiplicative scatter correction pretreatment
SNV	standard normal variate transformation
RMSEC	root mean square error of calibration
RMSEP	root mean square error of prediction
RPD	ratio of prediction to deviation
SD	standard deviation

This material is reserved for educational use only, not allowed for commercial use.
Forbidden to modify the content, and cite the document when use

CHAPTER 1

INTRODUCTION

1.1 Statement of the problems

The quality of agricultural products is important for the food industry. Consumers require agricultural products which have good qualities and an affordable price. Consumers often buy agricultural products by only looking at the external appearance. The external qualities of agricultural products such as color, shape and defects. The external qualities are indexes that can be visible to select the agricultural products but internal qualities can't be sorted to by visual inspection. The near infrared spectroscopy (NIRs) has been successfully used to evaluate internal qualities of agricultural products, due to it is nondestructive, fast, reliable and accurate (Cen and Hen, 2007). The hyperspectral imaging is the nondestructive technique which combines the methodology of the conventional spectroscopy and the image processing in order to evaluate quality of samples (Valous et al., 2009). The conventional NIR spectroscopy can only provide spectrum while the hyperspectral imaging can provide spectrum and spatial information of composition in samples (Manley et al., 2009).Thus, the spectral and spatial information which acquire from samples were used for analysis in the hyperspectral imaging technique (Wu and Sun, 2013).

There were many reports about NIR to evaluate qualities of fruits, vegetables and meat products such as Ariana and Lu (2010) detected an internal defect of cucumber, Lorente et al. (2012) and Nicolai et al. (2007) detected surface defects of apple, cherry and citrus. In addition, the quality of meat product is important factor for meat industry. There were many reports for detecting internal qualities of meat products by NIRs such as intact and minced pork (Barbin et al., 2012), lamb meat (Kamruzzaman et al., 2012) beef (ElMasry et al., 2012), and cooked ham (Talens et al., 2013). In this paper, the internal quality of eggs and sweet corns were studied. Both of them are agricultural products. Eggs are a raw material from animal while sweet corns are a raw material from plant. Another reason is eggs and sweet corns can be found in all seasons, all food markets. Therefore, internal quality of eggs and sweet corns are important for consumers before they make a decision to purchase.

This material is reserved for educational use only, not allowed for commercial use.
Forbidden to modify the content, and cite the document when use

Hen egg is the staple food of household and food industries. It is a favorite food because it is worth when compared between its low price and high quality. It contains proteins and other useful substances such as vitamin E, lutein, selenium, omega-3 fatty acids which are served for health against disease conditions (Sim, 1998). Internal quality of hen egg can be changed by time of storage. Storage affects the hen egg's quality which includes the functional properties of egg yolk and egg albumen. The factors that affect the internal quality of eggs may occur due to loss of water, loss of carbon dioxide (CO_2), diffusing of fluids between compartments (Rossi et al., 1995; Walsh et al., 1995; Karoui et al., 2006). The loss of water content is caused by water evaporation. This process is the reason for decreasing egg's weight (Romanoff and Romanoff, 1949).The loss of CO_2 and rising of the albumen pH cause the liquefaction of albumen (Burley and Vadehra, 1989). The exchanging of gas through the shell pores makes the structure of interaction between ovomucin-lysozyme change (Stadelman and Cotterill, 1995) and then affects to a thinner and thickness of albumen layer which is one of variables for calculating Haugh unit to evaluate hen egg's freshness. The freshness cannot be classified by an external appearances or the visible inspection. Therefore, the nondestructive technique is required to evaluate the hen egg's freshness.

Sweet corn (*Zea mays* L. *saccharata*) is important cereal crops which are used for human consumption. In addition, the sweet corn is also processed for many corn products in factory such as canned sweet corn, corn milk and cream of sweet corn. The quality of sweet corn affects the final products. The sugar content and water-soluble hydrocarbon in the kernels are the key factors of consumption quality (Evensen and Boyer, 1986). That is described in terms of taste and texture. The taste which refers to the sweetness of sweet corn depends on the storage time after harvest. Longer storage affects to the corn's quality. It becomes hard and decreased its sweetness due to the sugar in sweet corn turns into starch. The sugar of sweet corn converts to starch quickly after harvesting. Therefore, sweet corn should be transported to market or processed in factory within 24 hours after harvest (National Food Institute, 2016). Generally, the appearance of the sweet corn is also important and the consumers can inspect before buying but internal qualities which relate to the storage time cannot be identified by visual inspection. Hence, it is necessary to find out a nondestructive technique which can detect the qualities of sweet corn in order to be satisfied by consumers.

The purpose of this study, NIR spectrophotometer (FQA- NIR GUN) in the wavelength range of 588-1091 nm, FT-NIR spectrophotometer (NIR Flex N-500) in the wavelength range of

This material is reserved for educational use only, not allowed for commercial use.
Forbidden to modify the content, and cite the document when use

1000-2500 nm and NIR hyperspectral image in the wavelength 900-1700 nm were used to predict the freshness of hen's egg and quality of sweet corn. The statistical analysis was considered to establish the calibration models using partial least squares regression (PLSR) for each quality characteristic.

1.2 Objective

1.2.1 In order to study near infrared spectroscopy (FQA- NIR GUN, NIR Flex N-500 and hyperspectral image) for nondestructive quality assessment of hens' eggs.

1.2.2 In order to study near infrared spectroscopy (FQA- NIR GUN and NIR Flex N-500) for nondestructive quality assessment of sweet corns.

1.3 Scope of research

1.3.1 Study the potential of near infrared spectroscopy and hyperspectral imaging for nondestructive prediction of egg's freshness and quality characteristic for egg's freshness using Haugh unit.

1.3.2 Study the potential of near infrared spectroscopy for nondestructive prediction of sweet corn's freshness and quality characteristic for sweet corn's freshness are total soluble solid (TSS), moisture content and hardness value.

This material is reserved for educational use only, not allowed for commercial use.
Forbidden to modify the content, and cite the document when use

CHAPTER 2

LITERATURE REVIEW

2.1 Hen egg

2.1.1 Structure of hen egg

A hen egg contains three main parts: shell, yolk and albumen. The yolk is covered with an albumen layer and this structure is protected by a hard eggshell (figure 2.1). The weight of a hen egg and the weight of the main three parts are varied depending on the kind of hens and their age. The eggs of a white leghorn weight from 50 to 63 gram and the weight distributions of shell, albumen and yolk are in the range 0g 9-11%, 60-63% and 28-29%, respectively (Takehiko et al., 1996).

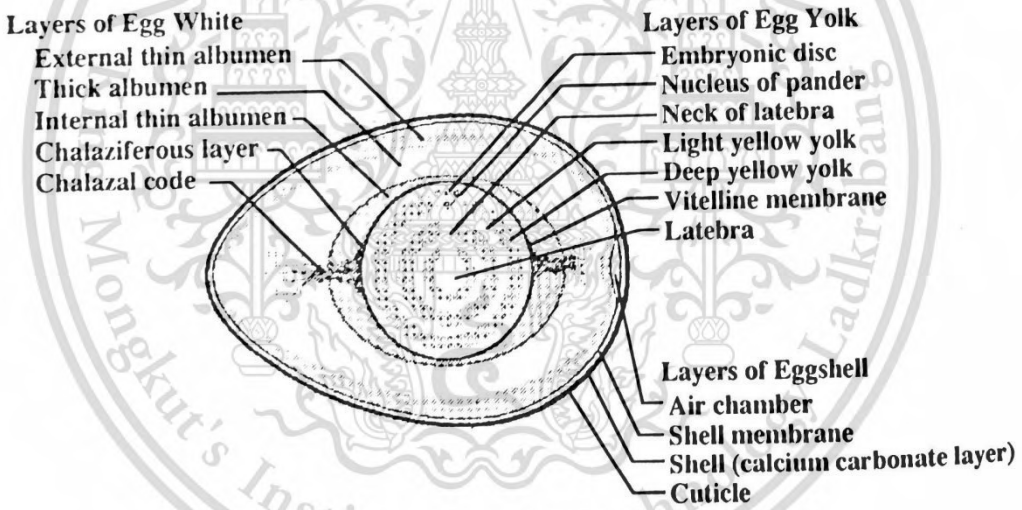

Figure 2.1 Composition of the egg

Sorce: Takehiko et al., (1996)

2.1.1.1 Egg shell

An egg shell is composed of cuticle carbonate layer and membranes. Figure 2.2 is an electron micrograph of a tangential section of the eggshell. The microstructure of the eggshell is depicted in figure 2.2. There are small holes called “pore canals” on the shell for gas transfer. The pore canals are at the palisade layers of the shell. The diameter of the pore canal is

This material is reserved for educational use only, not allowed for commercial use.
Forbidden to modify the content, and cite the document when use

about 10-30 μm. It is about 10,000 pore canals on the shell surface per one egg. The pore canal permits air and moisture to transfer, but does not permit liquid (Takehiko et al., 1996).

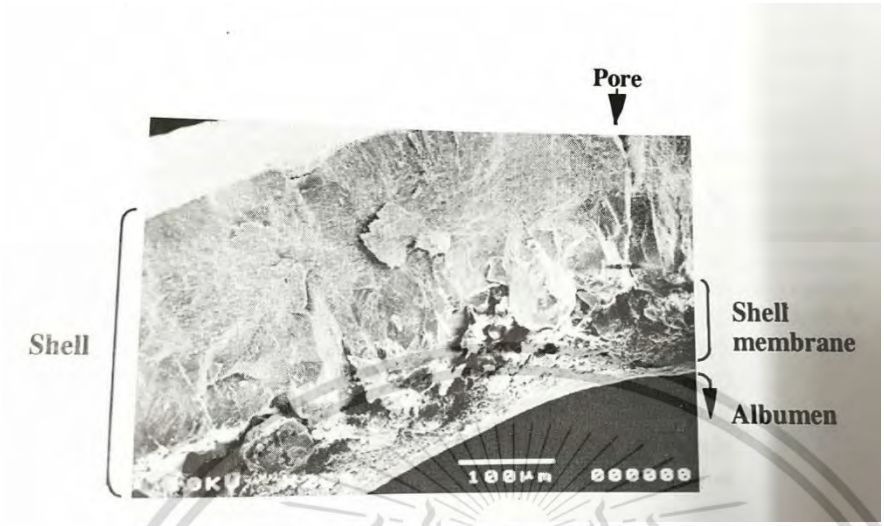

Figure 2.2 Scanning electron microscopic photograph of the shell of a hen egg.

Sorce: Takehiko et al., (1996).

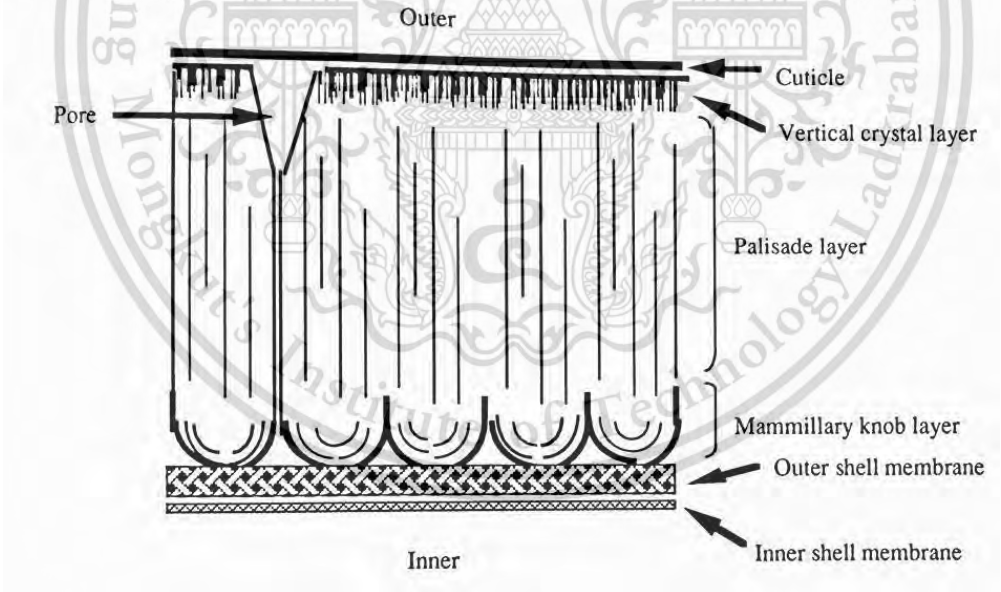

Figure 2.3 An illustrative representation of the hen eggshell.

Sorce: Takehiko et al., (1996).

This material is reserved for educational use only, not allowed for commercial use.
Forbidden to modify the content, and cite the document when use

1) Cuticle

The cuticle is the most external layer of egg. Its thickness is about 10 μm. The cuticle covers the pore canals. The cuticle protects microorganisms and moisture through the egg. But the cuticle permits gas through the egg. The cuticle contains protein, lipid and carbohydrates (Takehiko et al., 1996).

2) Shell stratum

The egg shell contains the vertical crystal layer and mammillary knob layer as shown in Figure 2.3. The compositions are inorganic materials (95%), protein (3.3%) and moisture (1.6%). Calcium carbonate is the main component of the inorganic materials. The vertical crystal layer is in a vertical direction of the shell. This layer has small vesicles. The palisade layer is called the spongy layer that is hard. Its structure is generated by calcification of calcium carbonate and collagen. The mammillary knob serves to harden the shell that is in contact to the outer shell membrane (Takehiko et al., 1996).

3) Egg shell membrane

The egg shell membrane contains with inner and outer membranes that is positioning between the inner surface of the egg shell and the albumen. The thickness is about 50 μm. The inner membrane is parallel to the egg shell and has three layers of fibers. The outer membrane is in different directions and has six layers of fibers. The thickness is about 15 μm. (Yoshinorui, 2008). The egg shell membrane contains with 20% moisture, 70% organic substance and 10% inorganic substance. The main organic substance is protein and some lipids and carbohydrates (Takehiko et al., 1996).

2.1.1.2 Albumen

Albumen contains with four layers: an outer thin white (23.3%), outer thick white (57.3%), inner thin white (16.8%) and inner thick layer (2.7%). The proportions of the contents in each layer may be varied based on environmental conditions, size of the egg, breed of the hen and rate of production (Yoshinorui, 2008).

Thick and thin albumen

The thick and thin albumen can be used to consider the freshness of eggs. For fresh eggs, thick albumen keeps the egg yolk in the center of the egg. The viscosity of thick albumen is higher than those of thin albumen due to it has high content of ovomucin. The thick albumen makes Haugh unit high while the thin albumen makes Haugh unit low. However the yield of ovomucin from thin albumen is not different. The thin albumen occurs naturally during

This material is reserved for educational use only, not allowed for commercial use.
Forbidden to modify the content, and cite the document when use

storage. The increasing of free sulfhydryl groups makes a loss of thick albumen. After electron beam irradiation, It results in a loss of foam volume and gel hardness (Yoshinorui, 2008).

The chalaziferous layer is a gelatinous layer which covers the egg yolk. The chalaziferous layer is twisted at both sides of the yolk membrane. The chalazae cord is forming. The chalazae cord is twisted clockwise at the sharp end of the egg and stretches into the thick albumen layer to both sides. The chalaziferous layer is elastic and allows the egg yolk in the position. Therefore the egg yolk is fixed in the center of egg (Yoshinorui, 2008).

2.1.1.3 Egg yolk

The egg yolk is covered by a vitelline membrane. The inner contains with yellow yolk and white yolk. The white yolk occurs from the white follicle that matures in the ovary. The weight of the white yolk is less than 2% of the whole egg yolk. The egg yolk contains with the layers of alternate light and deep yellow yolks. Several structure such as latebra, neck of latebra, nucleus of pander and embryonic disc are seen in egg yolk Latebra is located in the center of the egg yolk and is connected with the nucleus of pander, named “neck of latebra”. The embryonic disc is about 2-3 mm in diameter. It is in the nucleus of pander that is the place for the embryo to develop (Takehiko et al., 1996).

1) Vitelline membrane

The vitelline membrane contains with an inner layer (1.0-3.5 μm), continuous membrane (0.05-0.1 μm) and outer layer (3-8.5 μm). The structures of the inner and outer layers are consisting of fibers and three dimensionally mesh-worked. The structure of the continuous membrane is consisting of granules. The average weight of the vitelline membrane is about 51 mg per egg. It is about 20-30% of solid. The solid matter in the vitelline membrane contains with protein (87%), lipids (3%) and carbohydrates (10%). It consists of DNA and RNA. Due to its amino acid composition, the protein of the vitelline membrane is not classified in the categories of collagen, keratin or elastin (Takehiko et al., 1996).

2) Structure of yellow yolk

Obtaining the material through the mother hen’s blood stream, the white follicle rapidly accumulates yellow yolk to become a yellow follicle in about 9 days before it is ovulated into the oviduct. The yellow yolk contains with two types of lipoprotein emulsion such as the deep yellow yolk and the light yellow yolk. The deep yellow yolk is formed in the daytime while the light yellow yolk is formed at night. The protein concentration in blood serum is lower in the daytime. The thickness of the light yellow yolk layer is about 0.25-0.42 mm and the

This material is reserved for educational use only, not allowed for commercial use.
Forbidden to modify the content, and cite the document when use

thickness of the deep yellow yolk layer is about 2 mm. The structure of the egg yolk's layer is observed when an egg from a hen that has been injected with an oil-soluble pigment (Takehiko et al., 1996).

2.1.2 Identification in quality of eggs

Properties of eggs can be determined the internal and external quality. Internal quality is the quality of the albumen and yolk such as weight, pH, thickness and color. External quality is the shape of the egg and the eggshell. Egg properties are influenced by various factors such as genetics, hen age, body, weight and diet (Silversides, 1994; Monira et al., 2003; Silversides and Budgell, 2004; Van Den Brand et al., 2004). The properties such as egg shape index, egg weight, albumen height, Haugh units and eggshell weight and yolk color are described as follows:

2.1.2.1 Egg shape index

Shape index is acquired from the overall shape of the egg. To calculate shape index, the egg width and egg length are measured in cm using a Vernier caliper. The egg width is then divided by the egg length and that ratio multiplied by 100 (Van Den Brand et al., 2004).The shape index are classified in production as sharp (egg Shape Index of < 72), normal (egg Shape Index of 72-76), and round (egg Shape Index >76). The egg shape is important in commercial systems. If the eggs have an outside shape, eggs do not fit well into the packaging. The sharp eggs do not resist to the shipping and handling processes (Altuntas and Sekeroglu, 2007).

2.1.2.2 Egg weight

The egg weight is measured and used for analysis by placing an unbroken egg on a weighting scale and recording its value. Genetics and environment greatly influence body weight. Birds of heavier body weight lay smaller eggs related to their body size, while birds of lighter body weight lay larger eggs related to their body size (Hafez et al., 1955). Almost all egg quality properties decline as hen age, with the exception of egg weight, which increases (Ledur et al., 2002; Altunas and Sekeroglu, 2007).

2.1.2.3 Albumen height

Albumen contains with a thick and thin portion. The thick portion is surrounding the egg yolk, whereas the thin albumen consists of the rest of the white portion. The height of the albumen indicates the freshness of the eggs and can be measured using a tripod micrometer. The egg is broken onto a flat surface then a tripod micrometer is placed over the thick albumen. The height (mm) can be measured. The thicker the albumen is the better the quality of the egg, with heights of 8 to 10 mm being considered superior interior quality (Zeidler,

This material is reserved for educational use only, not allowed for commercial use.
Forbidden to modify the content, and cite the document when use

2002). Haugh unit can be calculated which is related the egg weight, albumen height. (Haugh, 1937; Williams, 1992). The calculation for Haugh unit is as follows:

$$\text{Haugh unit} = 100 \log (\text{albumen height} - 1.7\text{egg weight}^{0.37} + 7.57)$$

where albumen height is the height of the albumen in mm and egg weight is the weight of the egg in g (Silversides, 1994).

2.1.2.4 Eggshell weight

The eggshell weight is the weight of the shell portion of the egg. The eggshell is dry when weighed. It can be dried by hot air (Anderson et al., 2004) or in an oven at 100° C (Silversides, 1994). Egg shell weights have been varied to both increase and decrease as the hen ages (Silversides, 1994; Silversides and Budgell, 2004; Popova-Ralcheva et al., 2009)

2.1.2.5 Yolk color

The yolk color can be easily changed and it is variable. Consumers in the United States often prefer a light-to-medium yellow of the yolk color (Galobart et al., 2004), while producers of liquid, frozen and dried egg products prefer darker of the yolk color (Zeidler, 2002). The diet of the hen has the greatest influence on yolk color (Galobart et al., 2004). The yolk color can be easily manipulated by using synthetic additives, and this is frequently done in many countries. In the United States, however, only naturally occurring products can be used in chicken diets (Zeidler, 2002; Galobart et al., 2004). To achieve the basic yellow color of a typical egg yolk, yellow xanthophylls are needed (Galobart et al., 2004). The yolk color is influenced by the diet, the age and breed of hen. The yolk color is subjectively determined by the use of the Roche color fan (Stadelman, 1995; Vuilleumier, 1968).

2.2 Sweet corn

2.2.1 Botany and cultivars

Sweet corn or *Zea mays* L. *spp. rugosa* (or saccharata) belongs to the grass family Gramineae (Poaceae) which represents the majority of food plants in the world. Sweet corn is well-known for its high sugar content in the kernels at the early "dough" stage, and wrinkled, translucent kernels when dry (Magness et al., 1971). The plant is a single stemmed annual, grown from one seed (monocotyledon); the plant has drooping leaves and bears both male and female flowers (monoecious) (Food Encyclopedia, 1996). Each ear contains numerous silks that stick out from the top of the husk and through which pollination occurs. Corn cobs are classified in yellow, white or bicolor depending on the cultivar. While sweet corn grows best in a warm weather

This material is reserved for educational use only, not allowed for commercial use.
Forbidden to modify the content, and cite the document when use

requiring at least eight hours of direct sunlight daily, it can adapt to a wide range of climates such as in the cooler parts of North America. Cultivars are generally grouped into three main classes: early, medium, and late depending on the time of their edible maturity (Salunkhe, 1984). Due to many years of research and development of new technologies, recently sweet corn breeders have introduced new genes into the market which are sweeter in taste and much more resistant to climatic changes and diseases in order to extend their shelf life and eating quality. Based on the nature of kernel sugar amount and the conversion rate of sugar to starch, sweet corn can also be classified into four basic groups: standard or sugary normal (su), sugary enhanced (se), super sweet hybrids (sh2), and improved super sweet hybrids also knew as Sweetie class (Munro and Small, 1997):

2.2.1.1 Su is the most common corn grown for fresh consumption. It stops the conversion of sugar to starch after harvest.

2.2.1.2 Se is characterized by a slight increase in sugar level mainly maltose and a slower conversion of sugar to starch after harvest. This corn type has very tender kernels which is highly desirable for consumers but not favorable for mechanical harvesting.

2.2.1.3 Sh2 produces kernels with two to three times the sugar content of the standard corn varieties su and inhibits the conversion of sugar to starch right after harvest. Texture is relatively crispy than creamy as with the normal and sugary enhanced genes. They have longer shelf life due to their higher capacity of retaining moisture and sweetness inside their kernels. They are mainly destined for canning and freezing.

2.2.2 Advantages for use of hybrids (Inglett, 1970).

2.2.2.1 Yield

Hybrid varieties of sweet corn generally produce higher yields than the old, open pollinated types. The separate effect of the development of hybrid sweet corn on yield, however, is difficult to assess because a number of other factors have developed or evolved simultaneously. These ding factors include such important items as improved and increased use of fertilizers, better cultural practices, and greater control of insects and diseases affecting sweet corn. Hybrid sweet corn varieties today generally yield 2 to 4 times more than the old, open pollinated varieties but only a part of this increase is directly attributable to hybridization.

2.2.2.2 Quality

One of the most important quality factors related to hybridization is the improved uniformity of maturation of the sweet corn. This characteristic, typical of hybrids, not

This material is reserved for educational use only, not allowed for commercial use.
Forbidden to modify the content, and cite the document when use

only increases the yield of cut corn but reduces the variation in maturity which invariably improves quality of the processed product. Other quality factors, such as color, sweetness and pericarp tenderness can also be improved by hybridization. Quality is of considerable interest to sweet corn breeders and much improvement will be made in the future.

2.2.2.3 Disease and insect resistance

Improvement was made in developing insect and disease resistance in many sweet corn hybrids. The success of this work varies; a few specific problems were essentially solved, while in other cases the problem was only reduced. However, this approach is most worthwhile and, as the work continues, additional success is highly probable

2.2.3 Harvesting of sweet corn

2.2.3.1 Mechanical harvesting

Mechanical harvesting of sweet corn is a continuous process in which all the ears are harvested in one operation. The machine harvests two rows. The plants are destroyed in the harvesting process while the cars are conveyed to a wagon. The quality of the product a received at the factory has been increased by improvements made in these harvesters.

Mechanical harvesters can be operated day and night and this eliminates the necessity of storing large amounts of sweet corn at the factory during the day for the night shifts. Thus, use of mechanical harvesters allows an orderly harvest which is completely adequate to keep the plant running at all times but avoids excessive storage of unhusked corn. (Inglett, 1970).

2.2.3.2 Hand harvesting

The most common method of harvesting sweet corn involves pulling the ears by hand. Sweet corn is then transported by a truck to a packing house where it is graded and packed (Ryall and Lipton, 1979). Beside this method, more sophisticated ways using high-tech mechanical harvesters have been introduced to the market which cut the stalks near the ground, remove the ears, and transmit them to a bin attached to the harvester (Ryall and Lipton, 1979). Sweet corn harvest requires very careful supervision that can avoid some problems during postharvest processes (Boyette et al., 1990). Proper maturity of a corn cob occurs when sugar changes to starch, the hull becomes tougher, and the kernels pass through stages called pre-milk, milk, early dough, and dough. Corn will be ready for harvest at the milk stage, i.e., as soon as the kernels are fully developed and give out a milky liquid when squeezed (Schultheis, 1998). Other harvest indices can be considered when the silks have just turned brown and dry or approximately 18 to 22 days after the first silks appear (Peet, 1995). Whether harvested by hand or mechanically,

This material is reserved for educational use only, not allowed for commercial use.

Forbidden to modify the content, and cite the document when use

sweet corn should be collected early in the morning when its temperature is low in order to reduce cooling loads and to consume energy (Boyette et al., 1990).

Correct postharvest handling of sweet corn is necessary to maintain good quality in today's market (Herber, 1991). Every effort should be made to cool down sweet corn immediately after harvest to retard its deterioration. However, proper temperature management is very critical to ensure better quality and longer shelf life of this produce.

The technology for production and handling sweet corn for international markets is very particular and varies from those practices required for handling when this vegetable is proposed for home use or distributed through national markets; therefore, handling needs depend upon the market destination (Sargent, 1999).

Sweet corn or any other fresh horticultural commodity is a living organism and remains alive even after harvesting (Talbot et al., 1991). The taste and quality of sweet corn depends largely on its sugar content, which rapidly decreases after picking if not maintained at lower temperature (Boyette et al., 1990). Studies on sweet corn have showed that 60% of its sugar can be lost in 24 hours if kept at 30oC; this rate is four times less at 0^{o}C (Herber, 1991). To maintain its best quality, this vegetable must be cooled down to as near 0oC immediately after harvest and keep it refrigerated until it reaches the consumer. The delay between harvest and cooling is of critical importance, since sucrose, the compound primarily responsible for its sweetness, changes dramatically to starch (Salunkhe, 1984).

2.2.4 Quality evaluation of sweet corn

Quality is an important factor in the production and marketing of horticultural products (Bakker-Arkema, 1999). Producers are looking for good cultivar with high yield and low disease susceptibility. For wholesalers, good handling attributes and long storage life are important quality parameters. Consumers are more and more demanding in terms of food quality and safety, leading the producers towards higher standards in the production of fresh fruits and vegetables. Consumers are looking at several quality parameters such as good external appearance, firmness, and high quality flavor and nutritive value before making the decision to purchase (Kader, 2002). High quality sweet corn should have uniform size and color, hold fresh husks with sweet, milky and well-developed kernels and be free from any entomological defects or mechanical injuries (Sargent, 1999). Quantitative and qualitative attributes must be well described in order to determine the best quality conditions and to establish the storage length for sweet corn.

This material is reserved for educational use only, not allowed for commercial use.
Forbidden to modify the content, and cite the document when use

2.2.4.1 Qualitative attributes

Visual appearance of fruits and vegetables refers to physical characteristics such as shape, form, size, color, and defects (Kader, 2002). The qualitative factors play a dominant role in the selection of the commodity. The appearance of sweet corn is determined by the size and the uniformity in shape of the cob. The ear must be free from distortion or under development. The appearance is influenced by the color of the cob and mainly the husk that is covering it. The color of plant tissues are due to the presence of pigments such as chlorophylls (green) and flavonoids (yellow) (Clydesdale and Francis, 1976) which undergo significant modifications during storage.

Besides, many defects influence the appearance quality of the corn cob. They include damages on the external parts such as husks, shank, blades, and external silks and on the internal side like kernels and internal silks. The defects can be morphological due to malformation or underdevelopment of kernels. Pathological and entomological defects including fungi or bacteria and insects respectively cause serious problems inside the kernels (Kader, 2002). Mechanical defects consist of crushing, punctures and abrasion.

Measurement or evaluation of those parameters during storage of the produce sounds like a simple technique. However, it is much more complicated due to large variation between different corn cobs and different cultivars. Qualitative evaluation is usually based on scale charts composed of several rating.

2.2.4.2 Quantitative attributes

Other important factors for sweet corn are to look deeply inside kernels and see what happens at molecular level. Quantitative attributes including water content, mass loss and total soluble solids (TSS) percent can play a fundamental role in customer choice (Kader, 2002).

Water is the most abundant component in a plant cell. These cells can suck water from outside through the cell wall which gives the desirable crispness, firmness and turgidity for the crop tissue (Martens and Baordseth, 1987). For sweet corn, juiciness and succulence are important quality components to consider during storage (Kader, 2002).

The sweetness of sweet corn is due to sucrose and other sugars present in the juice (Harrill, 1994). Total soluble solids in a plant organism are primarily sugars; sucrose, fructose, and glucose. Brix readings are a widespread measure of the concentration of soluble

This material is reserved for educational use only, not allowed for commercial use.
Forbidden to modify the content, and cite the document when use

solids in a liquid sample. However, degree Brix or Refractive Index is a common method to measure the percentage sucrose using a small device known as refractometer.

For fresh sweet corn, the kernel carbohydrate composition decreases rapidly after harvest if left under field temperature resulting in unfavorable modification to kernel texture, flavor and consumer satisfaction (Olsen et al., 1990). By lowering the temperature immediately after harvest, the conversion of sugar to starch will gradually slow down. Therefore, sugar retention of the produce during postharvest storage is essential to maintain high quality produce with competitive prices.

2.3 Near infrared spectroscopy

2.3.1 Principle of NIR spectroscopy

Near infrared region between the visible and middle infrared (MIR) regions of the electromagnetic spectrum. It is defined as the range of electromagnetic radiation in the region of about 780-2500 nm (12,500-4,000 cm^{-1}). When near infrared radiation passes through the sample, the incident radiation may be reflected, absorbed or transmitted. The relative contribution of each phenomenon depends on the chemical constitution and physical parameter of the sample (Nicolai et al., 2008). The record of NIR region of the electromagnetic spectrum involves the response of the molecular bonds O-H, C-H, C-O and N-H of functional group. These bonds are subject to vibrational energy changes when irradiated by NIR frequencies, and two vibration patterns exist in these bonds including stretch vibration and bent vibration. The energy absorption of organic molecules in NIR region occurs when molecules vibrate or is translated into an absorption spectrum within the NIR spectrometer (Haiyan and Yong, 2007).

The whole measurement processing generally consists of the following several steps; (1) spectral data acquisitions; (2) data-preprocessing to eliminate noises and baseline shift from the instrument and background; (3) build calibration model using a set of samples with known analyzed concentration obtained by suitable reference method and (4) to validate the models using another set of samples without calibration set (Haiyan and Yong, 2007).

2.3.2 Vis/NIR measurments

"Sample presentation" or how to present or set a sample to an NIR instrument is one of the important factors considered in NIR measurement. Figure 2.4 illustrates some sample presentations known as "transmittance", "refelectance", transflectance" and "interactance"

This material is reserved for educational use only, not allowed for commercial use.
Forbidden to modify the content, and cite the document when use

2.3.2.1 Transmittance

Incident light illuminates one side of the sample and the transmitted light may be detected from the other side. This presentation is widely used for liquids by using a cuvette

2.3.2.2 Reflectance

Incident light illuminates the surface of the sample and the diffusely reflected light from the surface, or from the potion near the surface, may be detected. In this case, the sample should be opaque such as a powder sample and have more than one cm. depth

2.3.2.3 Transflectance

Transflectance was originally developed by Technicon for the InfraAlyzer and combines transmittance and reflectance. Incident light is transmitted through the sample and then scattered back from a reflector, which is made of ceramic or aluminium to be compatible with the diffuse reflectance characteristics of the instrument.

2.3.2.4 Interactance

In the case interactance, an interactance probe having a concentric outer ring of illuminator and an inner portion of receptor is usually used. The end of the probe should be in contact with the surface of the sample. Therefore, only the light transmitted through the sample can be detected

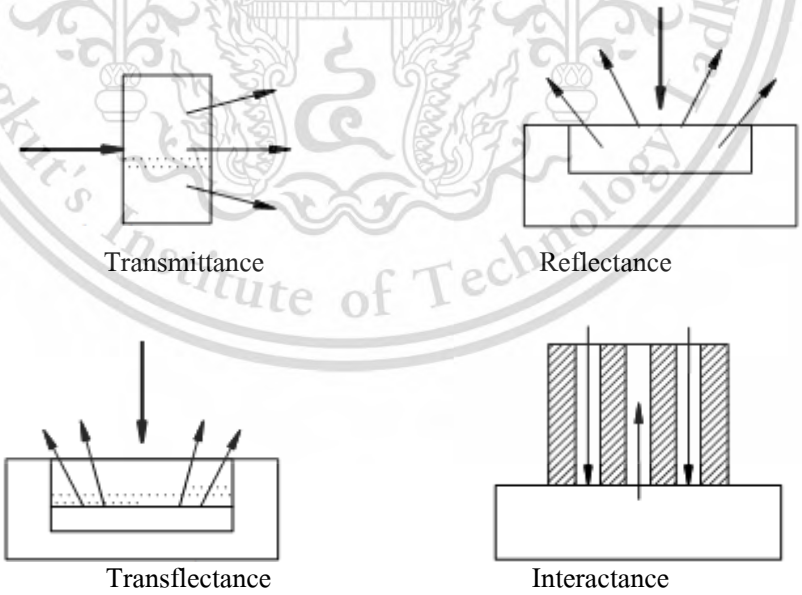

Figure 2.4 Sample presentations of transmittance, reflectance, transflectance and interactance

Source: (Kawano, 2002)

This material is reserved for educational use only, not allowed for commercial use.
Forbidden to modify the content, and cite the document when use

2.3.3 Data pretreatment

The raw data acquired from NIR spectrometer contain background information and many effects such as instrument source, sample source and operation source. In order to obtain reliable, accurate and stable calibration models, it is very necessary to pretreatment spectral data before modeling. Several pretreatment techniques are utilized to modify the spectra data.

2.3.3.1 Smoothing

The smoothing techniques have been proposed to remove random noise from NIR spectra. When smoothing obviously improves the visual aspect of NIR spectra, it does remove information at stage where it is not clear yet whether this information is useful (Nicolai, 2007). Popular smoothing methods are moving average filter and Savitzky-Goley algorithm (Nicolai, 2007)

2.3.3.2 Multiplicative scatter correction (MSC)

NIR spectral data may include additive (baseline shift) and multiplicative effects which are included by physical effects such as the non-uniform scattering through-out the spectrum as the degree of scattering is dependent on the wavelength of the radiation, the particle size and the refractive index (Nicolai, 2007). Those effects often happen on grain samples in which particle size of each grain is different. The bias of MSC lies in the fact that light scattering has wavelength dependence different from that of chemically based light absorbance (Geladi, 1985). MSC corrects spectra which rotates each spectrum with the average spectra over a set of samples (Imsil, 2012)

2.3.3.3 Derivatives

Derivatives are typically applied to correct for baseline effects for the purpose of removing nonchemical effects and creating robust calibration models. Moreover, it may also aid in resolving overlapped bands (CAMO, 2017). First and second derivatives are widely used in particle. Therefore, their concepts are summarized as following ways:

1) First derivative

The first derivative of spectrum is simply a measure of the slope of the spectral curve at every point. Its slope is not affected by purely additive baseline offsets in the spectrum. Hence, the first derivative is a very effective method for removing the offsets (CAMO, 2017).

This material is reserved for educational use only, not allowed for commercial use.
Forbidden to modify the content, and cite the document when use

2) Second derivative

The second derivative is used to measure the change in the slope of the curve pure additive offset. It is not affected by any linear “tilt” that may exist in the data. Hence, it is a very effective method for removing both the baseline offset and slope from a spectrum, especially the peaks in a raw spectra change sign and turn to negative peaks with lobes on either side in the second derivative (CAMO, 2017).

2.3.3.4 Standard normal variate (SNV)

Standard normal variate (SNV) is a technique usually applied to pre-process spectral data. This method can be used to remove scatter effects by centering and scaling each individual spectrum. The results of SNV are similar to multiplicative scatter correction (MSC) which removes multiplicative interferences of scatter and particle size effect from spectral data

2.3.4 Calibration models for qualitative and quantitative analysis

2.3.4.1 Principal component analysis (PCA)

Principal component analysis (PCA) is multivariate analysis technique uses to reduce the number of variable and solve the multicollinearity problem. The aim of PCA is explaining most of the variance in the data while reducing the number of variable to few uncorrelated component (Imsil, 2012). The information carried by the original variables is projected onto a smaller number of underlying (latent) variables called principle components (PCs). The first principal components (PC_1) covers as much of the variation in the data as possible. The second principal components (PC_2) is orthogonal to the first and covers much of the remaining variation as possible. Benefits of PCA are identification groups of variable. Identification groups of variables by PCA based on the loadings that is correlation between the variables and the principle component and groups of individual based on the principle scores. The result of PCA is generally called “score” (equivalent to the variable) which is concentrated onto a few underlying variables. Each sample has a score along each model component. The score shows the locations of the samples along each model component and can be used to detect sample patterns, grouping, similarities and differenced (Imis, 2012; Anderson, 2003).

2.3.4.2 Partial least squares regression (PLSR)

Partial least squares regression (PLSR) is mathematical technique which has been used in chemometric analysis. The PLS is the most popular multivariate techniques which have been used for creating NIR spectroscopy calibration model. The PLSR is a technique that

This material is reserved for educational use only, not allowed for commercial use.
Forbidden to modify the content, and cite the document when use

generalizes and combines features from principal component analysis (PCA) and multiple linear regression (MLR).Formula of PLSR shows in equation

$$Y=Xb$$

Where: X = a matrix containing the predictor variable.

Y = a column matrix containing the dependent variable.

b = a parameter that is determined by least-square regression.

In practice, PLSR can be applied to create calibration model on 2 models (i.e., PLS1 and PLS2). The PLS1 is developed for prediction one dependent variable by one model. While, the PLS2 is used to predict many dependent variables by one model.

2.3.4.3 Soft independent modeling of class analogies (SIMCA)

Generally PCA is not useful for classification because the class information is not used in the construction of the PCA model. Thus, the PCA model just describes to overall variation in the data. Anywise PCA can be worked together with the class information by soft independent modeling of class analogies (SIMCA). SIMCA is the first and one of the best-known modeling classification methods (Ballabio and Todeschini, 2009). SIMCA model each class independently by PCA, for each class, an acceptance boundary defined by the maximum residuals of the samples from that group is created. Each class is expected to be modeled by a different number of principal components (PCs) (Shiqiang et al., 2015). Ballabio and Todeschini (2009) explained SIMCA algorithm that "the PCA is separately calculated on Each class; since the number of significant component can be different for each category, cross-validation has been proposed as a way of choosing the number of retained components of each class model. In this way, SIMCA defined the number of classes subspaces (class models); then, a new object is projected in each subspace and compared to it in order to assess its distance from the class. Finally, the object from the class model".

2.3.4.4 Partial least square discriminant analysis (PLS-DA)

Primarily, the class models is SIMCA are calculated with the aim of describing variation within each class: when PCA is applied on each category, it finds the directions of maximum variance in the classes, on the opposite of, for example, partial least square discriminant analysis (PLS-DA), which directly models the classes on the basis of the descriptors. Partial least square discriminant analysis (PLS-DA) is classification method based on modeling the differences between several classes with PLSR. Nowdays, the PLS-DA is one of the most popular techniques used in MIR spectroscopy. The PLS-DA bases on the PLS2 algorithm

This material is reserved for educational use only, not allowed for commercial use.
Forbidden to modify the content, and cite the document when use

that searches for latent with a maximum covariance with Y variables. The main difference is related to the dependent variables, since these represent qualitative values, when dealing with classification. In PLS-DA the Y-block describes which objects are in the classes of interest. In binary classification problem, the Y variable can be easily defined by setting its values to 1 if the objects are in the class and 0 if not. Then, the model will give a calculated Y, in the Same way as for a regression approach; the calculated Y will not have either 1 or 0 values perfectly, so a threshold (equal to 0.5, for example) can be defined to decide if an object is assigned to the class (calculated Y greater than 0.5) or not (calculated Y low than 0.5). When dealing with multiclass problems, the same approach cannot be used: if Y is defined with the class numbers (1, 2, 3,…,N) this would mean that a mathematical relationship between the class exits (for example, that class g is somehow in-between class g-1 and class g+1). The solution to this is to unfold the class vector and apply the PLS2 algorithm for multivariate qualitative responses (PLS-DA). For each object, PLS-DA will return the prediction as a vector of classes, with values in-between 0 and 1. Since predicted vectors will not have the form but real values in the range between 0 and 1, a classification rule must be applied; the object can be assigned to the class with maximum value in the Y vector or, alternatively, a threshold between zero and one can be determined for each class (Ballabio and Todeschini, 2009).

2.3.5 Statistical evaluation of accuracy and precision

Performances of NIR spectroscopy are checked statistical. Typically, statistics are usually used for evaluation performances of NIR spectroscopy which are coefficient of determination R, standard error of calibration (SEC), standard error of prediction (SEP), bias and ratio of standard error of prediction to the standard deviation (RPD). The R value, the bias and the RPD are the most meaningful statistics for “instant” appraisal of analytical efficiency by NIR spectroscopy (Williams, 2007).

This material is reserved for educational use only, not allowed for commercial use.
Forbidden to modify the content, and cite the document when use

Table 2.1 Guidelines for the interpretation of R^2

Value of R	Value of R^2	Interpretation
Up to ± 0.5	5 Up to 0.25	Not usable in NIRS calibration
± 0.51 – 0.70	0.26 – 0.49	Poor correlation, research the reasons
± 0.71 – 0.80	0.50 – 0.64	Rough screening
± 0.81 – 0.90	0.66 – 0.81	Screening and approximate calibration
± 0.91 – 0.95	0.83 – 0.90	Usable with caution for most applications, including research
± 0.96 – 0.98	0.92 – 0.96	Usable in most applications, including quality assurance
± 0.99 >	0.98 >	Usable in any application

Source: Williams (2007)

2.3.6 Near hyperspectral image

Hyperspectral image is a form of NIR spectroscopy imaging that capture images at many wavelength bands in the NIR region (Geladi et al., 2004; Tatzer et al., 2005). It is an expansion of multispectral NIR imaging, where images are captured at a much smaller number of wavelength bands, usually two or three (Koehler et al., 2002, 2004; Geladi., 2004). NIR hyperspectral imaging is an exciting, new analytical advance that answers frequently posed questions such as: what chemical species are present and most importantly, where are they located? These questions can be answered simultaneously, in a single rapid measurement, through the unification of traditional NIR spectroscopy with powerful microscopic and macroscopic imaging capabilities of a hyperspectral imaging system. NIR hyperspectral imaging empowers researches with spatial and spectral information that permits characterization of samples with exceptional simplicity, speed and improves spatial and spectral resolution (Koehler et al., 2002).

2.3.6.1 Relationship between spectroscopy imaging, and hyperspectral imaging

Image processing and image analysis are the core of computer vision which became an integral of the industry's move forwards automation. However, the computer vision system has some drawbacks that are inefficient in the case of objects of similar color and unable to quality attributes. Because, the products' quality index can be identified based on the correlation between the spectral response and the specific quality attributes of the products, usually a chemical parameters (Park et al., 2002). Recently, optical techniques using NIRs is able to obtain information about the sample components based on the light absorption of the sample,

This material is reserved for educational use only, not allowed for commercial use.
Forbidden to modify the content, and cite the document when use

but it is not easy to know the location or position information. The combination of the strong and weak points of conventional spectroscopy and conventional imaging techniques are the hyperspectral image techniques which has been regarded as a promising analytical tool for analyses conducted in research and industries. While a gray scale image typically reflects the light intensity over the electromagnetic spectrum in a single band, a color image reflects the intensity over the red, blue and green bands of the spectrum. Increasing the number of bands can greatly increase the amount of information with different resolution values. Hyperspectral image been invented to integrate spectroscopy and spatial image (Chen et al., 2002) which be impossibly achieved with either vision system or NIRs techniques. Hyperspectral image can be carried out in reflectance, transmission or fluorescence modes while the majority of published research on hyperspectral image has been performed in reflectance mode. The main differences among imaging, spectroscopy and hyperspectral imaging techniques are shown in Table 2.2.

Table 2.2 Main differences among imaging, spectroscopy and hyperspectral imaging techniques.

Features	Hyperspectral imaging	Spectroscopy	Imaging
Spectral information	✓	✓	x
Spatial information	✓	x	✓
Multi-constituent information	✓	✓	x
Detectability to objects with small size	✓	x	✓
Flexibility of spectral extraction	✓	x	x
Generation of quality-attribute distribution	✓	x	x

Source: Wu and Sun (2013)

2.3.6.2 Calibration of hyperspectral image

The goals of calibration process in hyperspectral image are

1) Standardize the spectral axis of the hyperspectral image,

2) Determine whether a hyperspectral image system is operating properly,

3) Provide information about the accuracy of the extracted spectral data and thus validate their acceptability and credibility,

4) Diagnose instrument errors, measurement accuracy and

This material is reserved for educational use only, not allowed for commercial use.
Forbidden to modify the content, and cite the document when use

5) Reproducing under different operating conditions.

The most significant step in the calibration process is the spectral wavelength calibration that identifies each spectral channel with a specific wavelength. To determine the relation between distance (in pixels) on the spectral axis and wavelength, the spectral axis, must be calibrated by using a standard emission lamp as a light source. In the practice, the calibration lamp is first scanned by the hyperspectral image system under controlled operating conditions. Once the calibration lamp is scanned, its peaks are then assigned to standardize the spectral axis. Then a polynomial regression of first or second order can be established to convert spectral axis (in pixels) to its corresponding wavelength using the reference wavelength of calibration lamp. Finally, after acquiring hyperspectral images of real samples, another calibration step. Called reflectance calibration, should be performed to account for the background spectral response of the instrument and the "dark" current of the camera. The background is obtained by acquiring a spectral image from a uniform, high reflectance standard or white ceramic (-100% reflectance) and dark response (-0% reflectance) is acquired by recording an image when the light source is turned off and the camera lens is completely covered with its non-reflective opaque black cap. These two reference images are then used to calculate the pixel-based relative reflectance for the raw line-scan images using the following formula (Eq. 2.1):

$$I = \frac{I_0 - D}{W - D} \qquad \text{(Eq. 2.1)}$$

Where; I is the relative reflectance image, I_o is the raw reflectance image

D is the dark reflectance image

W is the white reference image

The corrected hyperspectral image can also be expressed in absorbance (A) by taking logarithms of the above equation 8.2 as:

$$\mathrm{A} = log_{I0}\frac{I_0 - D}{W - D} \qquad \text{(Eq. 2.2)}$$

2.3.6.3 Acquisition modes of hyperspectral image

There are three conventional ways to build one-spectral image: area scanning, point scanning, and line scanning. We concentrated on the line scanning which is also called push-broom. It involves acquisition of spectral measurements from a line of sample which are simultaneously recorded by an array detector and the resultant is stored in the Band Interleaved

This material is reserved for educational use only, not allowed for commercial use.
Forbidden to modify the content, and cite the document when use

by Line (BIL) format. This method is particularly well suited to conveyor belt systems and may therefore be more practicable than the former ones for food industry applications.

Line scanning devices record a whole line of an image rather than a single pixel at a time using a two-dimensional dispersing element (grating) and the two-dimensional array. A narrow line of the specimen is imaged onto a row of pixels on the sensor chip and the spectrograph generates a spectrum for each point on the line, spread across the second dimension of the chip. Therefore, hyperspectral images are acquired by a wavelength system that incorporates a diffraction grating or prism. These instruments typically require an entrance aperture, usually a slit, which is imaged onto the focal plane of the spectrograph at each wavelength simultaneously. Therefore, an object imaged on the slit will be recorded as a function of its entire spectrum and its location in the sample. This configuration is normally used when either the specimen or the imaging unit is moving one in respect to the industrial applications. The sensor detectors in a push-broom scanner are lined up in the row called a linear array. HSI systems can be conducted either in reflectance or transmittance modes. To acquire images in transmittance mode, thin sample sizes are usually used to allow light to travel through the sample. Thicker samples can be used in reflectance HSI measurements. Thus, food materials can be inspected as a whole in reflectance mode without the need to make slices. For instance, Peng & Lu (2008) studied about firmness and TSS of apples using HSI in reflectance mode. In this research we employed Sisu CHEMA that is a complete chemical imaging system, characterized by speed, simplicity and superior performance. SiSu CHEMA employs a push-broom imaging technology providing several advantages for the users, such as high speed, low heat load from illumination and flexibility to most sample shapes and sizes. Push-broom approaches these characteristics: (1) It is a line-scale device, (2) Full spectra of the all spatial positions along the imaged line is recorded in one single snapshot; and (3) Target must be imaged line-by-line from the 2D image.

The penetration depth could have effects on the HSI detection. By providing references for thickness determination, which could be valuable for designing an appropriate and accurate sensing configuration, penetration depth would prove beneficial. Light penetration depth is defined as the depth at which the incident light was reduced by 99%. It can vary according to the status, type of sample, and the detection waveband. Optical features of the light penetration depth are mainly determined by strong absorbing constituents in the sample. Lammertyn et al. (2000) proved that light penetration depth in apples was dependent on the detection wavelength

This material is reserved for educational use only, not allowed for commercial use.
Forbidden to modify the content, and cite the document when use

by putting forward a non-linear model describing the correlation between the reflectance and thickness of apple slices. The penetration of apple is up to 4 mm in the 700-900 nm range and between 2 and 3 mm in the 900-1900 nm range. In the research of Qin and Lu (2008), the light penetration depth in tissues of apple, peach, pear, kiwifruit, tomatoes, zucchini, cucumber, and plum was calculated according to the absorption and reduced scattering spectra of the test samples at different wavelengths. The minimum light penetration depths ranged from 7.1 mm at 535 nm for the plum to 13.8 mm at 720 nm for the zucchini. The wavelengths were correlated to the absorption peaks of the major pigments in the fruits and vegetables. The maximum penetration depths ranged from 18.3 mm for the apple to 65.2 mm for the zucchini, study highlighted that penetration depth varies a great deal depending on the type of object being studied and the applied depth, and on surface and texture of sample. Long wavelength and short wavelength has different energy so penetration depth is different. Short wavelength has high energy so penetration depth is longer than long wavelength.

2.3.6.4 Hyperspectral image data

Hyperspectral image data consist of several congruent images representing intensities at different wavelength bands composed of vector pixels containing three-dimensional hyperspectral cube or hyper cube or data cube which can provide physiochemical information of the material under test (Cogdill et al., 2004). Intensity values of a spatial image in the hypercube at one wavelength may have 8-bit gray values meaning that 0 is the black and 255 is the white. In more precise system, the intensity values of each pixel having 12-bit (2^{12} gradations, i.e, 0-4095), 14-bit (2^{14} gradations, i.e., 0-16383) or 16-bit (2^{16} gradations, i.e, 0-65535) gray levels are used. For more demanding scientific applications such as cell, fluorescence or Raman imaging, a higher performance 16-bit cooled camera may be advantageous. Hyperspectral data volumes are very large and suffer from collinearity problems. This has implications for storage, management, and further image processing and analysis.

2.3.6.5 Advantages and disadvantages of hyperspectral imaging

The foremost advantages of using HSI technology in food analysis can be summarized in the following points;

1) No sample preparation

2) A chemical-free assessment method

3) It is noninvasive and nondestructive method, so that the same sample could be used for other purposes and analyses;

This material is reserved for educational use only, not allowed for commercial use.
Forbidden to modify the content, and cite the document when use

4) It is eventually economic because it save in labor, time and reagent cost in addition to the large saving in the cost of waste treatments;

5) Rather than collecting a single spectrum at one spot on a sample, as in spectroscopy, HSI records a spectral volume that contains a complete spectrum for every spot (pixels) in the sample;

6) It has the flexibility in choosing any region of interest (ROI) in the image even after image acquisition;

7) It is able to determine several constituents simultaneously in the same sample and

8) It allows for the visualization of different biochemical constituents presented in a sample based on their spectral signatures because regions of similar spectral properties should have similar chemical composition. This process is called building chemical images, or chemical mapping, for constructing detailed maps of the surface composition of foods which traditionally requires use of intense laboratory methods.

In spite of the abovementioned advantages, HSI does have some disadvantages, which can be summarized as follows;

HSI contains substantial amount of data, including much redundant information and present considerable computational challenges;

9) It takes a long time for image acquisition and analysis, therefore HSI technology has to a very limited extent been directly implemented in on-line systems for automated quality evaluation purposes

10) One of the main analytical drawbacks of HSI technique is that it is an indirect method, which means that it needs standardized calibration and model transfer procedures,

11) One major factor that limits its industrial applications for food inspection is the hardware speed needed for rapid image acquisition and analysis of the huge amount of data collected and

12) Depending on the spatial resolution and the structure of the sample investigated, spectra from individual image pixels may not represent a pure spectrum of one singular material, but a mixed spectrum consisting of spectral responses of the various materials that cover the region of interest (ROI) selected from the sample.

This material is reserved for educational use only, not allowed for commercial use.
Forbidden to modify the content, and cite the document when use

2.4 Application of NIR spectroscopy to detect quality of agricultural products

Lin et al. (2011) used reflectance NIRS for detection and classification of egg freshness. Egg were stored for 1–14 days and Haugh units is standard method to measure freshness of egg. Accuracy of classification eggs based on storage time is 92.4% in calibration set and 91.4% in prediction set, respectively. In addition, correlation coefficient (R) for prediction Haugh unit is 0.879 and root mean square error of prediction (RMSEP) is 2.443.

Giunchi et al. (2008) used FT-NIR spectroscopy for assessment of shell-egg. Samples were storage at 1, 4, 7, 10, 13 and 16 days. The air cell height, thick albumen heights and Haugh unit are parameter of freshness. The predictive model of air cell height, thick albumen heights and Haugh unit showed R^2 at 0.722, 0.789 and 0.676, respectively.

Liu et al. (2014) used hyperspectral imaging in the wavelength 1000–2500 nm to predict moisture content of porcine meat during salting process. Different spectra such as reflectance spectra, absorbance spectra and Kubelka–Munk spectra were examined of moisture content. The distribution map of moisture content were generated by PLSR model. The results showed that moisture contents of porcine meat could be determined accurately by hyperspectral imaging.

Xiong et al. (2015) used hyperspectral imaging for determining the total pigments in red meats. The partial least squares regression (PLSR) was applied to correlate the reference values of total pigments and spectral data. The overall results indicated hyperspectral imaging had the good method or predicting the total pigments in red meats because it showed high correlation coefficient (R_p^2 =0.953 and RMSEP = 9.896).

Cen et al. (2016) used hyperspectral imaging to detect chilling injury in cucumber fruit. The physiological disorders of cucumber fruit divided two-class (normal and chilling) and three-class (normal, lightly chilling, and severely chilling). The classify result showed high accuracy. The accuracy to classify physiological disorders between normal and chilling is 100% while the accuracy to classify normal, lightly chilling, and severely chilling is 91.6%. This research can be applied to using hyperspectral imaging system with supervised classification for detecting chilling injury in cucumbers.

Jia et al. (2017) evaluated pH of fresh chicken breast fillets by visible and near-infrared (VNIR) hyperspectral imaging in the wavelength range 400-900 nm. The best model was developed using Partial Least Squares Regression (PLSR) with the pretreatment of multiplicative scatter correction followed by second derivative. The coefficients of determination for validation (R_v^2) is 0.87, root mean square error for validation (RMSEV) is 0.16 and the ratio of percentage

This material is reserved for educational use only, not allowed for commercial use.
Forbidden to modify the content, and cite the document when use

deviation (RPD) is 2.02. The competitive adaptive reweighed sampling (CARS) method used to selected optimal 20 wavelengths for develop a new PLSR model. The result of new PLSR model was good accuracy (R^2_v = 0.94, RMSEV = 0.06 and RPD = 3.55 and R^2_p =0.73, $RMSE_P$ 0.29). The distribution map was generated to analyze the spatial context of pH values of each fillet. The results showed that VNIR hyperspectral imaging can be applied to predicted spatial and global pH values of fresh chicken breast meat.

Chu et al. (2017) used short wave infrared hyperspectral imaging in the wavelength range 1000-2500 nm to detect aflatoxin B_1 in single maize kernels. The AFB_1 contamination levels (<20 ppb, 20-100 ppb, $\geq$100 ppb) were used to classify by principal component analysis (PCA) with support vector machine (SVM) methods. The result showed good accuracy (83.75% and 82.50% for calibration and prediction set). Therefore, it indicated that hyperspectral imaging could be used to classify AFB_1 level in single maize kernels.

This material is reserved for educational use only, not allowed for commercial use.
Forbidden to modify the content, and cite the document when use

CHAPTER 3

RESERCH METHODOLOGY

3.1. Materials and equipments

3.1.1 Hen egg (esa brown variety)

3.1.2 Sweet corn ('Insee 2' variety of a hybrid sweet corn)

3.1.3 FQA-NIR GUN spectrophotometer (FANTEC inc., Japan)

3.1.4 FT-NIR spectrophotometer (NIR Flex N-500., Switzerland)

3.1.5 Hyperspectral imaging unit (Specim, Spectral Imaging Ltd., Finland)

3.1.6 Refractometer (Atago PAL-3, Japan)

3.1.7 Hand-held penetrometer (fruit firmness tester, FHR-5, Nippon Optical Work Co., Ltd., Tokyo)

3.1.8 Hot air oven (Memmert UFB 400, Germany)

3.1.9 Vernier caliper

3.2 Methods

The experiments in this thesis were divided into two parts. First part was the nondestructive quality assessment of hens' eggs by NIR spectrophotometer (FQA- NIR GUN), FT-NIR spectrophotometer (NIR Flex N-500) and NIR hyperspectral imaging. Second part was the nondestructive quality assessment of sweet corns (total soluble solids, hardness value and moisture content) by NIR spectrophotometer (FQA- NIR GUN) and FT-NIR spectrophotometer (NIR Flex N-500)

3.2.1 An experiment to evaluate the freshness of hen eggs.

3.2.1.1 Sample preparation

Hen eggs (Figure 3.1) were purchased from a poultry farm in Nakhon Ratchasima Province, Thailand. They were sorted for the same size of number 3 (National Bureau of ACFS, 2010) with good appearance. Samples for use in this study were inspected and cleaned to ensure that there were no dirt and breakage at the shell. The samples were divided into 7 groups in order to use for measurement at the different period of storage (0, 4, 7, 10, 14, 18 and 21 days).

This material is reserved for educational use only, not allowed for commercial use.
Forbidden to modify the content, and cite the document when use

Figure 3.1 Hen eggs (esa brown variety)

3.2.1.2 Measuring spectra

Three NIR spectrophotometers were used in this thesis. NIR spectrophotometer (FQA- NIR GUN) in the wavelength range of 588-1091 nm was used for interactance mode, FT-NIR spectrophotometer (NIR Flex N-500) in the wavelength range of 1000-2500 nm was used for reflectance mode and NIR hyperspectral image in the wavelength 900-1700 nm was used for reflectance mode. For, FT-NIR and FQA- NIR GUN measurement, each hen egg was scanned 4 times at the middle around the equator in every 90°. The position to scan hen egg shown in Figure 3.2

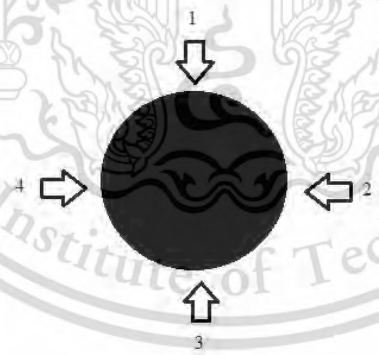

Figure 3.2 Scanned position of hen egg.

For NIR hyperspectral image data acquisition, samples were measured by a push-bloom NIR hyperspectral imaging system. The main parts of hyperspectral image system contained with an imaging spectrometer, a CCD camera, a light source, a translation stage at size 100 × 100 mm, and data acquisition software that controls the motor speed, exposure time and image acquisition. Each sample was placed horizontally on a tray and moved by stepper motor through the field of view (FOV) of the spectrograph at a constant speed of 33 mms^{-1} during

This material is reserved for educational use only, not allowed for commercial use.
Forbidden to modify the content, and cite the document when use

measurement. The exposure time of the CCD camera was adjusted to 1.5 ms. The white and dark reference was captured for each measurement. The white and dark spectra were recorded as reference spectra. A high speed shutter unit switched the optical path during measurement into three modes: target, white reference and dark reference. The white and dark reference was captured for each measurement. After scanning, the sample images were taken by CCD camera and transformed to a digital signal. After that, the hyperspectral image was created by a function of x, y and λ.

3.2.1.3 Haugh unit

After spectral measurement, each hen egg was determined Haugh unit by a standard method using the formula (3.1) that was a destructive method (Haugh, 1937). Each egg was weighed on a balance with a resolution of 0.01 gram and then broken onto a flat glass plate and the height of its albumen was measured at 3 points around the yolk using a micrometer with a resolution of 0.1 millimeter. The heights of albumen's thickness was calculated as the mean of three measurements. Each sample was measured albumen thickness at three points around the yolk. Each point of measuring albumen thickness was at the middle distance between outer border edges of yolk and albumen. The same procedure was used for all samples and then calculated of Haugh unit where h was averaged thick albumen height and W was egg weight:

$$\text{Haugh unit} = 100 \times \log (h - 1.7W^{0.37} + 7.6) \quad (3.1)$$

For the freshness classification by consideration of Haugh unit, Haugh unit is 72 or higher for 'AA' grade, 60–71 for 'A' grade and 60 or lower for 'B' grade. Hen egg is considered to be unfresh when Haugh unit is lower than 60 (United States Department of Agriculture, 2000).

3.2.1.4 Data analysis

For data from NIR spectrophotometer (FQA- NIR GUN)) which was interactance mode, all sample were scanned and divided into 2 sets. A first set was used for calibration and a second set was used for prediction. Calibration model was established using Haugh unit (dependent variable) and spectral data (independent variables) from a calibration set. Accuracy of calibration model was evaluated by test in a prediction set. As well as, for data from FT-NIR spectrophotometer (NIR Flex N-500) which was reflectance mode, all samples were divided for the calibration set and the prediction set, then did the same way as mentioned in the interactance part. The average spectrum was calculated from four measurements of each sample. The spectral pretreatments in calibration set were investigated. The spectral pretreatment were

This material is reserved for educational use only, not allowed for commercial use.
Forbidden to modify the content, and cite the document when use

applied to reduce noise, remove slope variation, reduce to scattering effects and enhance to contribution of the dependent variable (Haugh unit). The pretreatment which obtained the best results was selected to establish the calibration model. The calibration model was developed and cross-validated using Partial Least Squares Regression (PLSR). The acquired models were tested by cross-validation and used to test the samples in the calibration set. For cross-validation the samples were divided into 29 segments each of two samples. For each segment the first sample was set aside and the second sample was used to establish the model, which was then tested on the first sample. The same procedure was carried out on all 29 segments. From each spectral pretreatment, the correlation coefficient (R) and the root mean square error of cross-validation (RMSECV) were determined for the optimal conditions in order to establish the calibration model. To evaluate the performance of the calibration model, statistical results of R and root mean squared error of calibration (RMSEC) were considered. To assess the predictive accuracy of the model, the results of the correlation coefficient (R) and the root mean squared error of prediction the prediction (RMSEP) were considered. The Unscrambler program (CAMO, Oslo, Norway) was used for the statistical analysis in this research.

For data from NIR hyperspectral image, Spectral data of each sample and background were obtained from the HSI system. In order to analysis only spectral data of hen egg, the region of interest (ROI), a size 50×90 pixel was cropped in only the area of hen egg body excluding ‘the background. Spectral data in the ROI were averaged and used for to establish the calibration model for Haugh unit. The calibration model was developed and cross-validated using Partial Least Squares Regression (PLSR). In the calibration set, the spectral pretreatments method such as smoothing (Savitzky-Golay) , first derivative differentiation, second derivative differentiation, multiplicative scatter correction (MSC) and standard normal variate transformation (SNV) were investigated in order to obtain the optimal conditions. The best conditions were determined by considering the lowest root mean square error of cross validation (RMSECV) and the highest coefficient of determination (R). The performance of the calibration models were considering the R and the root mean square error of calibration (RMSEC) in calibration set and the accuracy were considering the R, the root mean square error of prediction (RMSEP) in prediction set and a ratio of prediction to deviation (RPD). For RPD, the levels of prediction accuracy were based on a value for the RPD. Saeys et al. (2005) gave levels of prediction accuracy based on the RPD where: less than 1.5 indicates that the model is not usable, 1.5 to 2.0 indicates that the model can distinguish between high and low values, 2.0 to 2.5

This material is reserved for educational use only, not allowed for commercial use.
Forbidden to modify the content, and cite the document when use

indicates that the model can be used for approximate prediction, 2.5 to 3.0 indicates that the model is good for prediction and > 3 indicates that the model is excellent for prediction. Unscrambler software (CAMO, Oslo, Norway) was used for the statistical analysis in this research. After that, generate distribution map of Haugh unit value by the best calibration model. For the visualization process in this study, the best calibration model was used to generate concentration image or distribution map and visualize the spatial variations of Haugh unit value. The distribution map each pixel of hyperspectral image used to prediction Haugh unit distribution of eggs. The prediction of distribution map was presented with color scale which the distribution map of Haugh unit value corresponded the color scale. Each sample was presented in distribution map which showed in different colors based on predicted Haugh unit. Evince program (2.7.5 version) was used for analysis in order to create the distribution map.

3.3.2 An experiment to evaluate quality of sweet corns

3.3.2.1 Sample preparation

Samples of sweet corns (Figure 3.3) were harvested from a farm in Nakhon Ratchasima province, Thailand. Sweet corns were harvested in July, 2015. The samples were selected to be of similar size, good appearance and without defect. They were carefully transported to the laboratory. The samples were taken for measurement in every 20 samples at 6 hr, 12 hr, 18 hr, 24 hr, 30 hr and 36 hr after harvest.

Figure 3.3 sweet corns (‘Inset 2’ variety of hybrid sweet corn)

3.3.2.2 Measuring spectrum

Three NIR spectrophotometers were used in this thesis. NIR spectrophotometer (FQA- NIR GUN) in the wavelength range of 588-1091 nm was used for interactance mode, FT-NIR spectrophotometer (NIR Flex N-500in the wavelength range of 1000-

This material is reserved for educational use only, not allowed for commercial use.
Forbidden to modify the content, and cite the document when use

2500 nm was used for reflectance mode and NIR hyperspectral image in the wavelength 900-1700 nm was used for reflectance mode. Determinations were done in 2 parts. In the first part, each sweet corn with husk was scanned 3 times at its top, middle and bottom, and in the second part, each sweet corn without husk was scanned 3 times at the same positions.

3.3.2.3 Quality of sweet corns

1) Total soluble solids content

After spectral measurements, juice was squeezed from sweet corns. Total soluble solids content of samples was measured using a digital refractometer (PR101, Palette Series, Atago Co., Ltd., Tokyo, Japan)

2) Hardness

The hardness was measured using a hand-held penetrometer (fruit firmness tester, FHR-5, Nippon Optical Work Co., Ltd., Tokyo)

3) Moisture content (AOAC, 2000)

Remove the corn kernels from the corn stalks. After that, corn kernels were randomly picked for measuring moisture content. Weigh samples immediately recorded as "wet weight of sample" and recorded "dry weight of sample" that was a constant weight from a hot air oven (Memmert, D 0601 Model 500, Germany).

Calculate moisture content using the following equation:

$$\% \text{ Moisture Content} = \frac{A - B}{A} \times 100$$

Where: A = Weight of wet sample (grams) and B = Weight of dry sample (grams)

3.3.2.4 Data analysis

For developing the model of total soluble solids, moisture content and hardness value, all samples were scanned and divided into 2 sets. A first set was used for calibration and a second set was used for prediction. The average spectrum was calculated from time measurements of each sample. In order to divide the calibration set and prediction set; all samples had been sorted according to their dependent variable (total soluble solids, hardness value and moisture content). One spectrum of every three spectra was selected into the prediction set. Therefore, the calibration set contained 70% of all spectra while the remaining 30% of all spectra constituted the prediction set. Different pretreatments such as derivative, smoothing Savitzky-Golay, MSC, SNV were applied to reduce noise, remove slope variation, reduce to scattering effects and enhance to contribution of the dependent variable (spectra data). All of the

This material is reserved for educational use only, not allowed for commercial use.
Forbidden to modify the content, and cite the document when use

spectra were developed into calibration models by using PLSR. The statistical results of correlation coefficient (R) and root mean squared error of cross-validation (RMSECV) were considered the best model. To evaluate the performance of the calibration model, statistical results of R and RMSEC were considered. To assess the predictive accuracy of the model, the results of R, RMSEP and RPD were considered. Statistical analysis was done with Unscrambler software (CAMO, Oslo, Norway).

This material is reserved for educational use only, not allowed for commercial use.
Forbidden to modify the content, and cite the document when use

CHAPTER 4

RESULTS AND DISCUSSIONS

4.1 Changed of hen egg quality during storage

Hen eggs were considered the external and internal appearance at the different period of storage. Hen eggs were broken on the mirror one by one and then capture the image. Picture of hen eggs during storage is shown in Figure 4.1. By considering Figure 4.1(left side), external of hen egg was an egg shell (calcium carbonate) that couldn't see the difference. Comparisons between a group of fresh and unfresh egg by looking only the shell egg, it couldn't identify between fresh egg and unfresh egg. From Figure 4.1(right side), internal of hen egg were composed of three main parts; egg yolk, thick albumen and thin albumen. Egg yolk was in the center of the egg. Next, the egg yolk had thick albumen and thin albumen, respectively. The result of averaged Haugh unit during storage period was presented in Table 4.1. Eggs with Haugh unit score below 60 were considered to be unfresh. The periods of storage at 0 day and 4 day, eggs were considered to be fresh. After periods of storage at 7 day, eggs were considered to be unfresh. During storage, internal appearance of hen eggs was changed and it was affected to its quality as follows; thick albumen was weak, thin, lacking in viscosity and egg yolk was flat. In during storage at 0-4 days, thick albumen and egg yolk is higher than hen egg which is storage at 7-21 days. The factors that affect the internal quality of eggs are loss of water, CO_2 through the shell, liquefaction of albumen and flaccidity of the vitelline yolk membrane (Rossiet al., 1995; Walsh et al., 1995; Karoui et al., 2006) The loss of water content which caused by water evaporation through the egg shell. These processes are the reason of the decreasing egg weight and the volume of the air cell between inner and outer shell membranes increases (Romanoff and Romanoff, 1949). In addition, the liquefaction of albumen increases because carbon dioxide (CO_2) is loss, albumen pH raises and the formation of egg in the reproductive system. (Burley and Vadehra, 1989). The structural change of interaction between ovomucin-lysozyme during storage is involved to reduction of freshness. The result of the structural changes is effect of albumen thinning and air cell increasing because CO_2 gas is lost through the pores on the egg shell.

This material is reserved for educational use only, not allowed for commercial use.
Forbidden to modify the content, and cite the document when use

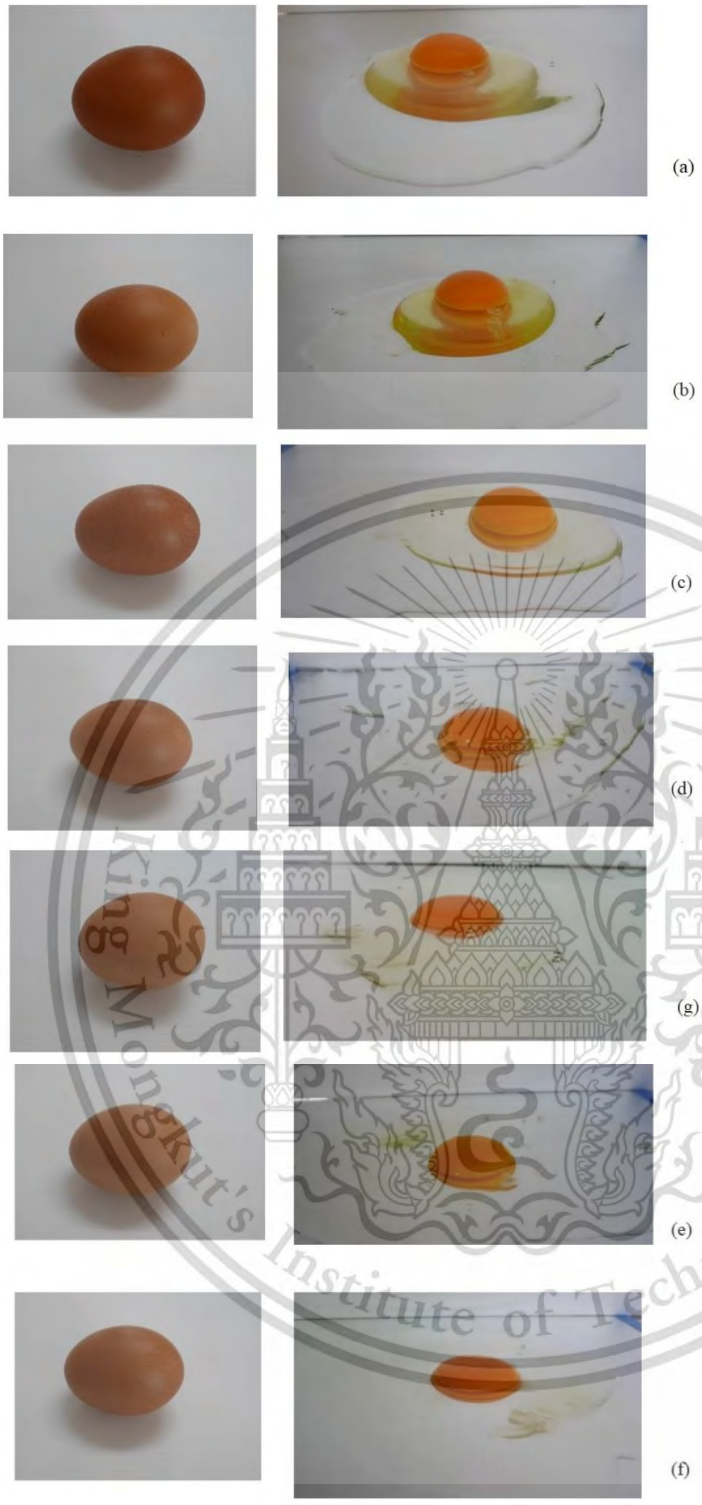

Figure 4.1 Samples of hen eggs with different periods of storage (a) 0 day, (b) 4 day, (c) 7 day,(d) 10 day, (e) 14 day, (f) 18 day and (g) 21 day.

This material is reserved for educational use only, not allowed for commercial use.
Forbidden to modify the content, and cite the document when use

Table 4.1 Averaged Haugh unit during storage period**.**

Parameter	Days						
	0	**4**	**7**	**10**	**14**	**18**	**21**
Haugh unit	73.55	64.73	49.55	36.20	31.33	24.79	22.18

4.2 Changed of sweet corn quality during storage

Sweet corns were considered the external and internal appearance at the different period of storage time after harvest (6 hr, 12 hr, 18 hr, 24 hr, 30 hr and 36 hr). Samples of sweet corns with different storage time after harvest shown in Figure 4.2. Normally, sweet corns should be transported to the factory and should be processed within 24 hours after harvest (National Food Institute, 2016). Due to quality of fresh sweet corns rapidly changes by time. It can indicate the sweet corn with storage time over 24 hr after harvest is unfresh. Comparisons between a group of fresh and unfresh sweet corns by only looking at external and internal appearance of sweet corns, it can't be identify between fresh sweet corns and unfresh sweet corns. But the quality of sweet corns can be judged by their texture and taste. External evaluation (shape, color and size) of sweet corns can't be estimated for texture and taste. The quality results of sweet corns with different storage time after harvest shown in Table 4.2. Parameter qualities of sweet corns were present in term of total soluble solids content, hardness and moisture content. From Table 4.2, quality of sweet corns was change during storage time. The taste and texture of sweet corns were related to sweetness and tenderness. The sweetness and tenderness of sweet corns depends on the storage time after harvest. The sugar of sweet corns was changed by converting to be starch after harvest. Longer storage time affected to its quality. It becomes hard and decreasing its sweetness. Internal quality relates the storage time but it couldn't be identified by visual inspection.

This material is reserved for educational use only, not allowed for commercial use.
Forbidden to modify the content, and cite the document when use

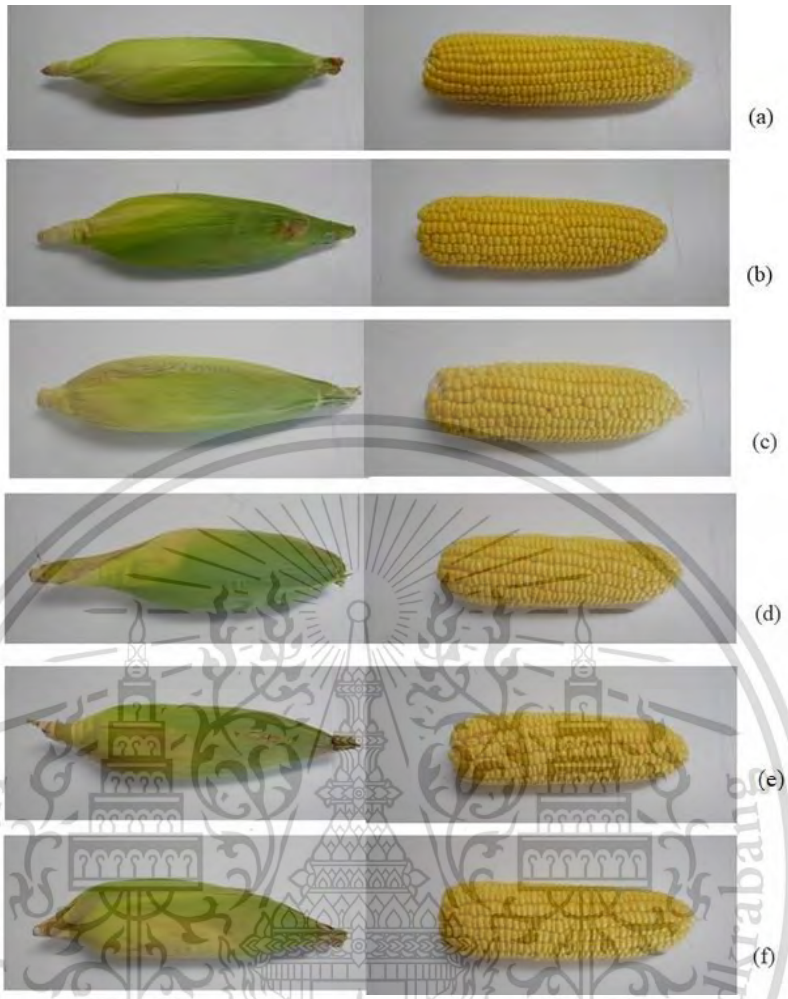

Figure 4.2 Samples of sweet corn with different storage period after harvest.
(a) 6 hr, (b) 12 hr, (c) 18 hr, (d) 24 hr, (e) 30 hr and (f) 36 hr.

Table 4.2 The quality results of sweet corns with different storage period after harvest.

Items	Storage period after harvest (hr)					
	6	12	18	24	30	36
Soluble solids content (^{o}Bx)	18.5	18.03	16.90	15.86	14.37	13.77
Hardness (N)	11.13	11.79	11.83	12.24	12.80	13.1
Moisture content (%)	17.53	13.37	11.68	11.65	11.61	11.55

N = Newton

This material is reserved for educational use only, not allowed for commercial use.
Forbidden to modify the content, and cite the document when use

4.3 An experiment to evaluate the freshness of hen eggs

4.3.1 Calibration model for Haugh unit by interactance NIRS

All samples (247 samples) were scanned and divided into two groups. The first group was used for calibration (165 samples) and the second group was used for prediction (82 samples). A dependent variable was Haugh unit and independent variables were spectra data. Calibration model was established by using the dependent variable and independent variables from a calibration set. The performance of the model was evaluated by test in a prediction set. Statistical characteristics of Haugh unit in calibration set and prediction set are shown in Table 4.3. In order to divide the calibration set and the prediction set, all samples were sorted according to the Haugh unit. Then, one sample of every three sample was selected into the prediction set. Finally, the calibration set contained 247 samples while the prediction set contained 82 samples.

Table 4.3 Statistical characteristics of samples in the calibration set and the prediction set for interactance NIRs.

Items	Calibration set	Prediction set
Number of samples	165	82
Range	22.2-84.31	25.25-82
Mean	50.42	50.98
SD	13.78	14.07
Wavelength	588-1091 nm	588-1091 nm

SD = standard deviation.

Figure 4.3 shows average spectra of all hen egg samples which were measured with the NIR spectrophotometer (FQA- NIR GUN). Figure 4.3 (a) shows the original spectra while Figure 4.3 (b) showed the processed spectra by second derivative. It was found that the peak of second derivative become clear. In the NIR region of 588-1091 nm, spectra could provide information of molecular bonds. The peak of NIR spectra related with C-H, H-O, C-O and N-H. The main peaks of spectra were identified at 750 and 970 nm. These absorption peaks related to O–H (Zhu et al., 2013). The peaks in the Figure 4.3 (b) were related to compositions of egg samples.

This material is reserved for educational use only, not allowed for commercial use.
Forbidden to modify the content, and cite the document when use

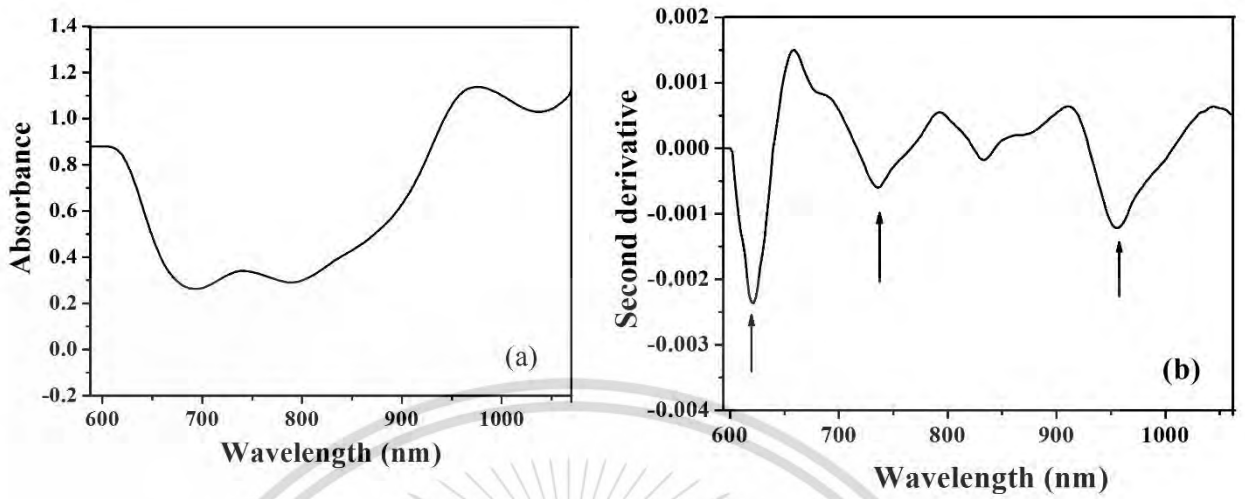

Figure 4.3 Average spectra of all egg samples which were measured with the NIR spectrophotometer (FQA- NIR GUN)

(a) original spectra

(b) second derivative

The NIR spectra are characterized by unfavorable spectral variations such as light scattering, noise and large baseline shifts in the spectra. They are influenced by physical properties such as variations in temperature, density and particle of shape or size etc. (Leonardi and Burns 1999). The size of hen egg samples in this research was number three, it was used the same size in order to reduce the effects of the noise and baseline shifts in the spectra. However the shape of egg samples was oval that the width and length was different which might be affected to accuracy of model. In this study, the samples were divided for a calibration set and a prediction set. The samples in the prediction should be more than 30% of the total samples. The dependent variable value in the calibration set should be cover (maximum and minimum value should be in the calibration set) and similar deviation in the prediction set in order to ensure that an acquired model could be accepted for use. In the calibration set, samples were used to establish the model using PLSR. The best model was selected for prediction in the further step. To acquire the best model, the spectral pretreatments were investigated for finding out the best conditions for establishing the best model. In this step, there were acquired models. The models were tested by cross-validation namely acquired models were used to test by samples in the calibration set. For cross-validation, samples were divided to 29 segments and each segment contained 2 samples.

This material is reserved for educational use only, not allowed for commercial use.
Forbidden to modify the content, and cite the document when use

The first step, samples from 1st segment were leaved out and the other samples were used to establish the model. Then the acquired model was tested by samples in 1st segment. The second step, samples from 2nd segment were leaved out and the other samples were used to establish the model. Then the acquired model was tested by samples in 2nd segment. The next step was done in the same procedure until all segments were tested. The results from cross-validation were presented by factor, R and RMSECV. The best model obtained from the results of highest R and lowest RMSECV and PC. The acquired calibration model were tested its performance. This step, the model was tested by all samples in the calibration set. The results in this step obtained R and RMSEC for the model. After that the model was used to evaluate the accuracy by the samples in the prediction set. The results of accuracy of the model were presented by PC, R and RMSEP. Therefore, the selection of suitable pretreatment methods were important step to reduce noise, remove slope variation, reduce to scattering effects and enhance to contribution of the spectra data. The best condition of the calibration was investigated by statistical of spectral pretreatments. Statistical results of spectral pretreatments for prediction of Haugh unit by interactance NIR were shown in Table 4.4. It showed that combination smoothing and first derivative pretreatment obtained the best results (R = 0.89, RMSECV = 6.19). The Savitzkye-Golay smoothing method used to moving average. (Blanco and Villarroya 2002) So, smoothing method was applied for noise reduction in the process of spectral analysis. The first derivatives method of pretreatment was used to solving problems in correcting light scattering contributions (Leonardi and Burns, 1999).

This material is reserved for educational use only, not allowed for commercial use.
Forbidden to modify the content, and cite the document when use

Table 4.4 Statistical results of spectral pretreatments for prediction of Haugh unit by interactance NIRs.

Spectral Pretreatments	N	Wavelength	F	R	RMSECV
Original	165	588-1091 nm	9	0.89	6.21
Smoothing	165	588-1091 nm	6	0.88	6.27
1st derivative	165	588-1091 nm	7	0.88	6.26
2nd derivative	165	588-1091 nm	8	0.87	6.65
MSC	165	588-1091 nm	5	0.88	6.27
Mean	165	588-1091 nm	6	0.88	6.35
SNV	165	588-1091 nm	5	0.87	6.68
Smoothing + 1st derivative	165	588-1091 nm	8	0.89	6.19
Smoothing + 2nd derivative	165	588-1091 nm	16	0.85	7.20
Mean + Smoothing + 1st derivative	165	588-1091 nm	8	0.89	6.22
Mean + Smoothing + 2nd derivative	165	588-1091 nm	16	0.84	7.48
SNV+ Smoothing + 1st derivative	165	588-1091 nm	5	0.87	6.63
SNV+ Smoothing + 2nd derivative	165	588-1091 nm	7	0.86	6.86

F = Factors, R= correlation coefficient, RMSECV= root mean square error of cross validation, Smoothing = Savitzky-Golay smoothing, 1st derivative = Savitzky-Golay first derivative and MSC = multiplicative scatter correction pretreatment

Calibration models for Haugh unit by interactance NIRs was established using the above-mentioned pretreatments (combination smoothing and first derivative). The PLSR calibration and prediction results for prediction Haugh unit by interactance NIRS are shown in Table 4.5. The results of calibration and prediction obtained good accuracy (R= 0.91, RMSEC=5.69 and R=0.91, RMSEP=5.64). These results were corresponding to the published report for classification of eggs based on storage time at 1-3 days, 4-9 days and 5-14 days which the accuracy was presented by 92.4% in calibration set and 91.4% in prediction set (Hao et al., 2011). In addition, the results for Haugh unit prediction of published reports were corresponding to this experiment. The accuracy of published reports were presented by R=0.879 and RMSEP=2.443 (Hao et al., 2011).The result of this experiment meaning that the PLSR model could be usable with caution for most

This material is reserved for educational use only, not allowed for commercial use.
Forbidden to modify the content, and cite the document when use

applications (Williams 2007). All results of this experiment showed high R and low RMSEP which was possible to predict Haugh unit for online application.

Table 4.5 PLSR calibration and prediction results for prediction Haugh unit by interactance NIRs.

Items	Calibration set	Prediction set
Pretreatment	Smoothing + Fist derivative	Smoothing + Fist derivative
N	165	82
F	8	8
R	0.91	0.91
RMSEC	5.69	-
RMSEP	-	5.64
RPD	-	2.49

F = Factors, N=number of samples, R= correlation coefficient, RMSEC= root mean square error of calibration, RMSEP= root mean square error of prediction and RPD = ratio of prediction to deviation

Figure 4.4 shows the scattered plots of the actual values and predicted values of Haugh unit in the calibration set and prediction set which were acquired by PLSR calibration model. The R value between the actual and the predicted in the calibration set and prediction set as well as the RMSEC value and RMSEP value were satisfied. The Haugh unit was predicted with R of 0.91 in the calibration set and prediction set. The values of RMSEP represented the standard deviation of the differences between the predicted and actual values of Haugh unit in the prediction set. The low value of RMSEP and high value of R indicated a good performance of the PLSR model in prediction. Considering these results, it showed clearly demonstrated that the model as shown in Figure 4.4 had a good accuracy in predicting Haugh unit.

This material is reserved for educational use only, not allowed for commercial use.
Forbidden to modify the content, and cite the document when use

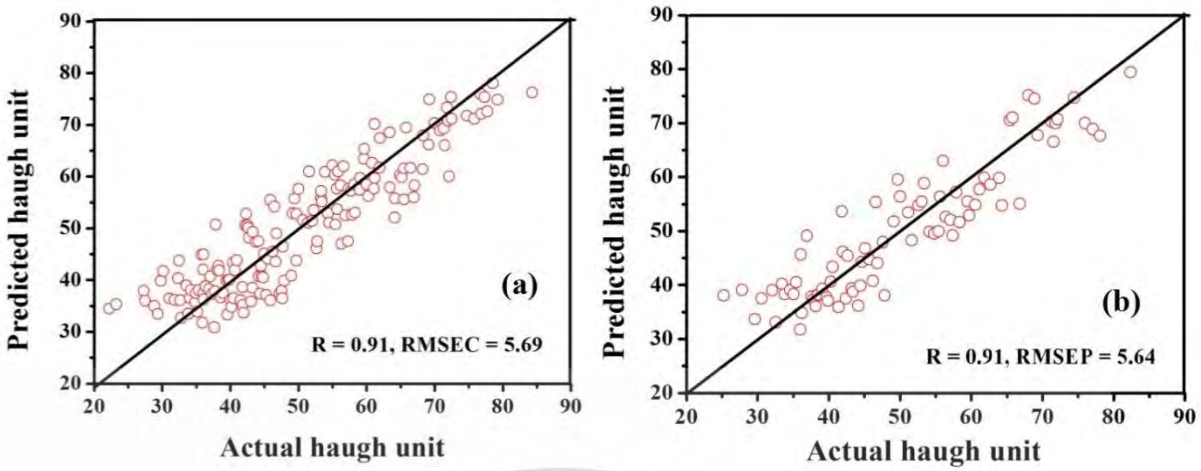

Figure 4.4 Predicted and actual values for Haugh unit by interactance NIRs

(a) in the calibration set

(b) in the prediction set

4.3.2 Calibration model for Haugh unit by reflectance NIRs

Table 4.6 shows statistical characteristics of samples in the calibration set and the prediction set for quantitative analysis. The spectra in every wavelength were used as independent variables while Haugh unit was used as the dependent variable. The calibration set (102 samples) was used to build the model while the prediction set (48 samples) was used to test the robustness of the model. To avoid bias between calibration set and prediction set; all samples had been sorted according to value Haugh unit. After that, all samples were divided to the calibration and prediction set. The prediction set were chosen one spectrum of every three samples. Finally, the calibration set contained 102 spectra while the prediction set contained 48 spectra. The standard deviation and of Haugh unit was quite similar in the calibration and prediction set. It was shown in the table 4.6.

Table 4.6 Statistical characteristics of samples in the calibration set and the prediction set for reflectance NIRs.

Items	Calibration set	Prediction set
number of samples	102	48
Range	23.4-83.38	29.63-77.72
Mean	49.53	49.43
SD	13.01	12.70
wavelength	1000-2500 nm	1000-2500 nm

SD = standard deviation

This material is reserved for educational use only, not allowed for commercial use.
Forbidden to modify the content, and cite the document when use

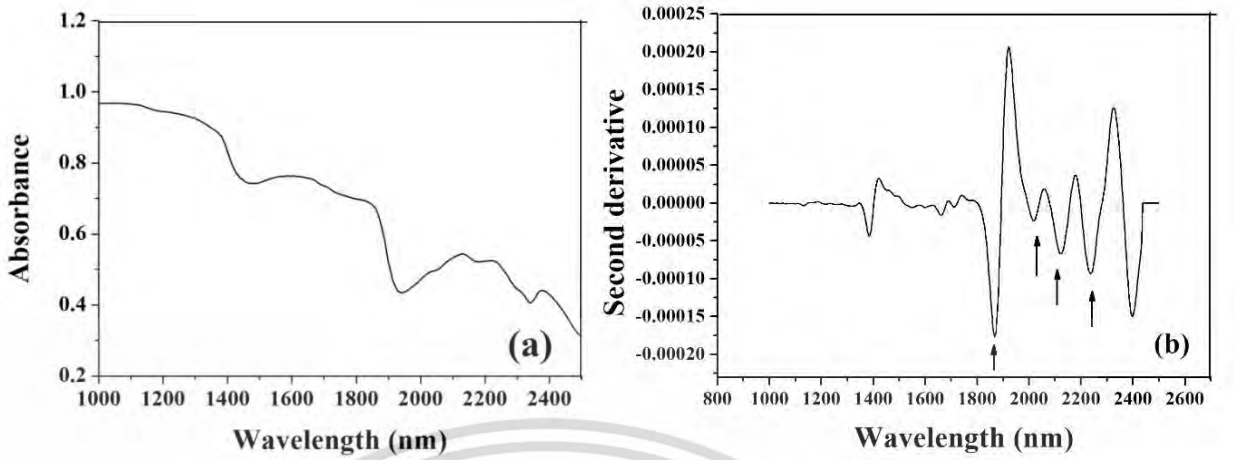

Figure 4.5 Average original spectra and second derivative of samples which were measured with the FT-NIR spectrophotometer (NIR Flex N-500).

(a) original spectra

(b) second derivative

Figure 4.5 shows the average original spectra and second derivative spectra of egg samples with the different Haugh unit. They were clear different between the original spectra and the second derivative spectra. Several clear absorption bands of the second derivative spectra were observed at 2060 nm that related to protein absorption (Berzaghi et al., 2005). The peaks were 2136 nm and 2298 nm that related to C-H combination tones (Cozzolino et al., 2002; Hoving-Bolink et al., 2005).

The spectral pretreatments were test during establishing of the calibration model. The statistical spectral pretreatments for prediction of Haugh unit by reflectance NIR in the wavelength range of 1000 - 2500 nm are shown in Table 4.7. Spectral pretreatments were investigated to improve the predictability. Spectra pretreatments such as smoothing, first derivative, second derivative, mean, MSC, SNV and different combinations of these treatments were evaluated. From the Table 4.7, the MSC pretreatments obtained the best results (highest R and lowest RMSECV). The R of MSC pretreatment was 0.82 while RMSECV was 7.27. In Table 4.7, MSC spectra pretreatment of hen egg obtained the optimum results for the model, then it implied that it was applied to reduce scattering due to refraction of brown from the egg shell.

This material is reserved for educational use only, not allowed for commercial use.
Forbidden to modify the content, and cite the document when use

Table 4.7 Statistical results of spectral pretreatments for prediction of Haugh unit by reflectance NIRs.

Spectral pretreatments	N	Wavelength	F	R	RMSECV
Original	102	1000-2500 nm	7	0.81	7.49
smoothing	102	1000-2500 nm	7	0.81	7.55
1^{st} derivative	102	1000-2500 nm	5	0.77	8.18
2^{nd} derivative	102	1000-2500 nm	3	0.79	7.98
Mean	102	1000-2500 nm	7	0.81	7.52
MSC	102	1000-2500 nm	8	0.82	7.27
SNV	102	1000-2500 nm	7	0.79	7.90
Smoothing + 1^{st} derivative	102	1000-2500 nm	7	0.78	8.17
Smoothing + 2^{nd} derivative	102	1000-2500 nm	4	0.77	8.17
Mean + Smoothing + 1^{st} derivative	102	1000-2500 nm	5	0.78	8.05
Mean + Smoothing + 2^{nd} derivative	102	1000-2500 nm	5	0.76	8.46
SNV+ Smoothing + 1^{st} derivative	102	1000-2500 nm	6	0.75	8.56
SNV+ Smoothing + 2^{nd} derivative	102	1000-2500 nm	5	0.75	8.68

F = Factors, R= correlation coefficient, RMSECV= root mean square error of cross validation, Smoothing = Savitzky-Golay smoothing, 1^{st} derivative = Savitzky-Golay first derivative and MSC = multiplicative scatter correction pretreatment

In Table 4.8, it is reported the results of PLSR model for calibration and prediction. Haugh unit by interactance NIRs, the accuracy of the model was evaluated on the basis of the R values (Williams and Sobering, 1996). The R showed correlation of the percentage variation in the Y variable (Haugh unit) that was accounted by the X variables (spectra). The R values above 0.80 indicated that it could be used for screening and approximate quantitative predictions (Williams, 2007). Model with R value at 0.87 could be used to predict Haugh unit, and the results of prediction obtained good quantitative information (R = 0.83). In Figure 4.6, it shows the results between the predicted value and actual value of the Haugh unit. The PLSR model could be used to predict the Haugh unit that was presented in the scatter plots as shown in Figure 4.6(a) and 4.6(b).

This material is reserved for educational use only, not allowed for commercial use.
Forbidden to modify the content, and cite the document when use

Table 4.8 PLSR calibration and prediction results for prediction Haugh unit by interactance NIRs.

Items	Calibration set	Prediction set
Pretreatment	MSC	MSC
N	102	48
F	8	8
R	0.87	0.83
RMSEC	6.32	-
RMSEP	-	7.11
RPD	-	1.78

F = Factors, N=number of samples, R= correlation coefficient, RMSEC= root mean square error of calibration, RMSEP= root mean square error of prediction and RPD = ratio of prediction to deviation

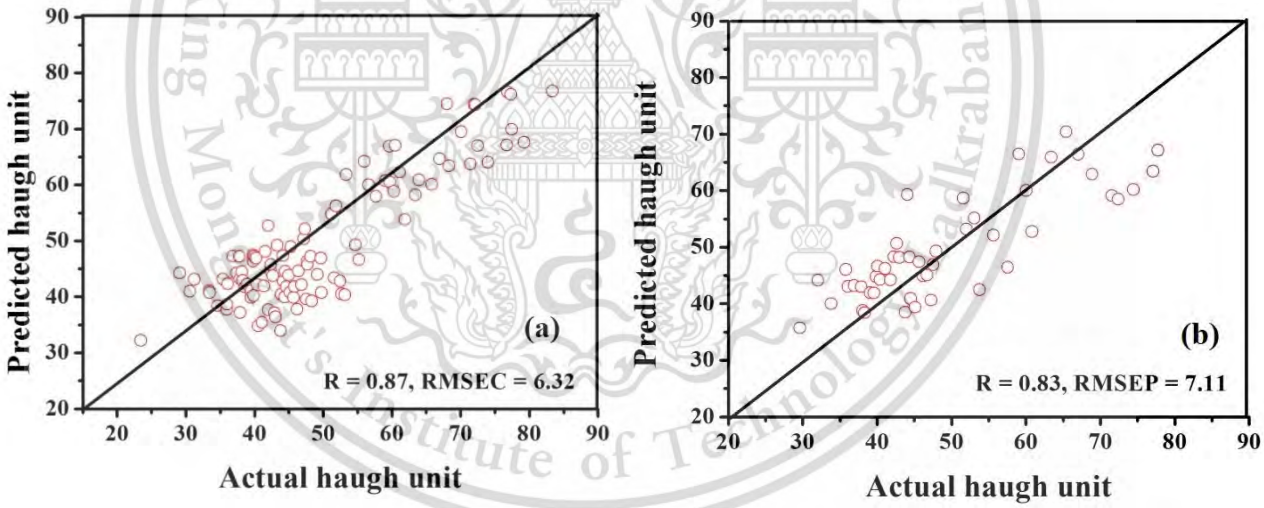

Figure 4.6 Predicted and actual values for Haugh unit by reflectance NIRs

(a) in the calibration set

(b) in the prediction set

4.3.3 Calibration model for Haugh unit by hyperspectral image NIRs

4.3.3.1 Data acquisition

Averaged spectra of samples with different freshness are shown in Figure 4.7. Samples of fresh eggs and unfresh eggs were completely separated by high Haugh unit (62.41-

This material is reserved for educational use only, not allowed for commercial use.
Forbidden to modify the content, and cite the document when use

80.57) and low Haugh unit (17.29-60.64) respectively. Hyperspectral imaging data in the wavelength ranged 900-1700 nm of fresh eggs (≥60 of Haugh unit) and unfresh eggs (<60 of Haugh unit) were considered by the averaged original spectra (Figure 4.7a) and also by the second derivative spectra (Figure 4.7b) which could be presented more information and clearly divided peaks of chemical components on the spectra. The second derivative spectra showed water peak at 1450 nm (Osborne et al., 1993), protein (N-H functional group) peak at 1,020 nm and oil peaks at 1151 nm (Ortiz-Somovilla et al., 2007)

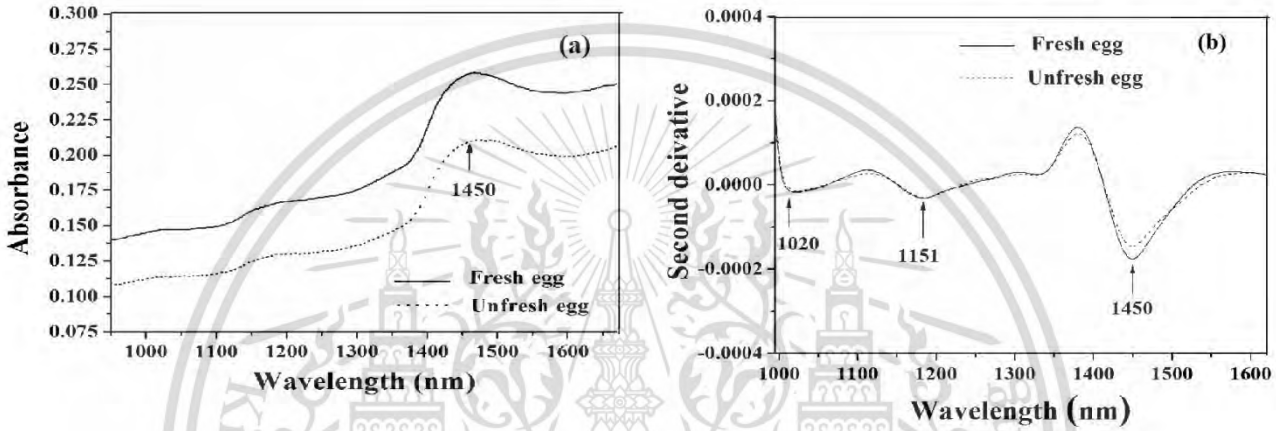

Figure 4.7 Average absorbance spectra of samples in two groups with different freshness

(a) Original spectra

(b) Second derivative spectra

The acquired absorbance spectra contained many peaks which occurred due to the vibration energy of compositions in the scanned material. In reflectance NIR spectroscopy, the light penetration depth was 2-4 mm. In this reason, the light could pass through eggshell and get information inside of egg. Therefore protein and oil showed in the acquired spectra. Due to eggshell didn't relate to Haugh unit of hen egg and it couldn't see peaks of calcium carbonate in this study. Haugh unit was related to two main variables such as the thickness of albumen and the weight which were corresponding to the freshness of hen egg. The water content inside egg was evaporated and passed through the shell during storage time therefore its weight was decreased (Romanoff and Romanoff, 1949). It could be described by consideration of absorbance peak of water. The absorbance at 1450 nm of fresh eggs and unfresh eggs were clearly different. The average original spectra of fresh eggs at the peak of 1450 nm appeared higher absorbance when compared to unfresh eggs as well as the average second derivative spectral of fresh eggs at 1450 nm showed clear higher opposite peak than unfresh eggs. It implied that fresh eggs contain more

This material is reserved for educational use only, not allowed for commercial use.
Forbidden to modify the content, and cite the document when use

water or higher weight than those of unfresh eggs. The most composition of albumen is protein and the most composition yolk is lipid. The peak of protein and in fresh egg and unfresh egg is slightly different. Due to the thick albumen is loss structure and becomes to liquefaction of albumen in during storage time. Yuceer and Caner (2014) explained that the protease enzymes were depolymerized by hydroxyl ions at high pH and interaction between ovomucin-lysozyme will be change. These affects with thick albumen, then thick albumen becomes thinner and HU values will decrease. In addition, the valtelline membrane of yolk in fresh egg and unfresh egg is different in during storage time. The fresh egg will has vatelline membrane on the surface of yolk. The vitelline membrane in fresh egg is composed of fibers connected to the chalaziferous layer. During storage, the fibers network disappear and the strength of vitelline membrane decrease (Stadelman and Cotterill, 1995). Yolk will become flat. Therefore, fresh eggs have high yolk and unfresh eggs have flat yolk. These are the reasons why peak of lipid and protein are slightly different.

4.3.3.2 Establishment of the calibration model and prediction of Haugh unit

Haugh unit of samples were acquired and presented in Table 4.9. A set of 58 samples were used for the calibration set and the prediction set contained 33 samples. Haugh unit of samples in the prediction set were in the range of samples' Haugh unit in the calibration set. A minimum and maximum value of Haugh unit from the experiment in the calibration set covered the minimum and maximum value in the prediction set. It indicated that the distribution of the Haugh unit value in the calibration set was a suitable to build the calibration model for prediction. The region of interest (ROI) of the image in each sample (50×90 pixels) was investigated. Each ROI contained absorbance spectra from hyperspectral imaging data in the wavelength ranged 900-1700 nm. Spectra in each ROI was average and then used as a representative of each sample for analysis. The calibration model for Haugh unit was established using PLSR. Haugh units of samples in the calibration set was varied from 17.29-83.64 that were minimum and maximum value of Haugh unit in this experiment. While Haugh unit of samples in the prediction set were varied from 17.82-80.57 as shown in Table 4.9.

This material is reserved for educational use only, not allowed for commercial use.
Forbidden to modify the content, and cite the document when use

Table 4.9 Statistical characteristics of samples Haugh unit in the calibration set and the prediction set for measurement in the wavelength range 900-1700 nm.

Items	The calibration set	The prediction set
Number of samples	58	33
Range	17.29-83.64	17.82-80.57
Mean	43.52	42.18
SD	19.44	19.34
Wavelength	900-1700 nm	900-1700 nm

SD = standard deviation

Spectral pretreatments of averaged spectra in the calibration set were investigated as shown in Table 4.10 The SNV spectral pretreatment obtained the best results (R=0.92 and RMSECV=5.79) for the establishment of the calibration model for Haugh unit. Therefore, the calibration model using SNV spectral pretreatment (R=0.95 and RMSEC = 4.58) was acquired and carried out for prediction. Measured Haugh unit and predicted Haugh unit of samples in the calibration set were plotted as shown in Table 4.11 and Figure 4.8 (a). In order to present accuracy for prediction Haugh unit value, SNV spectra pretreatment of the prediction set contains 33 samples which used to test the robustness of model. The prediction result was plotted between actual value from and predicted values which presented in Figure 4.8 (b). The results obtained good accuracy (R=0.92, RMSEP = 6.29 and RPD = 3.07) for the prediction of Haugh unit value.

This material is reserved for educational use only, not allowed for commercial use.
Forbidden to modify the content, and cite the document when use

Table 4.10 Statistical results for prediction of Haugh unit with difference techniques of spectral.

Spectral pretreatments	N	Wavelength	F	R	RMSECV
Original	58	900-1700 nm	3	0.92	5.91
Smoothing	58	900-1700 nm	6	0.89	6.77
1st derivative	58	900-1700 nm	7	0.86	7.73
2nd derivative	58	900-1700 nm	3	0.85	7.85
MSC	58	900-1700 nm	7	0.91	6.11
SNV	58	900-1700 nm	6	0.92	5.79

F = Factors, R= correlation coefficient, RMSECV= root mean square error of cross validation, Smoothing = Savitzky-Golay smoothing, 1st derivative = Savitzky-Golay first derivative and MSC = multiplicative scatter correction pretreatment

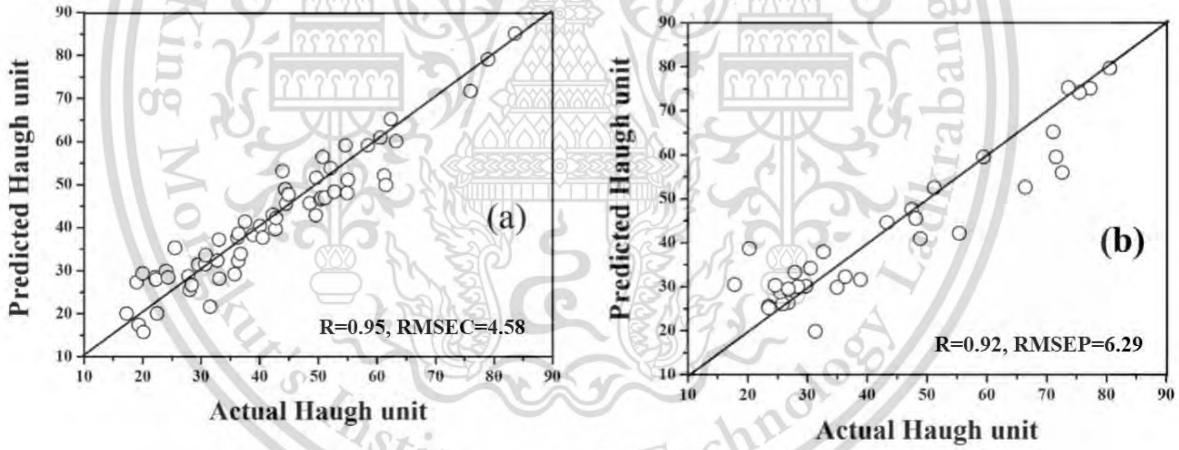

Figure 4.8 Scattered plots of measured Haugh unit and predicted Haugh unit

(a) in the calibration set.

(b) in the prediction set

This material is reserved for educational use only, not allowed for commercial use.
Forbidden to modify the content, and cite the document when use

Table 4.11 PLSR calibration and prediction results for prediction Haugh unit in the wavelength range 900-1700 nm.

Items	Calibration set	Prediction set
Pretreatment	SNV	SNV
N	58	33
F	6	6
R	0.95	0.92
RMSEC	4.58	-
RMSEP	-	6.29
RPD	-	3.07

F = Factors, N=number of samples, R= correlation coefficient, RMSEC= root mean square error of calibration, RMSEP= root mean square error of prediction and RPD = ratio of prediction to deviation

4.3.3.3 Distribution map of Haugh unit value

The calibration model from the SNV spectral pretreatment was used for determining of Haugh unit in every pixel of images for prediction. The prediction of Haugh unit in all spots of each sample's image in the prediction set was the final step. The acquired image by prediction of Haugh unit related to a linear color scale at all spots of each sample was generated which was called the distribution map. The distribution map explained the linear color scale which defined for showing the difference of Haugh unit. The value of Haugh unit was related to the linear color scale, therefore Haugh unit in each pixel was predicted and transferred to color. Distribution map of samples based on predicted Haugh unit and the linear color scale at each pixel which obtained in different colors was shown at Figure 4.9. Highest value of predicted Haugh unit was presented by red color as well as the lowest value of predicted Haugh unit was presented by blue color. Other colors of predictive image in the linear color scale were changed according to the level of predicted Haugh unit. Figure of distribution map shows red, blue and other colors which were spread throughout the image based on the predicted Haugh unit. Due to the weight of each color in each image was different related to Haugh unit of each sample, it implied that each sample was different in the functional properties of both egg yolk and egg albumen. During storage time, water content was loss by water evaporation through the egg shell.

This material is reserved for educational use only, not allowed for commercial use.
Forbidden to modify the content, and cite the document when use

This process was the reason of the decreasing egg weight. The loss of water content was effect with distribution maps of colors for predicted Haugh unit. The freshness of eggs could be predicted by considering colors of image. The fresh eggs contained more red color while the unfresh eggs contain more blue color. In the method of during measurement, each hen egg was placed on tray and moved by stepper motor at a constant speed of 33 mms^{-1}. The line in distribution maps might be caused by scanning speed. If reduce the scanning speed, distribution maps for predicted Haugh unit might not show the line. The compositions of the eggshell are calcium carbonate (94%), calcium phosphate (1%), magnesium carbonate (1%) and organic substances (4%). Therefore, the main component is calcium carbonate (Thapon and Bourgeois, 1994). The calcium carbonate has a strong absorbance at 2,550 and 2,350 nm (Workman, J., Weyer, L., 2012). Due to samples were scanned in the wavelength range of 900-1700 nm in this study, then we didn't see peaks of the calcium carbonate. But the distribution maps showed the blue border around the predictive image of eggs, its maybe colors of calcium carbonate.

A set of 33 samples was used for evaluation of prediction performance by consideration at the acquired predictive images based on Haugh unit and the linear color scale compared to real freshness of hen eggs in order to classify the freshness of eggs.

Generally in practice, the group of fresh eggs and unfresh eggs cannot be identified by the normal vision. But the distribution maps from the results of hyperspectral imaging technique based on Haugh unit can be used to classify the freshness of egg by visual inspection of color on the acquired image. It may be applied by paying attention to only red color in order to select only the fresh hen eggs. Due to as a result of the light penetrated through albumen the acquired spectra contained information of albumen that related to Haugh unit in each pixel. The predicted image showed irregular colors in each part of each egg, which implied that the quality of albumen in each part of egg was non-homogeneous. However, overall colors of the images from different storage times between fresh and unfresh eggs were clearly different. However it can be used the acquired predictive value from the predictive image compared to the cut off value, in order to classify groups of fresh eggs and unfresh eggs. These results demonstrated that hyperspectral imaging system has a potential to use in the online system in order to classify the freshness of hen eggs.

This material is reserved for educational use only, not allowed for commercial use.
Forbidden to modify the content, and cite the document when use

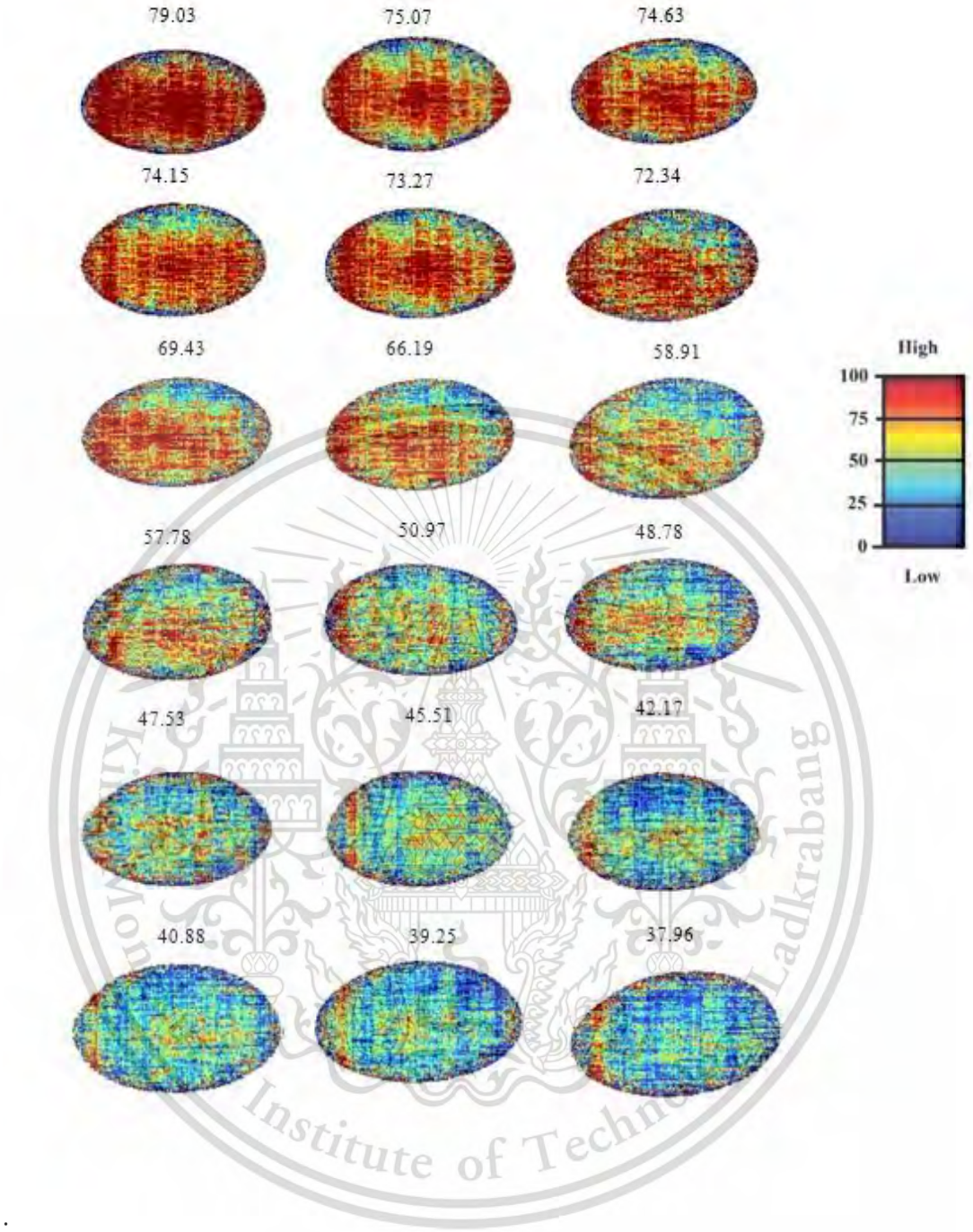

.

This material is reserved for educational use only, not allowed for commercial use.
Forbidden to modify the content, and cite the document when use

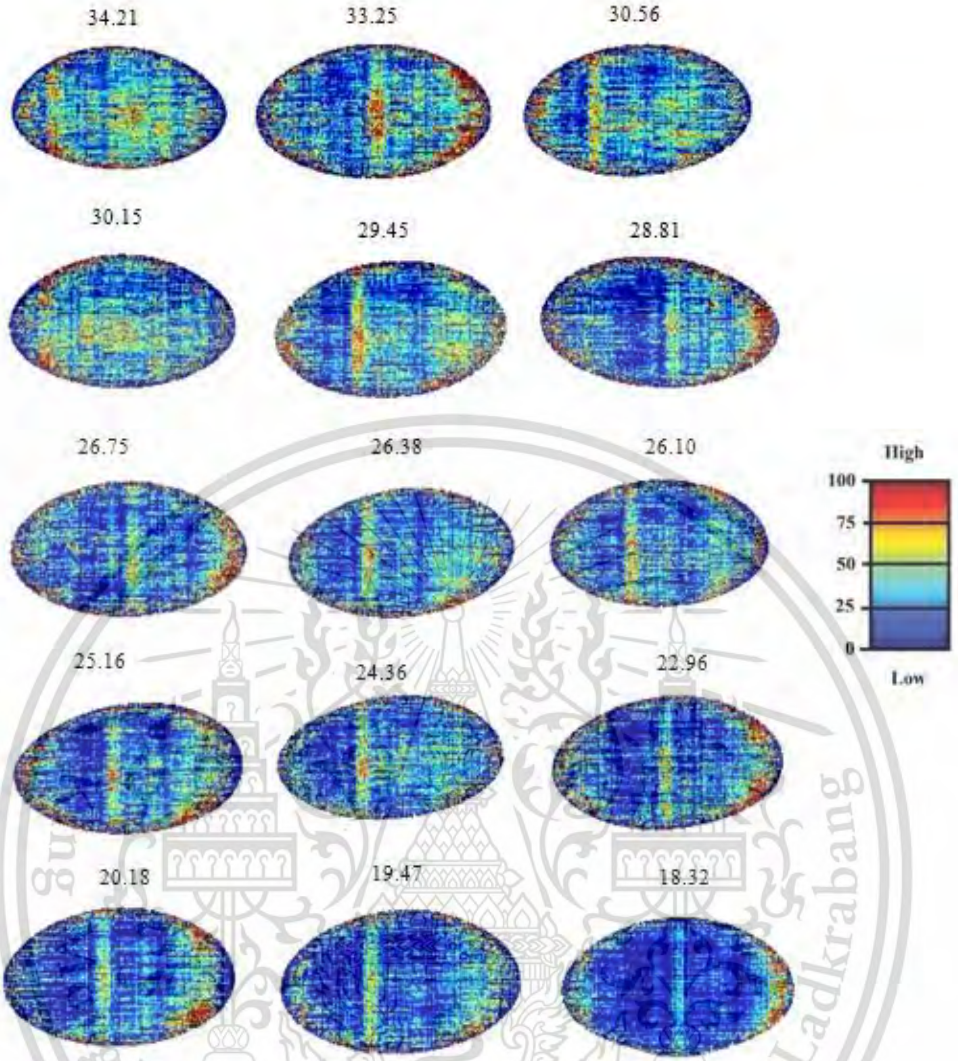

Figure 4.9 Distribution maps of colors for predicted Haugh unit in hen eggs.

4.4 An experiment to evaluate the freshness of sweet corns

Definition of sweet corns is corns with sweetness. The total soluble solid content is not less than 9 degrees of brix. The kernel shall be on the cob and sweet corns shall be whole with or without husk (National Bureau of ACFS, 2012). The quality (total soluble solids content, hardness value and moisture content) of sweet corns depends on its storage time after harvest. Sweet corns shall be transported and processed within 24 hours after harvest because sweet corns will become hard and less sweet. To evaluate the freshness of sweet corns in this study, corns will be divided into two parts. First part, evaluate the freshness of sweet corns with husk. Other part, evaluated the freshness of sweet corns without husk.

This material is reserved for educational use only, not allowed for commercial use.
Forbidden to modify the content, and cite the document when use

4.4.1 Calibration models for quality of sweet corns with husk and without husk by interactance NIRs

The average raw spectra of sweet corns with husk and sweet corn without husk shown in Figure 4.10. Average absorbance of sweet corns with husk was presented by red line color as well as average absorbance of sweet corns without husk was presented by black line color. The absorbance spectra of sweet corns with husk and sweet corns without husk showed a similar profile with absorbance at 978 nm. This absorbance is related with moisture content in the sample (Cozzolino et al., 2002; Ortiz- Somovilla et al., 2007). The absorbance spectra of sweet corns with husk and sweet corns without husk showed a different profile with absorbance at 650 nm. This absorbance was in the range of the visible wavelength. Absorbance at 650 nm might be the chlorophyll pigments of husk. This was similar to the published report for evaluation of defect pods for greens soybean (Sirisomboon et al., 2009). In addition, chlorophyll pigments absorbance of fruit was found at 960 nm (Abbott et al., 1997; Chauchard et al., 2004). It is clear that the spectra absorbance of moisture content and chlorophyll pigments are shown in Figure 4.10. It was not clear in some peaks of absorbance spectra. The true peaks were identified after doing the second derivatives spectral pretreatment. Average second derivative absorbance spectra of samples are shown in Figure 4.11. The moisture absorbance was found at 760 and 830 nm; oil absorbance was found at 964 nm; and protein absorbance was found at 1175 nm (Osborne et al., 1993). Due to sweet corns with husk and without husk having different colors, the spectral features between sweet corns with husk and without husk were different in the range of the visible wavelength.

This material is reserved for educational use only, not allowed for commercial use.
Forbidden to modify the content, and cite the document when use

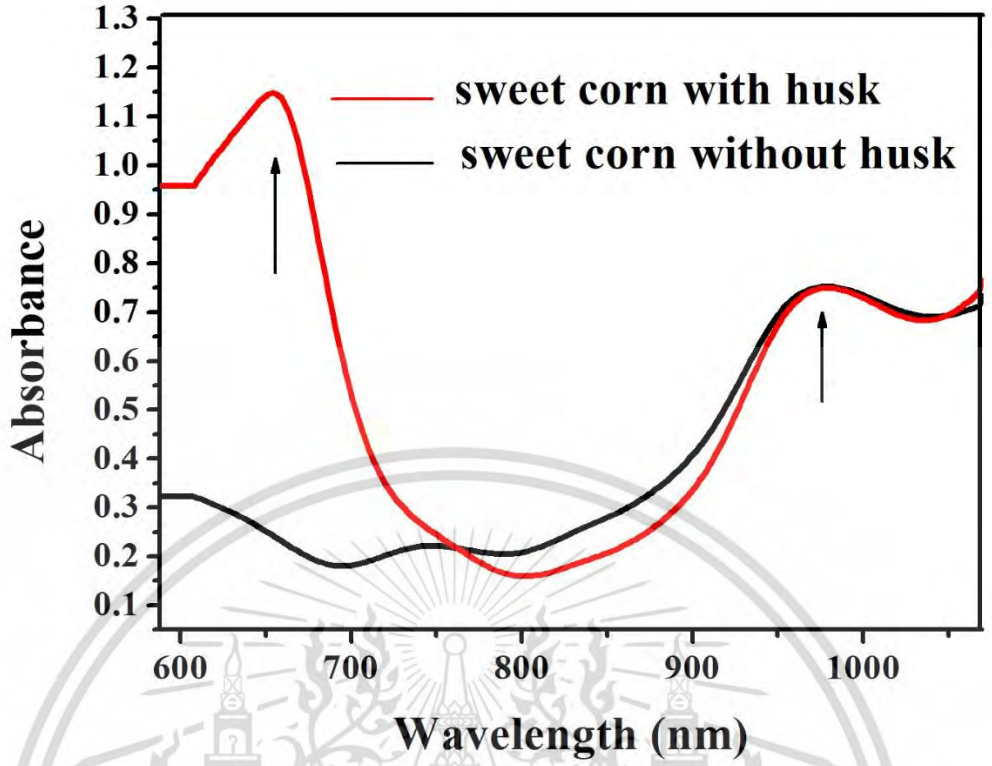

Figure 4.10 Averaged absorbance spectra of samples (sweet corns with husk and sweet corns without husk).

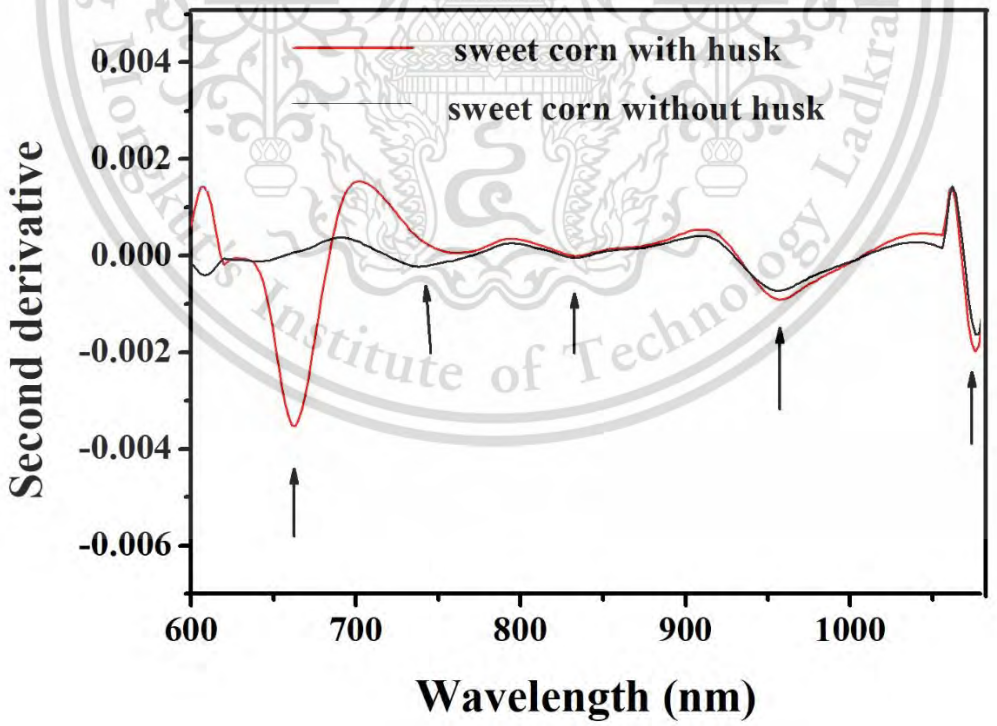

Figure 4.11 Average second derivative absorbance spectra of samples (sweet corns with husk and sweet corns without husk).

This material is reserved for educational use only, not allowed for commercial use.
Forbidden to modify the content, and cite the document when use

4.4.1.1 Calibration model for predicting total soluble solids content of sweet corns

Statistical characteristics of samples (sweet corns with husk and sweet corns without husk) in the calibration set and the prediction set are shown in Table 4.12. Acquired spectra of 180 spectra from 180 samples were prepared to two sets which were used for the in the calibration set and the prediction set. The statistics (range, mean and standard deviation) of each data set for total soluble solids content in the calibration set and prediction set are listed in Table 4.12.

Table 4.12 Statistical characteristics of soluble solids content of samples (sweet corns with husk and sweet corns without husk) in the calibration set and the prediction set for interactance NIRs.

Items	Sweet corns with husk		Sweet corns without husk	
	Calibration set	Prediction set	Calibration set	Prediction set
Number of samples	120	60	120	60
Range (%Brix)	12.2-21	12.5-20.1	12.2-21	12.5-20.1
Mean (%Brix)	16.21	16.27	16.21	16.27
SD	2.00	1.94	2.00	1.94
Wavelength	588-1091 nm	588-1091 nm	588-1091 nm	588-1091 nm

SD = standard deviation

Spectra of sweet corns with and without husk in wavelength range 588-1091 nm were investigated by spectra pretreatments and then calibration models were developed by cross-validation. Smoothing spectral pretreatment of sweet corns with husk obtained the best results of cross-validation in the calibration set (R=0.70, RMSECV=1.45°Bx) as shown in Table 4.13. For establishment the calibration models of sweet corn without husk, MSC spectra pretreatment of sweet corn without husk was used to predict total soluble solid content (R=0.76, RMSECV=1.26°Bx).

This material is reserved for educational use only, not allowed for commercial use.
Forbidden to modify the content, and cite the document when use

Table 4.13 Statistical results of spectral pretreatments for prediction of total soluble solids content in sweet corns with husk and sweet corns without husk

Spectral pretreatments	N	Sweet corns with husk			Sweet corns without husk		
		F	R	RMSECV (°Bx)	F	R	RMSECV (°Bx)
Original	120	15	0.68	1.50	12	0.70	1.47
Smoothing	120	15	0.70	1.45	12	0.75	1.30
1st derivative	120	12	0.69	1.49	8	0.74	1.33
2nd derivative	120	13	0.68	1.51	9	0.69	1.50
Mean	120	14	0.69	1.50	12	0.75	1.29
MSC	120	14	0.69	1.50	11	0.76	1.26
SNV	120	16	0.70	1.46	8	0.74	1.32
Smoothing + 1st derivative	120	15	0.70	1.47	12	0.74	1.33
Smoothing + 2nd derivative	120	16	0.70	1.49	2	0.71	1.42
Mean + Smoothing + 1st derivative	120	15	0.70	1.49	5	0.71	1.44
Mean + Smoothing + 2nd derivative	120	16	0.69	1.50	5	0.70	1.46
SNV+ Smoothing + 1st derivative	120	15	0.69	1.50	9	0.75	1.30
SNV+ Smoothing + 2nd derivative	120	16	0.68	1.53	4	0.72	1.40

This material is reserved for educational use only, not allowed for commercial use.
Forbidden to modify the content, and cite the document when use

Table 4.14 PLSR calibration and prediction results for prediction of total soluble solid content in (sweet corns with husk and sweet corns without husk)

	Sweet corns with husk		**Sweet corns without husk**	
Items	**Calibration set**	**Prediction set**	**Calibration set**	**Prediction set**
Pretreatment	Smoothing	Smoothing	MSC	MSC
N	120	60	120	60
F	15	15	11	11
R	0.83	0.77	0.84	0.84
RMSEC	1.10	-	1.05	-
RMSEP	-	1.23	-	1.07
RPD	-	1.58	-	1.81

The accuracy of prediction for total soluble solids content in calibration set and prediction set by regression are shown in Table 4.14. The accuracy result for prediction total soluble solids content in sweet corns without husk using smoothing obtained the good result (R = 0.84, RMSEP = 1.07^{o}Bx), while the accuracy of the model for prediction total soluble solids content in sweet corns without husk using MSC obtained unsatisfied results (R = 0.77, RMSEP = 1.23^{o}Bx). Comparisons between results of used NIRs to scan sweet corns without husk and sweet corns with husk, sweet corns without husk obtained better accuracy because the husk of the sweet corns was affected to its accuracy. These results were similar to the model for predicting soluble solids content in watermelon (Jie et al., 2014). The watermelon had the thick rind that had the effect on accuracy to predicting total soluble solids content. The result for predicting total soluble solids content of watermelon obtained poor result (correlation of prediction was 0.70). However, to compare between results of used NIRs to predict total soluble solids of sweet corns with husk and watermelon, it could be clear that the accuracy of the model for predicting total soluble solids content for sweet corns with husk had a better result.

Scatter plots are used to display correlations between actual total soluble solid content and predicted total soluble solid content as shown in Figure 4.12. It could be clearly seen that the accuracy for predicting total soluble solids content of sweet corns without husk obtained better accuracy.

This material is reserved for educational use only, not allowed for commercial use.
Forbidden to modify the content, and cite the document when use

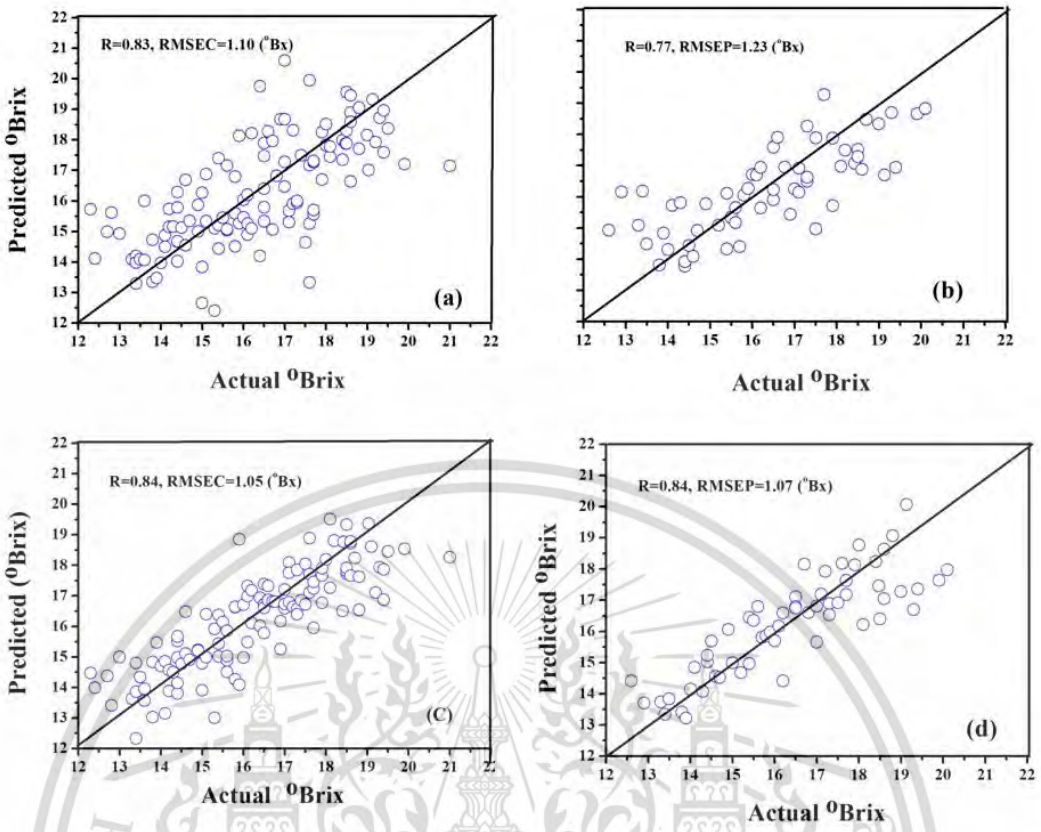

Figure 4.12 Predicted and actual values for total soluble solids content by interactance NIRs.

(a) in the calibration set of sweet corns with husk

(b) in the prediction set of sweet corns with husk

(c) in the calibration set of sweet corns without husk

(d) in the prediction set of sweet corns without husk

4.4.1.2 Calibration model for predicting the hardness of sweet corns

Table 4.15 shows the summary statistics for the calibration and prediction models for the prediction of the hardness of sweet corns with/without husk. The total of samples was divided into two groups, the calibration group (103 samples) and the prediction group (54 samples). The unit of hardness was newton. The maximum and minimum of the hardness and their standard deviations were presented.

This material is reserved for educational use only, not allowed for commercial use.
Forbidden to modify the content, and cite the document when use

Table 4.15 Statistical characteristics of the hardness of samples (sweet corns with husk and sweet corns without husk) in the calibration set and the prediction set for interactance NIRs.

Items	Sweet corns with husk		Sweet corns without husk	
	Calibration set	**Prediction set**	**Calibration set**	**Prediction set**
Number of samples	103	54	103	54
Range (Newton)	10.45-13.73	10.45-13.72	10.45-13.73	10.45-13.72
Mean (Newton)	12.18	12.20	12.18	12.20
SD (Newton)	2.00	1.94	2.00	1.94
Wavelength	588-1091 nm	588-1091 nm	588-1091 nm	588-1091 nm

SD = standard deviation

In Table 4.16, spectral pretreatments are investigated for hardness prediction. It was shown the original spectra gave the good results (R=0.79, RMSECV=052 N). So, the original spectra were used to build the model for predicting the hardness of sweet corn with husk. To build the calibration model of sweet corns without husk, MSC spectra pretreatment of sweet corns without husk was used to predict the hardness (R=0.80, RMSECV=0.50 N).

This material is reserved for educational use only, not allowed for commercial use.
Forbidden to modify the content, and cite the document when use

Table 4.16 Statistical results of spectral pretreatments for prediction of the hardness in samples (sweet corns with husk and sweet corns without husk).

Spectral pretreatments	N	Sweet corns with husk			Sweet corns without husk		
		F	R	RMSECV (N)	F	R	RMSECV (N)
Original	103	13	0.79	0.52	12	0.79	0.51
Smoothing	103	13	0.79	0.52	12	0.79	0.51
1st derivative	103	13	0.77	0.53	11	0.76	0.54
2nd derivative	103	13	0.77	0.53	13	0.75	0.55
Mean	103	13	0.79	0.52	12	0.79	0.51
MSC	103	13	0.73	0.59	11	0.80	0.50
SNV	103	13	0.77	0.55	13	0.78	0.52
Smoothing + 1st derivative	103	11	0.78	0.53	13	0.78	0.53
Smoothing + 2nd derivative	103	13	0.79	0.52	13	0.78	0.53
Mean + Smoothing + 1st derivative	103	11	0.78	0.52	13	0.78	0.53
Mean + Smoothing + 2nd derivative	103	13	0.78	0.52	13	0.77	0.53
SNV+ Smoothing + 1st derivative	103	12	0.77	0.54	13	0.78	0.52
SNV+ Smoothing + 2nd derivative	103	13	0.78	0.53	12	0.77	0.53

The results of prediction for hardness in sweet corns with husk and sweet corns without husk are shown in Table 4.17. The comparisons between the accuracy for sweet corns with husk and sweet corns without husk were shown. The accuracy of prediction for sweet corns without husk was higher. The accuracy to predict sweet corns without husk gave the good results (R=0.81, RMSEP=0.47 N) while the accuracy to predict sweet corns with husk was reduced a little when compared the results of sweet corns with husk (R=0.80, RMSEP=0.40 N).

This material is reserved for educational use only, not allowed for commercial use.
Forbidden to modify the content, and cite the document when use

Table 4.17 PLSR calibration and prediction results for prediction of the hardness in samples (sweet corns with husk and sweet corns without husk).

	Sweet corns with husk		**Sweet corns without husk**	
Items	**Calibration set**	**Prediction set**	**Calibration set**	**Prediction set**
Pretreatment	Original	Original	MSC	MSC
N	103	54	103	54
F	13	13	11	11
R	0.87	0.80	0.87	0.81
RMSEC	0.40	-	0.40	-
RMSEP	-	0.47	-	0.44
RPD	-	4.13	-	4.41

The relationship between measured hardness value and predicted the hardness of sweet corns is shown in Figure 4.13. It was shown that the performance of the PLSR model from sweet corns with and without husk was good in calibration (Figure 4.13 a and c) while the accuracy for predicting hardness value of sweet corns without husk obtained better accuracy (Figure 4.13 d)

This material is reserved for educational use only, not allowed for commercial use.
Forbidden to modify the content, and cite the document when use

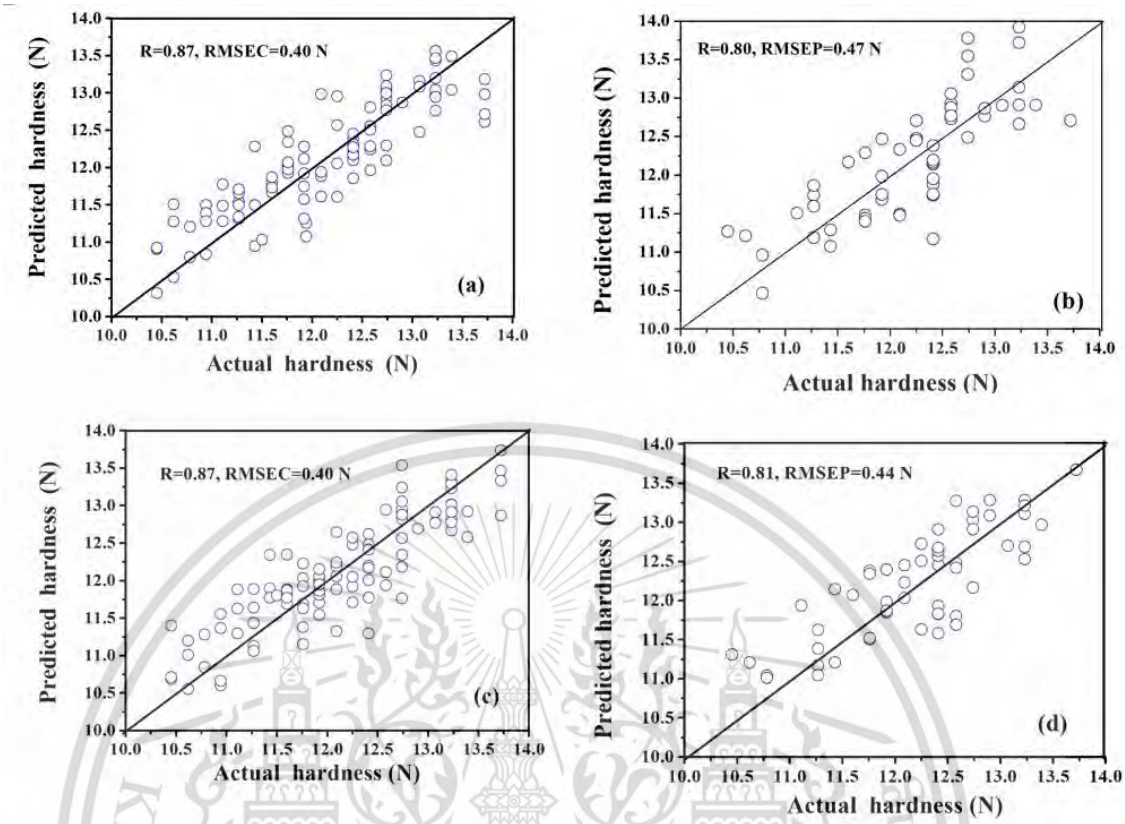

Figure 4.13 Predicted and actual values for hardness value by interactance NIRs.

(a) in the calibration set of sweet corns with husk

(b) in the prediction set of sweet corns with husk

(c) in the calibration set of sweet corns without husk

(d) in the prediction set of sweet corns without husk

4.4.1.3 Calibration model for predicting moisture content of sweet corns

The mean, range and standard deviation (SD) of moisture content in the sweet corn with/ without husk are shown in Table 4.18. The samples contained a wide range in moisture content of 10.34-15.0% in the calibration set and the wide range in moisture content of 10.38-14.9% in the prediction set. The relevant statistics for the moisture content in the sweet corns with/ without husk were presented.

This material is reserved for educational use only, not allowed for commercial use.
Forbidden to modify the content, and cite the document when use

Table 4.18 Statistical characteristics of samples (sweet corns with husk and sweet corns without husk) in the calibration set and the prediction set for interactance NIRs.

Items	Sweet corns with husk		Sweet corns without husk	
	Calibration set	**Prediction set**	**Calibration set**	**Prediction set**
Number of samples	105	45	105	45
Range (%)	10.34-15.0	10.38-14.9	10.34-15.0	10.38-14.9
Mean (%)	11.92	12.08	11.92	12.08
SD (%)	0.91	0.99	0.91	0.99
Wavelength	588-1091 nm	588-1091 nm	588-1091 nm	588-1091 nm

SD = standard deviation

Table 4.19 shows statistical results of spectral pretreatments for prediction of moisture content in samples (sweet corns with husk and sweet corns without husk). It showed that the prediction results of the sweet corns without husk had higher accuracy than the sweet corn with husk. The best model for moisture content of sweet corns with husk was obtained by using smoothing (R=0.65, RMSECV=0.69%) while the model for moisture content of sweet corns without husk was obtained by using SNV(R=0.75, RMSECV=0.59%).

The prediction results of moisture content in the sweet corns with husk and sweet corns without husk are shown in Table 4.20. The best results were from the sweet corns without husk obtained R=0.87 and RMSEC=0.45% while the prediction provided R=0.80 and RMSEP=0.52%. Accuracy of the sweet corns without husk for moisture content prediction using MSC obtained the best results while the accuracy of the sweet corns with husk for moisture content prediction using obtained the unsatisfied results R=0.71 and RMSEP=0.72%.

This material is reserved for educational use only, not allowed for commercial use.
Forbidden to modify the content, and cite the document when use

Table 4.19 Statistical results of spectral pretreatments for predicting moisture content in the samples (sweet corns with husk and sweet corns without husk).

Spectral pretreatments	N	Sweet corns with husk			Sweet corns without husk		
		F	R	RMSECV (%)	F	R	RMSECV (%)
Original	105	14	0.64	0.70	15	0.73	0.61
Smoothing	105	14	0.65	0.69	18	0.75	0.59
1st derivative	105	15	0.65	0.69	15	0.71	0.63
2nd derivative	105	12	0.63	0.71	12	0.74	0.60
Mean	105	14	0.64	0.70	16	0.75	0.59
MSC	105	13	0.64	0.70	14	0.75	0.59
SNV	105	14	0.64	0.70	17	0.75	0.59
Smoothing + 1st derivative	105	12	0.62	0.72	15	0.74	0.60
Smoothing + 2nd derivative	105	12	0.62	0.72	15	0.74	0.64
Mean + Smoothing + 1st derivative	105	13	0.64	0.70	15	0.71	0.63
Mean + Smoothing + 2nd derivative	105	12	0.62	0.72	14	0.74	0.60
SNV+ Smoothing + 1st derivative	105	12	0.62	0.72	13	0.74	0.60
SNV+ Smoothing + 2nd derivative	105	13	0.63	0.71	15	0.73	0.61

This material is reserved for educational use only, not allowed for commercial use.
Forbidden to modify the content, and cite the document when use

Table 4.20 PLSR calibration and prediction results for predicting moisture content in the sweet corns with husk and sweet corns without husk.

Items	Sweet corns with husk		Sweet corns without husk	
	Calibration set	**Prediction set**	**Calibration set**	**Prediction set**
Pretreatment	Smoothing	Smoothing	MSC	MSC
N	105	45	105	45
F	14	14	14	14
R	0.77	0.71	0.87	0.80
RMSEC	0.57	-	0.45	-
RMSEP	-	0.72	-	0.52
RPD	-	1.38	-	1.90

F = Factors, N=number of samples, R= correlation coefficient, RMSEC= root mean squares error of calibration, RMSEP= root mean square error of prediction and RPD = ratio of prediction to deviation

The relationship between measured moisture content and predicted moisture content of sweet corns are shown in Figure 4.14. It showed that the performance of the PLSR model from sweet corns with and without husk was satisfied in calibration (Figure 4.14 a and c) while the accuracy for predicting moisture content of sweet corns without husk obtained good results (Figure 4.14 d).

This material is reserved for educational use only, not allowed for commercial use.
Forbidden to modify the content, and cite the document when use

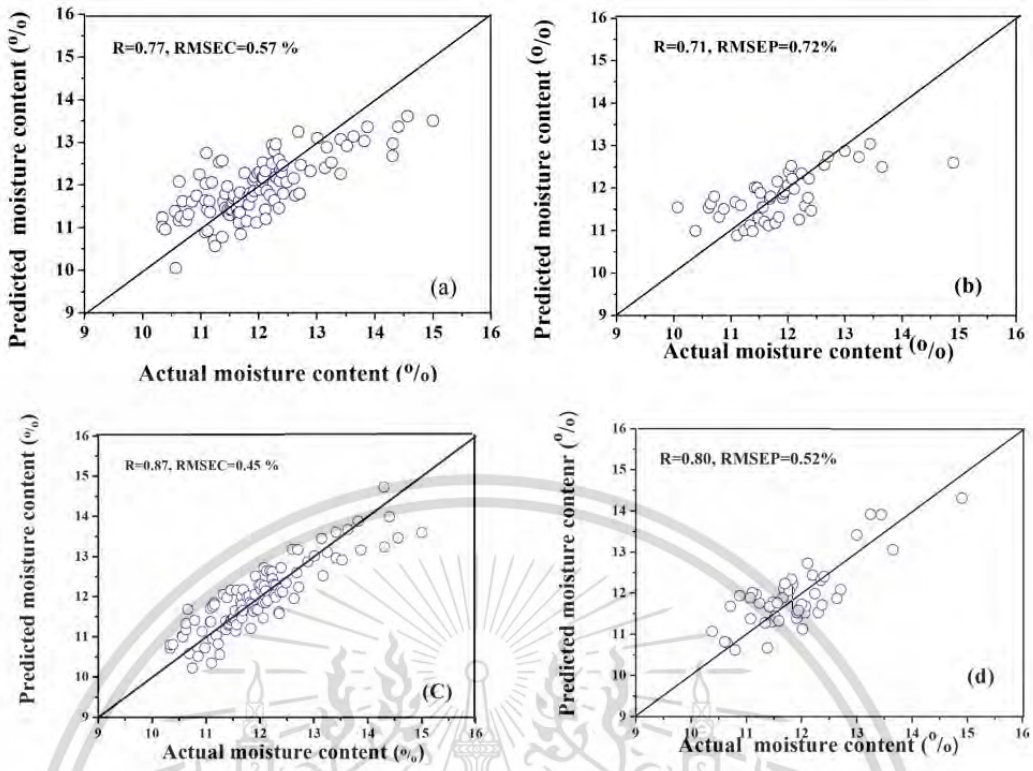

Figure 4.14 Predicted and actual values for moisture content by interactance NIRs.

(a) in the calibration set of sweet corns with husk

(b) in the prediction set of sweet corns with husk

(c) in the calibration set of sweet corns without husk

(d) in the prediction set of sweet corns without husk

4.4.2 Calibration model for quality of sweet corns with husk and without husk by reflectance NIRs

The averaged absorbance spectra of the sweet corns with husk and sweet corns without husk in the wavelength ranged 1000-2500 nm are shown in Figure 4.15.

This material is reserved for educational use only, not allowed for commercial use.
Forbidden to modify the content, and cite the document when use

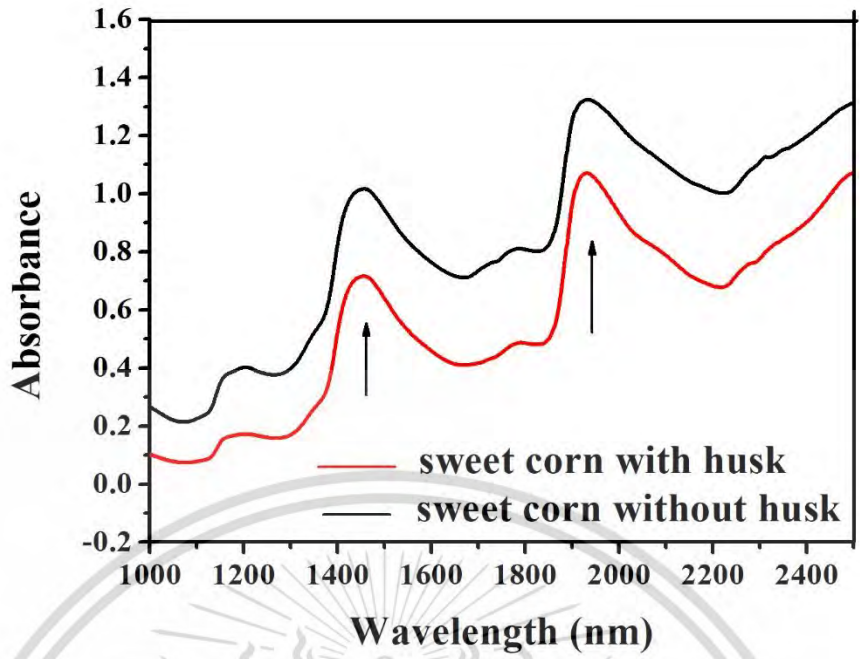

Figure 4.15 Averaged absorbance spectra of samples (sweet corns with husk and sweet corns without husk).

In Figure 4.15, it shows average raw spectra of the sweet corns with husk and sweet corns without husk. There were 2 lines (red and black). The red line was presented the sweet corns with husk while the black line was presented the sweet corns without husk. The absorbance of the sweet corns with husk had lower absorbance when compared with absorbance of the sweet corns without husk. In this case, the husk might be affected to the absorbance. The spectra showed absorbance peaks associated with the main constituents of sweet corns. The absorbance spectra of sweet corns with husk and sweet corns without husk showed a similar profile with absorbance at 1450 nm and 1920 nm. This absorbance was related with moisture content in sweet corns (Osborne et al., 1993). The water absorbance peaks (1450 nm and 1920 nm) were clear that they were related to the moisture content. But the other peaks of absorbance which were other constituents of sweet corns were not clear. Therefore, the second derivative spectra were used to separate absorption bands of other constituents. Average second derivative absorbance spectra of samples (sweet corns with husk and sweet corns without husk) are shown in Figure 4.16. From this figure, protein peaks were found at 1175 and 1705 nm; moisture peaks were found at 1450 nm and 1920 nm; starch peak was found at 1750 nm; carbohydrate peak was found at 2150 nm; and oil peaks were found at 2300 and 2350 nm (Osborne et al., 1993).

This material is reserved for educational use only, not allowed for commercial use.
Forbidden to modify the content, and cite the document when use

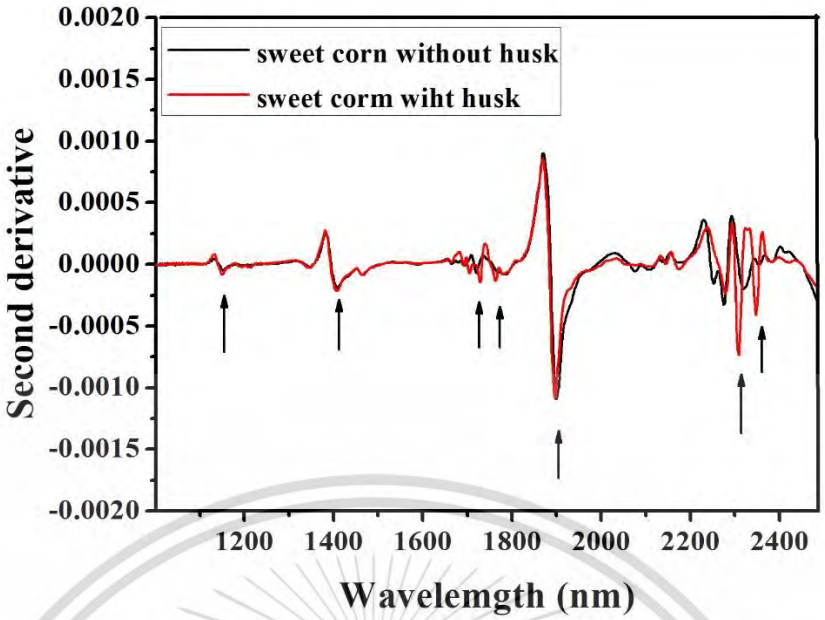

Figure 4.16 Average second derivative absorbance spectra of samples (the sweet corns with husk and sweet corns without husk).

4.4.2.1 Calibration model for predicting total soluble solids content of sweet corns

The minimum, maximum, mean and standard deviation values of sweet corns with husk and sweet corns without husk are analyzed and presented in Table 4.21. For calibration set of the sweet corns with and without husk, the total soluble solids content were varied from 11.4-21 °Bx with a mean value of 16.14 °Bx and a standard deviation of 1.98 °Bx. For prediction set of sweet corns with/without husk, the total soluble solids content were varied from 12.6-20.2 °Bx with a mean value of 16.3 °Bx and a standard deviation of 1.94 °Bx.

Table 4.21 Statistical characteristics of samples (sweet corns with husk and sweet corns without husk) in the calibration set and the prediction set for reflectance NIRs.

Items	Sweet corns with husk		Sweet corns without husk	
	Calibration set	Prediction set	Calibration set	Prediction set
Number of samples	111	53	111	53
Range (°Bx)	11.4-21	12.6-20.2	11.4-21	12.6-20.2
Mean (°Bx)	16.14	16.3	16.14	16.3
SD (°Bx)	1.98	1.94	1.98	1.94
Wavelength	1000-2500 nm	1000-2500 nm	1000-2500 nm	1000-2500 nm

SD = standard deviation

This material is reserved for educational use only, not allowed for commercial use.
Forbidden to modify the content, and cite the document when use

In Table 4.22, it shows the results of spectral pretreatments. Nine pretreatment methods were examined and shown in this table. The best model for total soluble solids content of sweet corns with husk was obtained by using second derivatives (R=0.81, RMSECV=1.15 ^{o}Bx) while model for total soluble solid content of sweet corns without husk was obtained by using original (R=0.86, RMSECV=0.97 ^{o}Bx).

Table 4.22 Statistical results of spectral pretreatments for prediction of total soluble solids content in samples (sweet corns with husk and sweet corns without husk).

Spectral pretreatments	N	Sweet corns with husk			Sweet corns without husk		
		F	R	RMSECV ^{o}Bx	F	R	RMSECV ^{o}Bx
Original	111	15	0.78	1.22	17	0.86	0.97
Smoothing	111	14	0.77	1.24	16	0.85	1.00
1st derivative	111	8	0.78	1.24	15	0.83	1.06
2nd derivative	111	5	0.81	1.15	17	0.85	1.00
Mean	111	14	0.78	1.23	15	0.83	1.05
MSC	111	13	0.79	1.21	16	0.83	1.05
SNV	111	14	0.79	1.23	15	0.84	1.04
Smoothing + 1st derivative	105	14	0.81	1.15	14	0.84	1.04
Smoothing + 2nd derivative	111	6	0.79	1.20	16	0.85	1.00
Mean + Smoothing + 1st derivative	111	13	0.79	1.21	13	0.83	1.05
Mean + Smoothing + 2nd derivative	111	12	0.79	1.22	14	0.84	1.03
SNV+ Smoothing + 1st derivative	111	12	0.77	1.24	12	0.82	1.10
SNV+ Smoothing + 2nd derivative	111	11	0.80	1.18	14	0.83	1.05

The predictive performances of PLSR models using full wavelength are summarized in Table 4.23. The best results for the sweet corns without husk obtained R=0.95 and

This material is reserved for educational use only, not allowed for commercial use.
Forbidden to modify the content, and cite the document when use

RMSEC=0.57°Bx while the prediction provided R=0.91 and RMSEP=0.88°Bx. Accuracy of the sweet corns without husk for total soluble solid content prediction obtained the best results while the accuracy of the sweet corns with husk for total soluble solid content prediction using second derivative obtained R=0.89 and RMSEP=0.81°Bx.

Table 4.23 PLSR calibration and prediction results for prediction of total soluble solid content in the sweet corns with husk and sweet corns without husk.

Items	**Sweet corn with husk**		**Sweet corn without husk**	
	Calibration set	**Prediction set**	**Calibration set**	**Prediction set**
Pretreatment	Second derivative	Second derivative	Original	Original
N	111	53	111	53
F	5	5	17	17
R	0.93	0.89	0.95	0.91
RMSEC	0.70	-	0.57	-
RMSEP	-	0.88	-	0.81
RPD	-	2.20	-	2.40

The quantitative relationship between predicted total soluble solids content and measured total soluble solids content of samples are presented in Figure. 4.17. Overall, the relationships between actual and predicted total soluble solids content confirmed the high correlation values as shown in Table 4.23. The range of soluble solids content of sweet corns were varied from 11.4-21 °Bx. The value of soluble solids content of the sweet corns had the wide range of values because sweet corns was measured soluble solids content at different time after harvest

This material is reserved for educational use only, not allowed for commercial use.
Forbidden to modify the content, and cite the document when use

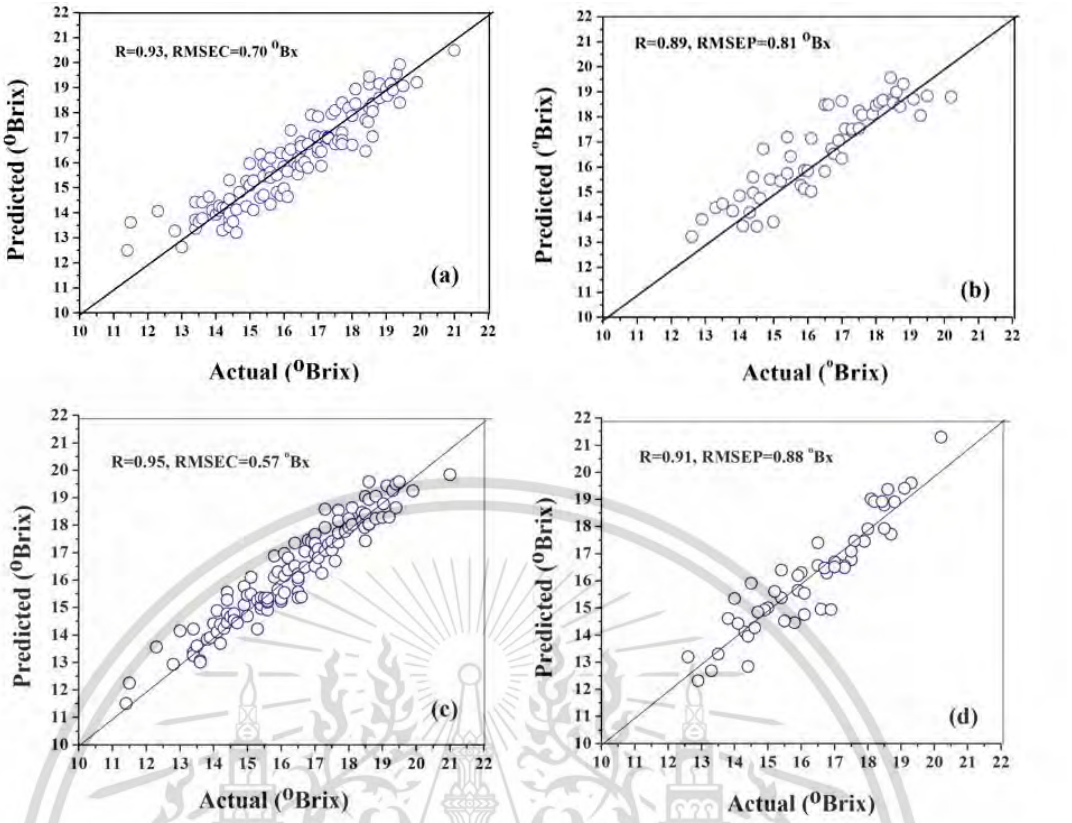

Figure 4.17 Predicted and actual values for total soluble solids contents by interactance NIRs.

(a) in the calibration set of sweet corns with husk

(b) in the prediction set of sweet corns with husk

(c) in the calibration set of sweet corns without husk

(d) in the prediction set of sweet corns without husk

4.4.2.1 Calibration model for predicting hardness of sweet corns

The measurement of the hardness and the statistic results are presented in Table 4.24. Samples (N=131) were used in this study. For calibration set of sweet corns with and without husk, the hardness was varied from 10.45-13.73 N with a mean value of 12.24 N and a standard deviation of 0.88 N. For prediction set of sweet corns with/without husk, the hardness was varied from 10.45-13.72 N with a mean value of 12.19 N and a standard deviation of 0.92 N.

This material is reserved for educational use only, not allowed for commercial use.
Forbidden to modify the content, and cite the document when use

Table 4.24 Statistical characteristics of samples (sweet corns with husk and sweet corns without husk) in the calibration set and the prediction set for reflectance NIRs.

Items	Sweet corns with husk		Sweet corns without husk	
	Calibration set	**Prediction set**	**Calibration set**	**Prediction set**
Number of samples	90	41	90	41
Range (Newton)	10.45-13.73	10.45-13.72	10.45-13.73	10.45-13.72
Mean (Newton)	12.24	12.19	12.24	12.19
SD (Newton)	0.88	0.92	0.88	0.92
Wavelength	1000-2500 nm	1000-2500 nm	1000-2500 nm	1000-2500 nm

SD = standard deviation

In the Table 4.25 shows the results of spectral pretreatments. Nine pretreatment methods were examined and shown in this table. The best model of the sweet corns with husk was obtained by using original spectra (R=0.75, RMSECV=0.51 N) while the model for hardness of the sweet corns without husk was obtained by the second derivative pretreatment (R=0.76, RMSECV=0.50 N).

The accuracy for predicting hardness in calibration set and prediction set by the model are shown in Table 4.26. The accuracy for prediction hardness in the sweet corns without husk using the second derivative obtained the good results (R = 0.85, RMSEP = 0.51 N while the accuracy of the model for prediction hardness in the sweet corns with husk was lower (R = 0.84, RMSEP = 0.49 N).

This material is reserved for educational use only, not allowed for commercial use.
Forbidden to modify the content, and cite the document when use

Table 4.25 Statistical results of spectral pretreatments for prediction of hardness in samples (sweet corns with husk and sweet corns without husk).

Spectral pretreatments	N	Sweet corns with husk			Sweet corns without husk		
		F	R	RMSECV (N)	F	R	RMSECV (N)
Original	90	12	0.75	0.51	15	0.70	0.56
Smoothing	90	13	0.75	0.52	15	0.73	0.53
1st derivative	90	12	0.75	0.52	7	0.71	0.55
2nd derivative	90	13	075	0.52	5	0.76	0.50
Mean	90	12	0.74	0.53	14	0.74	0.52
MSC	90	12	0.74	0.53	14	0.71	0.55
SNV	90	9	0.74	0.52	16	0.71	0.55
Smoothing + 1st derivative	90	11	0.74	0.52	10	0.71	0.55
Smoothing + 2nd derivative	90	12	0.75	0.51	14	0.72	0.54
Mean + Smoothing + 1st derivative	90	12	0.74	0.53	14	0.74	0.52
Mean + Smoothing + 2nd derivative	90	13	0.74	0.53	13	0.73	0.53
SNV+ Smoothing + 1st derivative	90	12	0.74	0.52	13	0.74	0.52
SNV+ Smoothing + 2nd derivative	90	11	0.74	0.53	14	0.74	0.52

This material is reserved for educational use only, not allowed for commercial use.
Forbidden to modify the content, and cite the document when use

Table 4.26 PLSR calibration and prediction results for prediction of hardness in samples (sweet corns with husk and sweet corns without husk).

	Sweet corns with husk		**Sweet corns without husk**	
	Calibration set	**Prediction set**	**Calibration set**	**Prediction set**
Pretreatment	Original	Original	Second derivative	Second derivative
N	90	41	90	41
F	12	12	5	5
R	0.87	0.83	0.91	0.85
RMSEC	0.37	-	0.34	-
RMSEP	-	0.51	-	0.51
RPD		1.80		1.80

F = Factors, N=number of samples, R= correlation coefficient, RMSEC= root mean squares error of calibration, RMSEP= root mean square error of prediction and RPD = ratio of prediction to deviation

Scattered plots were used to display correlations between actual hardness and predicted hardness as shown in Figure 4.18. Considering these results, it showed that the models obtained good results as shown in Figure 4.18 (b) and 4.18 (c) for predicting hardness value.

This material is reserved for educational use only, not allowed for commercial use.
Forbidden to modify the content, and cite the document when use

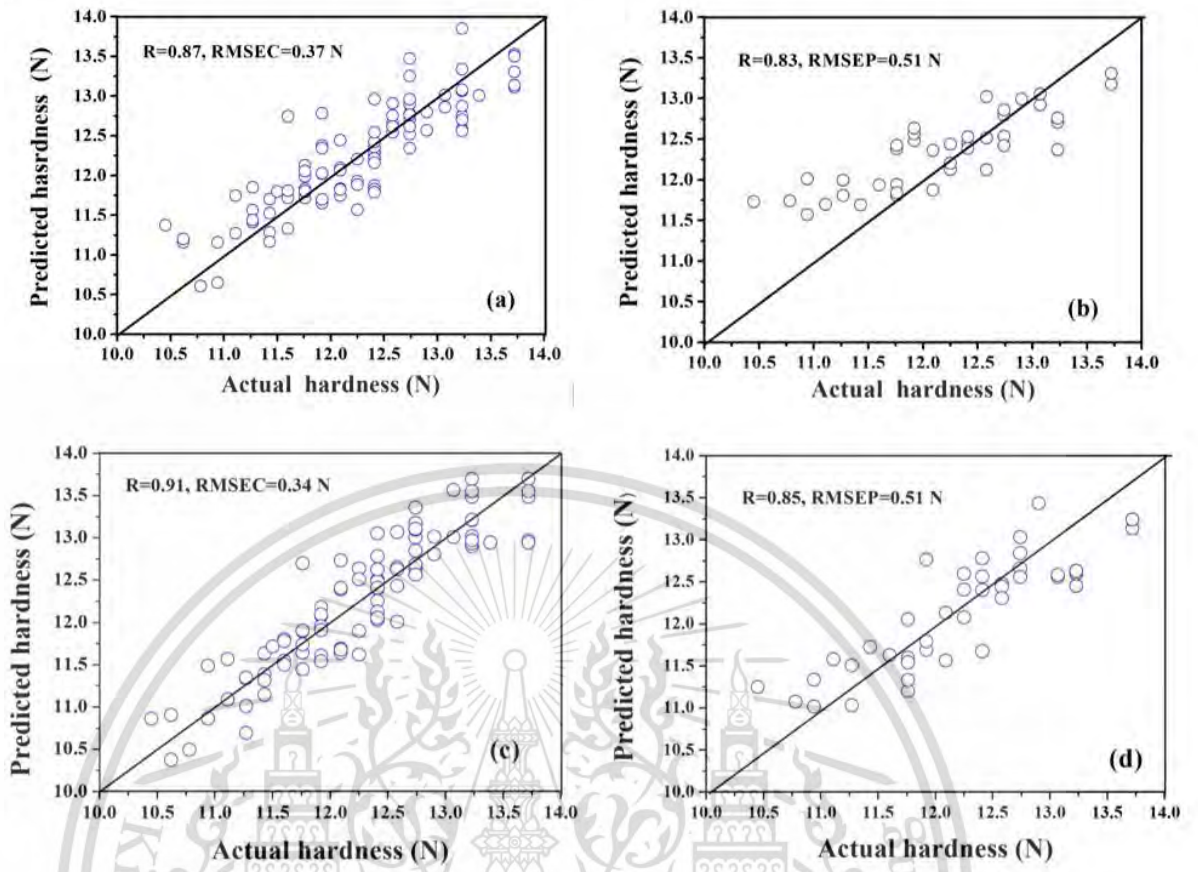

Figure 4.18 Predicted and actual values for hardness value by interactance NIRs.

(a) in the calibration set of sweet corns with husk

(b) in the prediction set of sweet corns with husk

(c) in the calibration set of sweet corns without husk

(d) in the prediction set of sweet corns without husk

4.4.2.1 Calibration model for predicting moisture content of sweet corns

The measurement of moisture content and the statistic results are presented in Table 4.27. For calibration set of the sweet corns with and without husk, the moisture content was varied from 10.24-14.7% with a mean value of 11.93% and a standard deviation of 0.87%. For prediction set of the sweet corns with/without husk, the moisture content was varied from 10.38-14.56% with a mean value of 11.95% and a standard deviation of 0.95%.

This material is reserved for educational use only, not allowed for commercial use.
Forbidden to modify the content, and cite the document when use

Table 4.27 Statistical characteristics of samples (the sweet corns with husk and sweet corns without husk) in the calibration set and the prediction set for reflectance NIRs.

Items	Sweet corns with husk		Sweet corns without husk	
	Calibration set	**Prediction set**	**Calibration set**	**Prediction set**
Number of samples	102	48	102	48
Range (%)	10.24-14.7	10.38-14.56	10.24-14.7	10.38-14.56
Mean (%)	11.93	11.95	11.93	11.95
SD (%)	0.87	0.95	0.87	0.95
Wavelength	1000-2500 nm	1000-2500 nm	1000-2500 nm	1000-2500 nm

SD = standard deviation

In Table 4.28 shows the results of spectral pretreatments. Nine pretreatment methods were examined and shown in this table. The best model for the moisture of sweet corns with husk was obtained by using original spectra (R=0.57, RMSECV=0.72%) while the model for the moisture content of sweet corns without husk was obtained by original spectra (R=0.71, RMSECV=0.72%).

This material is reserved for educational use only, not allowed for commercial use.
Forbidden to modify the content, and cite the document when use

Table 4.28 Statistical results of spectral pretreatments for prediction of moisture content in samples (the sweet corns with husk and sweet corns without husk)

Spectral pretreatments	N	Sweet corns with husk			Sweet corns without husk		
		F	R	RMSECV (%)	F	R	RMSECV (%)
Original	102	4	0.57	0.72	9	0.71	0.61
Smoothing	102	4	0.55	0.73	8	0.70	0.62
1^{st} derivative	102	6	0.55	0.72	9	0.70	0.62
2^{nd} derivative	102	8	0.55	0.74	10	0.71	0.62
Mean	102	6	0.56	0.74	11	0.70	0.62
MSC	102	4	0.56	0.74	9	0.71	0.62
SNV	102	6	0.55	0.74	11	0.71	0.60
Smoothing + 1^{st} derivative	102	5	0.57	0.72	11	0.70	0.62
Smoothing + 2^{nd} derivative	102	8	0.57	0.72	10	0.71	0.61
Mean + Smoothing + 1^{st} derivative	102	7	0.57	0.72	10	0.70	0.62
Mean + Smoothing + 2^{nd} derivative	102	7	0.56	0.74	9	0.70	0.62
SNV+ Smoothing + 1^{st} derivative	102	6	0.56	0.74	11	0.71	0.61
SNV+ Smoothing + 2^{nd} derivative	102	7	0.56	0.74	10	0.71	0.62

This material is reserved for educational use only, not allowed for commercial use.
Forbidden to modify the content, and cite the document when use

Table 4.29 PLSR calibration and prediction results for prediction of moisture content in samples (the sweet corns with husk and sweet corns without husk).

Items	**Sweet corns with husk**		**Sweet corns without husk**	
	Calibration set	**Prediction set**	**Calibration set**	**Prediction set**
Pretreatment	Original	Original	Original	Original
N	102	48	102	48
F	4	4	9	9
R	0.60	0.52	0.73	0.59
RMSEC	0.69	-	0.56	-
RMSEP	-	0.76	-	0.70
RPD		1.24		1.35

F = Factors, N=number of samples, R= correlation coefficient, RMSEC= root mean squares error of calibration, RMSEP= root mean square error of prediction and RPD = ratio of prediction to deviation

Scattered plots are used to display the correlations between actual moisture content and predicted moisture content as shown in Figure 4.19. Considering these results, it showed that the model had a poor accuracy for predicting moisture content as shown in Figure 4.20 (b).

This material is reserved for educational use only, not allowed for commercial use.
Forbidden to modify the content, and cite the document when use

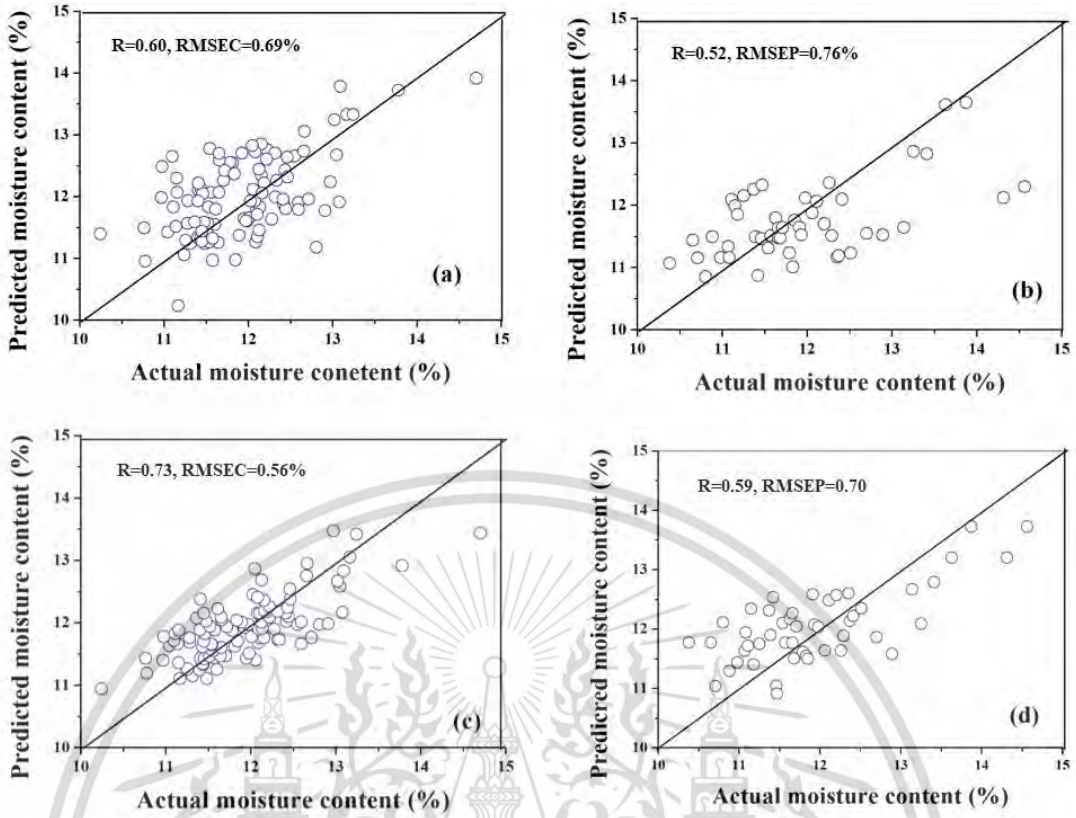

Figure 4.19 Predicted and actual values for moisture content by reflectance NIRs.

(a) in the calibration set of sweet corns with husk

(b) in the prediction set of sweet corns with husk

(c) in the calibration set of sweet corns without husk

(d) in the prediction set of sweet corns without husk

This material is reserved for educational use only, not allowed for commercial use.
Forbidden to modify the content, and cite the document when use

CHAPTER 5

CONCLUSIONS AND SUGGESTIONS

5.1 Conclusion

From the results of this research, the models were developed for predicting the quality of hen eggs and sweet corns by NIRs.

For the quality of hen eggs, the quality of hen eggs is described in term of Haugh unit, because Haugh unit of hen eggs is important index for freshness. Haugh unit of hen eggs were predicted by the near infrared spectroscopy at the different period of storage. Three NIR instruments were used in this research (FQA- NIR GUN, FT-NIR spectrophotometer and NIR hyperspectral image). The combination of smoothing and first derivative spectral pretreatments in the interactance mode (588-1091 nm) by FQA- NIR GUN obtained R of 0.91 and RMSEP of 5.64. The MSC spectral pretreatments in the reflectance mode (1000-2500 nm) by FT-NIR spectrophotometer obtained R of 0.83 and RMSEP of 7.11. The SNV spectral pretreatments in the reflectance mode (900-1700 nm) by NIR hyperspectral image obtained R of 0.92 and RMSEP=6.29. For NIR hyperspectral imaging, averaged spectra from ROI of hens' eggs by the hyperspectral imaging technique were used for establishing the calibration model in order to predict Haugh unit of eggs. The standard normal variate transformation spectral pretreatment gave the optimum conditions for the model. Distribution maps were generated from the model based on Haugh unit which can be used to classify the freshness of eggs by visual inspection of color on the acquired image simply be observing the level red color. However it can also be used for the acquired predictive Haugh unit from the image, compared to the cut-off Haugh unit value, in order to classify groups of eggs into fresh and unfresh. Therefore this demonstrates that hyperspectral imaging has a potential for use as a non-destructive, rapid online system to classify hens' eggs. Accuracy comparison of all results, it was found that results from NIR hyperspectral image obtained the best accuracy. Different wavelength of three NIRs instruments was affected to accuracy.

For the quality of sweet corns, the qualities of sweet corns were described in terms of total soluble solids content, hardness and moisture content. Sweet corns were measured at the different storage time after harvest (6 hr, 12 hr, 18 hr, 24 hr, 30 hr and 36 hr). Total soluble solids content of the sweet corns with/without husk were predicted by the interactance mode in the

This material is reserved for educational use only, not allowed for commercial use.
Forbidden to modify the content, and cite the document when use

wavelength range 588-1091 nm. Comparisons accuracy results between sweet corns with/without husk, it found that sweet corns without husk obtained better accuracy (R=0.84 and RMSEP=1.07 ^{o}Bx) while the results of the sweet corns with husk obtained poor results (R = 0.77, RMSEP = 1.23 ^{o}Bx). Hardness of the sweet corns with/without husk was predicted by the interactance mode in the wavelength range 588-1091 nm. Comparisons accuracy results between of the sweet corns with/without husk, it found that sweet corns without husk obtained better accuracy (R=0.81 and RMSEP=0.44 N) while the accuracy to predict hardness of the sweet corns with husk was lower when compared the result of sweet corns with husk (R=0.80, RMSEP=0.40 N). Moisture content of sweet corns with/without husk were predicted by the interactance mode in the wavelength range 588-1091 nm. Comparisons accuracy results between of the sweet corns with/without husk, it found that the sweet corns without husk obtained better accuracy (R=0.80 and RMSEP=0.52%) while results of the sweet corns with husk obtained poor accuracy (R = 0.71, RMSEP = 0.72%). Total soluble solids content of sweet corns with/without husk was predicted by the reflectance mode in the wavelength range 1000-2500 nm. Comparisons accuracy results between the sweet corns with/without husk, it found that the sweet corns without husk obtained better accuracy (R=0.91 and RMSEP=0.88 ^{o}Bx) while results of the sweet corns with husk obtained R of 0.89, RMSEP of 0.81 ^{o}Bx. Hardness of the sweet corns with/without husk was predicted by the reflectance mode in the wavelength range 1000-2500 nm. Comparisons accuracy results between of the sweet corns with/without husk, it found that the sweet corns without husk obtained better accuracy (R=0.85 and RMSEP=0.51 N) while the accuracy to predict sweet corns with husk was lower when compared with the results of the sweet corns with husk (R=0.84, RMSEP=0.49 N). Moisture content of sweet corns with/without husk were predicted by the reflectance mode in the wavelength range 1000-2500 nm. Comparisons accuracy results between of the sweet corn with/without husk, it found that the sweet corns without husk obtained better accuracy (R=0.59 and RMSEP=0.70%) while results of the sweet corns with husk obtained poor results (R = 0.52, RMSEP = 0.76%). The accuracy results of moisture content obtained the poor result because reference analysis is not accurate. The author removes the corn kernels from the corn stalks and then randomly picked corn kernels 3 times for measured moisture content while sweet corns was scan NIR at the top, middle and bottom. If reference analysis was randomly picked corn kernels 3 times at the same position of scanning NIR, the accuracy results of moisture content maybe good.

This material is reserved for educational use only, not allowed for commercial use.

Forbidden to modify the content, and cite the document when use

The comparison between results of the sweet corns with husk and without husk, the thickness of the husk had an effect on the accuracy of predicting qualities of sweet corn.

5.2 Suggestion

5.2.1 The thickness of husk was affected to the accuracy of prediction and it was different in each sample. Therefore the thickness of husk should be measured.

5.2.2 For measuring hardness value of sweet corns by destructive method, the hand-held penetrometer was used in this study. If a texture analyzer was used, the acquired hardness value for establishing the model maybe obtained the better results.

This material is reserved for educational use only, not allowed for commercial use.
Forbidden to modify the content, and cite the document when use

BIBLIOGRAPHY

Abbott, J.A., Lu, R., Upchurch, B.L. and Stroshine, R.L., 1997. Technologies for non destructivee quality evaluation of fruits and vegetables. Horticultural Reviews –Technologies for Non-destructive Quality Evaluation of Fruits and Vegetables, vol. 20. John Wiley & Sons, Inc, pp. 1–120.

Altuntas E., and Sekeroglu, A. 2007. Effect of egg shape index on mechanical properties of chicken eggs. Food Engineering. 85: 606-612.

Anderson, T.W. 2003. An Introduction to Multivariate Statistical Analysis. (3rd ed.). New York: Wiley and Sons.

Anderson, K. E., Tharrington, J.B., Curtis, P.A. and Jones, F.T. 2004. Characteristics of eggs from historic strains of single comb White Leghorn chickens and the relationship of egg shape to shell strength. Poultry Science. 3: 17-19.

Ariana, D. P., and Lu, R. 2010. Hyperspectral imaging for defect detection of pickling cucumbers. In D. -W. Sun (Ed.), Hyperspectral imaging for food quality analysis and control (pp. 431–448) (1st ed.). San Diego, California, USA: Academic Press/Elsevier.

Bakker-Arkema, F.W. (ed). 1999. CIGR Handbook of Agricultural Engineering, Volume IV: Agro-Processing Engineering. American Society of Agricultural Engineering, St. Joseph, MI. 527p.

Ballbio, D. and Todeschini, R. 2009. Multivariate Classification for Qualitative Analysis. Page 83-104. In Sun, D.A. Infrared Spectroscopy for Food Quality Analysis and Control. New York: Elsevier.

Barbin, D. F., ElMasry, G., Sun, D.W. and Allen, P. 2012. Non-destructive determination of chemical composition in intact and minced pork using near-infrared hyperspectral imaging. Food Chemistry. 138: 1162–1171.

Berzaghi, P., Dalle, Zotte, A., Jansson, L. M. and Andrighetto, I. 2005. Near-infrared reflectance spectroscopy as a method to predict chemical composition of breast meat and discriminate between different n-3 feeding sources. Poultry Science, 84: 128–136.

Blanco, M. and Villarroya, I. 2002. NIR spectroscopy: a rapid-response analytical tool. Trends in Analytical Chemistry. 21: 240–250.

This material is reserved for educational use only, not allowed for commercial use.
Forbidden to modify the content, and cite the document when use

Boyette, M.D. Wilson, L.G. and Estes, E.A. 1990. Postharvest cooling and handling of sweet corn. Extension Service State Agricola N.e. State University, Raleigh. November. 413-414.

Burley, R.W., Vadehra, D.V., 1989.TheAlbumen: Chemistry. In: The Avian Egg. Chemistry and Biology. Wiley, NewYork.

CAMO. The Unscambler Appendices: Method Refernces. [online]. Available: http://www.camo.com/Theunscambler/Appendices. Accessed on March 7, 2017.

Cen, H. and Hen. Y. 2007. Theory and application of near infrared reflectance spectroscopy in determination of food quality. Trends in Food Science & Technology. 18: 72-83.

Cen, H., Lu, R., Zhu, Q. and Mendoza, F. 2016. Nondestructive detection of chilling injury in cucumber fruit using hyperspectral imaging with feature selection and supervised classification. Postharvest Biology and Technology. 111: 352-361.

Chauchard, F., Cogdill, R., Roussel, S., Roger, J.M. and Bellon-Maurel, V. 2004. Application of LS-SVM to non-linear phenomena in NIR spectroscopy: development of a robust and portable sensor for acidity prediction in grapes. Chemometrics and Intelligent Laboratory Systems. 71: 141–150.

Chen, Y.R., Chao, K. and Kim, M. 2002. Machine vision technology for agricultural application. Computers and Electronic in Agricultural. 36(2): 173-191.

Chu, X., Wang, W., Yoon, S.C., Ni, X. and Heitschmidt, G.W. 2017. Detection of aflatoxin B1 (AFB1) in individual maize kernels using short wave infrared (SWIR) hyperspectral imaging. Biosystems Engineering. 157: 13-23.

Clydesdale, F.M. and Francis, F.J. 1976. *Pigments.* In: Fennema, O.R. (ed). Principles of food science. Part 1. Marcel Dekker, Inc. New York. 386-426.

Cozzolino, D., De Mattos, D. and Vaz Martins, D. 2002. Visible/near infrared reflectance spectroscopy for predicting composition and tracing system of production of beef muscle. Animal Science, 74: 477–484.

ElMasry, G., Sun, D.W. and Allen, P. 2012. Near-infrared hyperspectral imaging for predicting colour, pH and tenderness of fresh beef. Food Engineering. 110(1): 127–140.

Evensen, K.B. and Boyer, C.D.1986. Flavour qualities of frozen sweet corn are effected by genotype and blanching. American Society for Horticultural Science. 111(5): 734-738.

Food Encyclopedia. 1996. Corn. Les editions Queec/Amerique, Inc. Montreal, Quebec, Canada. 685p.

This material is reserved for educational use only, not allowed for commercial use.
Forbidden to modify the content, and cite the document when use

Galobart, J., Sala, R., Rincon-Carruyo X., Manzanilla, E.G., Vila, B. and Gasa, J. 2004. Egg yolk color as affected by saponification of different natural pigmenting sources. Applied Poultry Research. 13: 328-334.

Geladi, P. 1985. Linearization and scatter-correction for near-infrared reflectance spectra of meat. Apply Spectroscopy. 39: 491.

Geladi, P., Burger, J. and Lestander, T. 2004. Hyperspectral imaging: calibration problems and solution. Chemometrics and Intelligent Laboratory Systems. 72: 209-217.

Giunchi, A., Berardinelli, A., Ragni, L., Fabbri, A. and Silaghi, F.A. 2008. Non-destructive freshness assessment of shell eggs using FT-NIR spectroscopy. Food Engineering. 89: 142-148.

Hafez, E. S. E., Badreldin, A.L. and Kamar, G.A.R. 1955. Egg components in the Fayomi fowl during the first laying year. Poultry Science. 34: 400-410.

Haiyan, C. and Yong, H. 2007. Theory and application of near infrared reflectance spectroscopy in determination of food quality. Trends in Food Science & Tecnology. 18: 72-83.

Hao, L., Jiewen, Z., Li, S., Quansheng, C. and Fang, Z. 2011. Freshness measurement of eggs using near infrared (NIR) spectroscopy and multivariate data analysis. Innovative food science and emerging technology. 12: 182-186.

Harrill, R. 1994. Using a refractometer to test the quality of fruits and vegetables. Pineknoll Publishing, Keedysville, MD.

Haugh, R. R. 1937. The Haugh unit for measuring egg quality. U. S. Egg Poultry Magazine. 43: 552-555 and 572-573.

Herber, R. 1991. Postharvest handling of sweet corn. Speech m: The great lakes vegetable growers news. Michigan State University. 1p.

Hoving-Bolink, A. H., Vedder, H. W., Merks, J. W. M., de Klein, W. J. H., Reimert, H. G. M., Frankhuizen, R,. Van den brok, W.H.A.M. and Lambooij, E. 2005. Perspective of NIRS measurements early post mortem for prediction of pork quality. Meat Science. 69: 417–423.

Imsil, A. 2012. Effect of degree of milling on physicochemical qualities and discrimination of Thai Hom Mali rice by FT-NIR spectroscopy. Ph.D. Thesis of King Mongkut's Institute of Technology Ladkrabang.

Inglett, G.E. 1970. Corn: Culture, Processing and Products. The AVI publishing Co. Westpot, CT.

This material is reserved for educational use only, not allowed for commercial use.
Forbidden to modify the content, and cite the document when use

Jia, B., Yoon, S.C., Zhuang, H., Wang, W. and Li, C. 2017. Prediction of pH of fresh chicken breast fillets by VNIR hyperspectral imaging. Food Engineering. 208: 57-65.

Jie, D., Xie, L., Rao, X and Ying, Y. 2014. Using visible and near infrared diffuse transmittance technique to predict soluble solids content of watermelon in an on-line detection system. Postharvest Biology and Technology. 90: 1-6.

Kader, A.A. (ed). 2002. Postharvest technology of horticultural crops. 3rd edition. Coop. Ext. Uni. of Ca. Division of Agriculture and Natural Resources. Univ. of CA, Davis, CA. Publ. no. 3311. 535p.

Kamruzzaman, M., ElMasry, G., Sun, D. W. and Allen, P. 2012. Non-destructive prediction and visualization of chemical composition in lamb meat using NIR hyperspectral imaging and multivariate regression. Innovative Food Science & Emerging Technologies. 16: 218–226.

Karoui, R., Kemps, B.F., Bamelis, D., De Ketelaere, B., Decuypere, E., De Baerdemaeker, J., 2006. Method to evaluate egg freshness in research and industry: a review. European Food Research and Technology. 222: 727–732.

Kawano, S. 2002. Sampling and Sample Presentation. In: H.W. Siesler, Y. Ozaki, S. Kawata and H.M. Heise, (eds.), Near-Infrared Spectroscopy. WILEY-VCH Verlag Gmbh, Federal Republic, Germany. 115-124.

Koehler, F.W., Lee, E., Kidder, L.H. and Lewis, E.N. 2002. Near infrared spectroscopy: the practical chemical imaging solution. Spectoscopy Europe. 14: 12-19.

Lammertyn, J., Peirs, A., De Baerdemaeker, J., and Nicolai, B. 2000. Light penetration properties of NIR radiation in fruit with respect to non-destructive quality assessment. Postharvest biology and technology. 18 (1): 121-132.

Lin, H., Zhao, J., Sun, L., Chen, Q. and Zhou, F. 2011. Freshness measurement of eggs using near infrared (NIR) spectroscopy and multivariate data analysis. Innovative Food Science and Emerging Technologies. 12: 182–186.

Liu, D., Sun, D. W., Qu, J., Zeng, X. A., Pu, H. and Ma, J. 2014. Feasibility of using hyperspectral imaging to predict moisture content of porcine meat during salting process. Food Chemistry. 152: 197-204.

Ledur, M. C., Liljedahl, L.E., McMillan, I., Asselstine, L. and Fairfull, R.W. 2002. Genetic effects of aging on egg quality traits in the first laying cycle of White Leghorn strains and strain crosses. Poultry Science. 81: 1439-1447.

This material is reserved for educational use only, not allowed for commercial use.
Forbidden to modify the content, and cite the document when use

Leonardi, L. and Burns, D. H. 1999. Quantitative multiwavelength constituent measurements using single-wavelength photo time of flight correction. Applied Spectroscopy. 53: 637–646.

Lorente, D., Aleixos, N., Gomez-Sanchis, J., Cubero, S., Garcia-Navarrete, O. L. and Blasco, J. 2012. Recent advances and applications of hyperspectral imaging for fruit and vegetable quality assessment. Food and Bioprocess Technology. 5(4): 1121–1142.

Magness, J.R., Markle, G.M. and Compton, C.C. 1971. Food and feed crops of the United States. New Jersey. Bul. 828p.

Manley, M., Williams, P., Nilsson, D., Geladi, P., 2009. Near infrared hyperspectral imaging for the evaluation of endosperm texture in whole yellow maize (*Zea maize* L.) kernels. Agricultural and Food Chemistry. 57: 8761-8769.

Martens, M. and Baordseth, P. 1987. Ch. 21: *Sensory quality*. In: Weichmann, J. (ed). Postharvest physiology of vegetables. Marcel Dekker, Inc. New York, USA. 597p.

Monira, K. N., M. Salahuddin, and G. Miah. 2003. Effect of breed and holding period on egg quality characteristics of chicken. Poultry Science. 2: 261-263.

Munro, B.D. and Small, E. 1997. Vegetables of Canada. NRC Research Press. Ottawa, Ontario. 417p.

National Bureau of Agricultural Commodity and Food Standards (ACFS). Thai agricultural satandard for sweet corn. TAS 1512-2011. Effective 10 January, 2012.

National Food Institute. Food intelligence center. [Online] resource http://www.nfi.or.th (7 February 2016).

Nicolai, B.N. 2007. Nondestructive measurement of fruit and vegetable quality by means of NIR spectroscopy: A review. Postharvest Biology and Technology. 46 (2): 99-118.

Nicolai, B.M. Berna, A. Beullens, K. Vermeir, S. Saevels, S. and Lammertyn, J. 2008. High throughput flavor profiling of Fruit. 287-308. in Brückner, B. and Wyllie, S.G. editors.

Olsen, K.J., E.J. Giles and R.R. Jordan. 1990. Postharvest carbohydrate changes and sensory quality of three sweet corn cultivars. Scientia Horticulturae. Elsevier Science Publishers. B. V. Amesterdam. 44: 179-189.

Ortiz-Somovilla, V., Espana-Espana, F., Gaitan-Jurado, A. J., Perez-Aparicio, J. and De Pedro-Sanz, E. J. 2007. Proximate analysis of homogenized and minced mass of pork sausages by NIRS. Food Chemistry. 101: 1031–1040.

This material is reserved for educational use only, not allowed for commercial use.
Forbidden to modify the content, and cite the document when use

Osborne, B.G., Fearn, T. and Hindle, P.H. 1993. Practical NIR spectroscopy with Application in Food and Beverage Analysis. Longman Scientific & Technical. 1-7.

Park, B., Chen, Y. R., Hruschka, W. R., Shackelford, S. D. and Koohmaraie, M. 2001. Principal component regression of near-infrared reflectance spectra for beef tenderness prediction. Transactions of ASAE. 44(3): 609–615.

Park, B., Abbott, A.J., Lee, K.J. and Choi, C.H. and Choi, C.H. 2002. Near-infrared spectroscopy to predict soluble sold and firmness of apple. Pare number 023066, ASAE/CIGR Annual International Meeting, Chicago, Illinois, USA.

Peet, M. 1995. Sustainable practices for vegetable production in the south. North Carolina State University.

Popova-Ralcheva, S., Sredkova, V., Valchev, G. and Bozakova, N. 2009. The effects of the age and genotype on morphological egg quality of parent stock hens. Archiva Zootechnica. 12: 24-30.

Qin, J. and Lu, R. 2008. Measurement of the optical properties of fruits and vegetables using spatially resolved hyperspectral diffuse reflectance imaging technique. Postharvest Biology and Technology. 49: 355-365.

Romanoff, A.L., Romanoff, A.J., 1949. Physicochemical properties. In: The Avian Egg. John Wiley & Sons Inc, NewYork.

Rossi, M., Pompei, C., Hidalgo, A., 1995. Freshness criteria based on physical and chemical modifications occurring in eggs during aging. Food Science. 7 (2): 147–156.

Ryall, A.L. and Lifton, J.W. 1979. Handling, transportation and storage of fruits and vegetables.2nd edition. Vol. 1. 587p.

Salunkhe, D.K. and Desai, B.B. 1984. Postharvest biotechnology of vegetables. CRC Press, Inc. Boca Raton, Florida. Vol. 1. 194p.

Saeys, W., Mouazen, A.M., Ramon, H., 2005. Potential for Onsite and Online Analysis of Pig Manure using Visible and Near Infrared Reflectance Spectroscopy. Biosystems Engineering. 91(4), 393–402.

Sargent, S. 1999. Handling Florida vegetables: sweet corn. Florida cooperative extension Service. IFAS. University of Florida. Gainesville, FI. SS-VEC 925.

Schultheis, RJ. 1998. Sweet corn production. North Carolina Cooperative Extension service. North Carolina University.

This material is reserved for educational use only, not allowed for commercial use.
Forbidden to modify the content, and cite the document when use

Shiqiang, J. et al. 2015. Variety identification method of coated maize seed based on near-infrared spectroscopy and chemometrics. Cereal Science. 63: 21-26.

Silversides, F. G. 1994. The Haugh unit correction for egg weight is not adequate for comparing eggs from chickens of different lines and ages. Applied Poultry Research. 3: 120-126.

Silversides, F. G., and K. Budgell. 2004. The relationship among measures of egg albumen height, pH, and whipping volume. Poultry Science. 83: 1619-1623.

Sim, J. S., 1998. Designer eggs and their nutritional and functional significance. In: A. P. Simopoulos (Ed.), The Return of Omega-3 Fatty Acids into the Food Supply, 1. Land-Based Animal Food Products and Their Health Effects. Basel, Switzerland, pp. 89-101.

Sirisomboon, P., Hashimoto, Y. and Tanaka, M. (2009). Study on non-destructive evaluation methods for defect pods for green soy bean processing by near-infrared spectroscopy. Food Engineering. 93: 502–512.

Stadelman, W.J., Cotterill, O.J., 1995. Egg Science and Technology, fourth ed. Food Product Press, New York.

Takehiko, Y., Lekh, R.J., Hajime, H. and Mujo, K. 1996. Hen egg, theie basic and applied science, New York.

Talbot, M.T., Sargent, S.A. and Brecht, J.K. 1991. Cooling Florida sweet corn. Florida Cooperative Extension Service, IFAS. University of Florida. Circular 941. 21p.

Talens, P., Mora, L., Morsy, N., Barbin, D. F., Elmasry, G. and Sun, D. W. 2013. Prediction of water and protein contents and quality classification of Spanish cooked ham using NIR hyperspectral imaging. Food Engineering. 117(3): 272–280.

Tatzer, P., Wolf, M. and Panner, T. 2005. Industrial application for inline material sorting using hyperspectral imaging in the NIR range. Real-Time Imaging. 11: 99-107.

Thapon, J.L., Bourgeois, C.M., 1994. L'uf et les ovoproduits. Paris: Technique et Documentation, Lavoisier.

Valous, N.A., Mendoza, F., Sun, D.-W., Allen, P., 2009. Colour calibration of a laboratory computer vision system for quality evaluation of pre-sliced hams. Meat Science. 81(1): 132–141.

Van Den Brand, H., Parmentier, H.K. and Kemp, B. 2004. Selection for antibody response against sheep red blood cells and layer age affect egg quality. British Poultry Science. 45: 787-792.

This material is reserved for educational use only, not allowed for commercial use.
Forbidden to modify the content, and cite the document when use

Vuilleumier, J. P. 1968. The Roche yolk colour fan℠-An instrument for measuring yolk colour. Poultry Science. 48: 767-778.

Walsh, T.J., Rizk, R.E., Brake, J., 1995. Effects of temperature and carbon dioxide on albumen characteristics, weight loss, and early embryonic mortality of long stored hatching eggs. Poultry Science. 74: 1403–1410.

Williams, K. C. 1992. Some factors affecting albumen quality with particular reference to Haugh unit score. World's Poultry Science Journal. 48: 5-16.

Williams, P.C.and Sobering, D.C., 1996. How do we do it: a brief summary of the methods we use in developing near infrared calibrations. In: Davies, A.M.C., Williams, P.C. (Eds.), Near Infrared Spectroscopy: The Future Waves. NIR Publications, Chichester, pp. 185–188.

Williams, P. C. 2007. Application of Near-Infrared Spectroscopy (NIRS) in the Agricultural and Food Industries. July 4th, 2007. Kasetsart University, Bangkok, Thailand. 26 pp.

Wu, D., Sun, D.W., 2013. Advanced applications of hyperspectral imaging technology for food quality and safety analysis and assessment: A review — Part I: Fundamentals. Inovative Food Science & Emerging Technologies. 19: 1-14.

Xiong, Z., Sun, D.W., Xie, A., Pu, H., Han, Z. and Luo, M. 2015. Quantitative determination of total pigments in red meats using hyperspectral imaging and multivariate analysis. Food Chemistry. 178: 39-345.

Yoshinori, M. Egg bioscience and biotechnology. 2007. John Wiley & Sons Inc, NewYork.

Zeidler, G. 2002. Shell Egg Quality and Preservation. Pages 1199-1217 in Commercial Chicken Meat and Egg Production. 5th rev. D. D. Bell and W. D. Weaver, Jr., ed. Kluwer Academic Publishers, Norwell, MA.

Zhu, F., Zhang, D., He, Y., Liu, F. and Sun, D. W. 2013. Application of visible and near infrared hyperspectral imaging to differentiate between fresh and frozen– thawed fish fillets. Food and Bioprocess Technology. 6(10): 2931–2937.

This material is reserved for educational use only, not allowed for commercial use.
Forbidden to modify the content, and cite the document when use

APPENDIX

This material is reserved for educational use only, not allowed for commercial use.
Forbidden to modify the content, and cite the document when use

Journal of Food Engineering 215 (2017) 97–103

Contents lists available at ScienceDirect

Journal of Food Engineering

journal homepage: www.elsevier.com/locate/jfoodeng

Non-destructive quality assessment of hens' eggs using hyperspectral images

Sineenart Suktanarak, Sontisuk Teerachaichayut*

Department of Food Engineering, Faculty of Agro-Industry, King Mongkut's Institute of Technology Ladkrabang, Bangkok 10520, Thailand

ARTICLE INFO

Article history:
Received 3 January 2017
Received in revised form
5 July 2017
Accepted 10 July 2017
Available online 14 July 2017

Keywords:
Egg
Hyperspectral imaging
Freshness
Haugh unit
Prediction
Image

ABSTRACT

Freshness of hens' eggs is important for consumers and the food processing industry and the Haugh unit (HU) is a commonly used index for freshness. Measurement of HU is destructive and also assumes that the sample that is tested accurately reflects the batch of eggs being processed. This research tests the use reflectance near infrared hyperspectral imaging in the wavelength range of 900–1700 nm for nondestructive prediction of eggs freshness and compared these measurements to HU. To achieve this fresh eggs were stored at 25 °C and were measured after storage for 0, 4, 7, 10, 14, 18 and 21 days by hyperspectral imaging technique and compared to HU for each egg. Hyperspectral imaging technique combines between conventional imaging and NIR spectroscopy to achieve spatial and spectral information from eggs. The acquired near infrared hyperspectral imaging data from samples in the calibration set were analyzed in order to develop a calibration model for HU using partial least squares regression (PLSR) and then crossvalidated. The standard normal variate transformation (SNV) spectral pretreatment gave the optimum conditions for establishing the calibration model with a coefficient of determination (R2) of 0.91 and root mean square error of calibration (RMSEC) of 4.58. Distribution maps of HU were generated from the acquired calibration model by interpretation of predicted HU to different colors using image processing algorithms. Displayed colors of acquired image of eggs were different correspond to the freshness of the eggs based on HU. The results show that the near infrared hyperspectral imaging technique can be possible to use for presenting the images of egg related to HU in order to nondestructively evaluate hens' eggs freshness.

© 2017 Elsevier Ltd. All rights reserved.

1. Introduction

Hens' eggs are a staple food and contain many essential nutrients including proteins, vitamin E, omega-3 fatty acids, selenium and lutein (Sim, 1998). Internal quality of eggs can change during storage including loss of water and CO_2, as well as diffusion of fluids between different parts of the egg (Karoui et al., 2006). Water is lost by evaporation through the shell and its loss together with loss of CO_2 and increases in acidity results in the liquefaction of albumen (Burley and Vadehra, 1989). Gas exchange through the shell can cause changes in two of the albumen proteins, ovomucin and lysozyme, which then affects the thickness of albumen layer and can be used as a measure of their freshness (Stadelman and Cotterill, 1995). External appearance of an egg gives no indication of its freshness, so Haugh unit (HU) was developed, which involves breaking the egg onto a flat surface and measuring the height of the albumen with a micrometer. Measurement of HU is destructive and also assumes that the sample that is tested accurately reflects the batch of eggs being processed. Therefore, a non-destructive technique would be a major contribution for the evaluation of the freshness on eggs. Previous work on non-destructive assessment of eggs have used dielectric detection in the range of radio frequency of 40 kHz to 20 MHz (Soltani and Omid, 2015), visible (UV/VIS 200–800 nm) transmittance spectroscopy (Liu et al., 2007) and proton NMR relaxation (Laghi et al., 2005). Hyperspectral imaging is a non-destructive technique which integrates the conventional spectroscopy and image processing for quality evaluation of samples (Valous et al., 2009). Conventional NIR spectroscopy can only provide a spectrum while hyperspectral imaging can provide both spectrum and spatial information of the composition of samples (Manley et al., 2009). Wu and Sun (2013) showed that the spectral and spatial information acquired from samples could be used for analysis in hyperspectral imaging. The hyperspectral imaging technique has been used for both qualitative and quantitative analysis in order to evaluate qualities of products. Dai et al. (2015)

* Corresponding author.
E-mail address: sontisuk.te@kmitl.ac.th (S. Teerachaichayut).

http://dx.doi.org/10.1016/j.jfoodeng.2017.07.008
0260-8774/© 2017 Elsevier Ltd. All rights reserved.

This material is reserved for educational use only, not allowed for commercial use.

Forbidden to modify the content, and cite the document when use

showed its effectiveness for qualitative analysis, such as freshness classification of fresh and frozen prawns using total volatile basic nitrogen (TVB-N) values. Wang et al. (2015) showed it to be an index of discrimination of aflatoxin B_1 at different concentrations on maize kernel surfaces and Cen et al., 2016) in the classification of chilling injury in cucumbers. For quantitative analysis (Lee et al., 2014) showed it to be effective in detection of bruise damage on pears and Xiong et al. (2015a,b) in the prediction of 2-thiobarbituric acid reactive substances (TBARS) in chicken meat during refrigerated storage and the prediction of total pigments in red meat. The spectral information in the wavelength range of 400–1000 nm has also been used for the prediction of total soluble solids content and firmness in blueberry (Leiva-Valenzuela et al., 2013) and the evaluation of anthocyanin content of lychee pericarp (Yang et al., 2015). The purpose of this study was to determine whether NIR hyperspectral imaging could be used to measure the freshness of hens' eggs and to compare the method with the standard HU test.

2. Materials and methods

2.1. Sample preparation

Fresh eggs were obtained from a poultry farm in Nakhon Ratchasima in Thailand on the day they were laid. They were selected for good appearance and to be within the size grade number 3 (National Bureau of ACFS, 2010). The samples were carefully transported from the poultry farm to the laboratory where they were then inspected and cleaned and any cracked or broken eggs were rejected. The samples were divided randomly into 7 groups of 13 (N = 91) for measurement after storage for 0, 4, 7, 10, 14, 18 or 21 days at 25 °C.

2.2. NIR hyperspectral image measurement

Samples were scanned by a pushbroom NIR hyperspectral imaging system (Specim, Spectral Imaging Ltd., Finland), reflectance mode, in the wavelength range of 900–1700 nm with 256 spectral bands at 6 nm resolution and 3.12 nm wavelength intervals. The main elements of the hyperspectral image system consists of a CCD camera, an imaging spectrometer, a light source of a 300 W tungsten halogen lamp, a translation stage at size 100 × 100 mm, and data acquisition software (ChemaDAQ, Spectral Imaging Ltd., Finland) that controls the motor speed, exposure time and image acquisition. The halogen lamp was situated at an angle of 45° and light in the translation stage was moved to the scan. The hyperspectral imaging system was opened for preheating 30 min before the scan samples were taken. Each sample was placed on a tray and moved by stepper motor through the field of view (FOV) of the spectrograph at a constant speed of 33 mms^{-1} during measurement. The exposure time of the CCD camera was adjusted to 1.5 ms in order to obtain good quality images. The white and dark reference was captured for each measurement. After scanning, the sample images were taken by CCD camera and transformed to a digital signal. After that, the hyperspectral image was created by a function of x, y and λ. The two spatial dimensions (x and y) displayed the spatial data which was used for the generation of a distribution map. The λ displayed the spectral data which was used for the prediction of quality attributes. The main elements of hyperspectral image system are shown in Fig. 1.

2.3. Freshness measurement

After hyperspectral image measurement, the Haugh unit (HU) of each egg was measured by the standard method using formula (1) (Haugh, 1937). Each egg was weighed on a balance with a resolution of 0.01 g and then broken onto a flat glass plate and the height of its albumen was measured at 3 points around the yolk using a micrometer with a resolution of 0.1 mm.

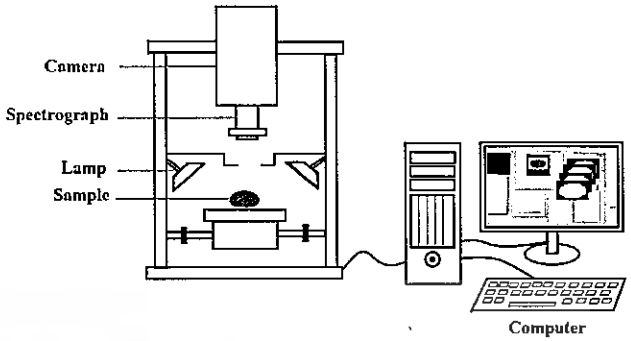

Fig. 1. Schematic diagram of the hyperspectral image system.

$$HU = 100 \times \log\left(h - 1.7w^{0.37} + 7.6\right) \quad (1)$$

Where: h is average height of the albumen in millimeters and w is weight of egg in grams (Monira et al., 2003).

The HU is a commonly used method of classifying the quality of eggs into: 'AA' grade = HU > 72, 'A' grade = HU 60–72 and 'B' grade = HU < 60 (United States Department of Agriculture, 2000). Eggs are considered to be "fresh" when HU is 60 or higher and "unfresh" when HU is lower than 60 (Zhao et al., 2010).

2.4. Hyperspectral image acquisition

The experimental procedure is shown in Fig. 2. Ninety one eggs were scanned. Samples were divided into 2 groups; one for calibration with 58 eggs and one for prediction with 33 eggs. There were 8 fresh eggs and 50 unfresh eggs in the calibration set and 8 fresh eggs and 25 unfresh eggs in the prediction set. The region of interest (ROI), a size 50 × 90 pixel, was cropped at the center of each egg image. Spectra of the ROI were averaged for each sample. Acquired averaged spectrum was used as a representative of each egg before the establishment of the calibration model. Partial least squares regression (PLSR) is a method of establishing the calibration model for HU. The dependent variable was HU and independent variables were spectra of egg in the wavelength range of 900–1700 nm. A similar deviation and

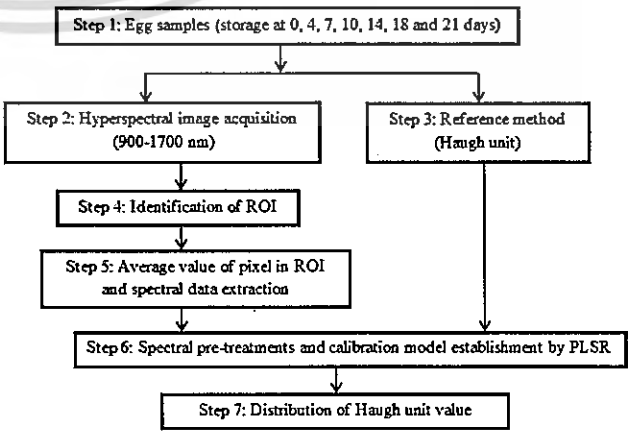

Fig. 2. Flow diagram for the process of hyperspectral image analysis.

This material is reserved for educational use only, not allowed for commercial use.
Forbidden to modify the content, and cite the document when use

the range of HU in the calibration set should cover the range of HU in the prediction set, therefore HU of all the samples had to be considered in order to ensure that the samples in the calibration set and the prediction set were distributed appropriately (Lin et al., 2011). The spectral pretreatment methods such as Savitzky-Golay smoothing, Savitzky-Golay derivative, multiplicative scatter correction pretreatment (MSC) and standard normal variate transformation (SNV) were investigated in order to obtain the optimal conditions of the calibration model for HU. The acquired models were tested by cross-validation and used to test the samples in the calibration set. For cross-validation the samples were divided into 29 segments each of two samples. For each segment the first sample was set aside and the second sample was used to establish the model, which was then tested on the first sample. The same procedure was carried out on all 29 segments. From each spectral pretreatment, the coefficient of determination (R^2) and the root mean square error of cross-validation (RMSECV) were determined for the optimal conditions in order to establish the calibration model. The optimum conditions should give the highest R^2 value and lowest RMSECV with low numbers of principal components in a model from partial least squares regression factors giving the number of principal components in a model from partial least squares regression. The process of spectral pretreatment is important because it reduces noises that can affect the physical properties such as variation in shape and size of samples (Leonardi and Burn, 1999). The R^2 value and the RMSEC were used to evaluate the performance of the calibration model. The calibration model was used to evaluate the accuracy of the samples in the prediction set by PC, R^2, RMSEP and a ratio of prediction to deviation (RPD). Saeys et al. (2005) gave levels of prediction accuracy based on the RPD where: less than 1.5 indicates that the model is not usable, 1.5 to 2.0 indicates that the model can distinguish between high and low values, 2.0 to 2.5 indicates that the model can be used for approximate prediction, 2.5 to 3.0 indicates that the model is good for prediction and >3 indicates that the model is excellent for prediction.

2.5. Visualization of HU in distribution map

The acquired calibration model for HU, which was created from the absorbance spectra at the optimal conditions by spectral pretreatments, was used for image processing. An image for prediction by HU measurement was transferred to colors in each pixel based on a color scale generated from the PLSR model. Therefore the predictive HU was implied by color in each pixel of the image. Each predictive image of each sample called "distribution map" was acquired. The acquired calibration model for HU was used to generate the distribution map of samples in the prediction set. For prediction of the freshness of the eggs by visualization, the distribution map showed the spatial variations of HU values, which corresponded to the color in the egg's predictive image. The freshness of each egg was assessed by the distribution map which showed in different colors based on the predicted HU. The accuracy of prediction was by comparative evaluation between the acquired distribution maps and the eggs whose freshness were known from the prediction set, one by one for the 33 samples. Evince program (2.7.5 version) was used for analysis in the whole process in order to create the distribution map.

3. Results and discussion

3.1. Data acquisition

The freshness of the sample of eggs was separated into high HU (62.41–83.64) and low HU (17.29–60.64). Hyperspectral imaging data in the wavelength ranged over 900–1700 nm of fresh eggs (≥60 of HU) and (<60 of HU) for unfresh eggs were considered. The original absorbance spectra from ROI of fresh eggs (N = 16) and unfresh eggs (N = 75) were averaged and plotted as shown in Fig. 3a. Pretreatment of spectra using the Savitzky-Golay second derivative was provided in order to clearly divide the peaks of chemical components on the spectra as shown in Fig. 3b. The second derivative spectra showed a water peak at 1450 nm, which was consistent with Osborne et al. (1993), protein (N-H functional group) peak at 1020 nm and oil peak at 1151 nm, which were both consistent with Ortiz-Somovilla et al. (2007).

Measurement of HU of the eggs takes into account their freshness, their weight and the thickness of albumen. Water is evaporated from eggs through their shells during storage therefore their weight decreases and this could be measured by changes in absorbance peak of the water in hyperspectral imaging. The absorbance of the average original spectra at 1450 nm of fresh eggs was higher than that of unfresh eggs (Fig. 3). Also the average second derivative spectra of fresh eggs at 1450 nm showed a higher opposite peak than unfresh eggs indicating that fresh eggs contained more water or a higher weight than the unfresh eggs. The albumen contains high levels of protein and the yolk high levels of

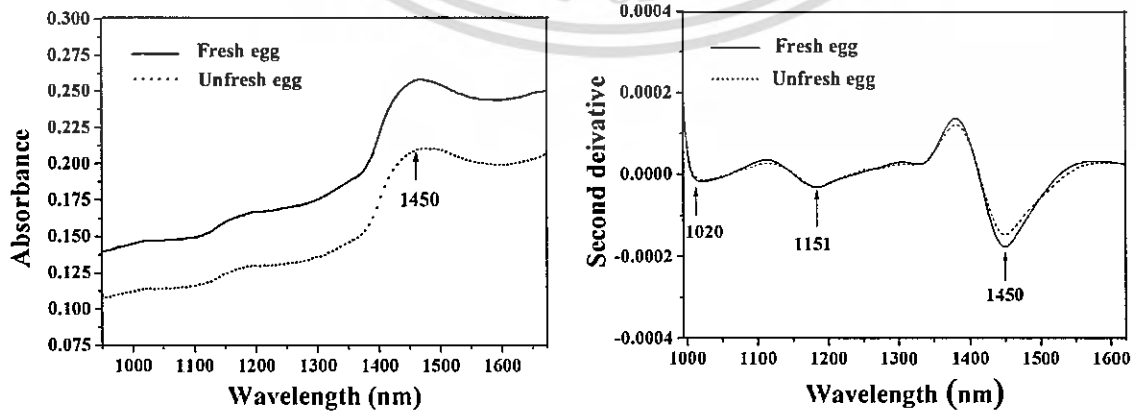

Fig. 3. Mean hyperspectral imaging spectra of all egg samples with different freshness.
(a) Original spectra.
(b) Second derivative spectra.

This material is reserved for educational use only, not allowed for commercial use.
Forbidden to modify the content, and cite the document when use

Table 1
Characteristics of egg samples in HU in the calibration set and the prediction set in the wavelength range of 900–1700 nm.

Items	The calibration set	The prediction set
Number of samples	58	33
range	17.29–83.64	17.82–80.57
mean	43.52	42.18
SD	19.44	19.34

SD = standard deviation.

Table 2
Analysis of the results of various spectral pretreatments for prediction of HU in the calibration set.

Spectral pretreatments	N	F	R^2	RMSECV
Original	58	3	0.84	5.91
Savitzky-Golay1st derivative	58	7	0.74	7.73
Savitzky-Golay2nd derivative	58	3	0.73	7.85
MSC	58	7	0.83	6.11
SNV	58	6	0.85	5.79
Savitzky-Golay smoothing	58	6	0.80	6.77

Where: N = number of samples, F = factor (the number of principal component from partial least squares regression), R^2 = coefficient of determination, RMSECV = root mean square error of cross validation, MSC = multiplicative scatter correction pretreatment and SNV = standard normal variate transformation.

lipid. The peak for protein in both fresh and unfresh eggs was different due to the loss of their structure and liquefaction of the albumen during storage. Yuceer and Caner (2014) reported that the reasons for albumen thinning include the fact that protease enzymes are depolymerized by hydroxyl ions which affects the structure of ovomucin-lysozyme. Also swollen ovomucin gel is broken down because of the insolubility of the ovomucin-lysozyme complex (Hawthorne, 1950). This results in the albumen becoming thinner and HU value decreasing. The vitelline membrane of the yolk of both fresh and unfresh eggs varies during storage. Fresh eggs have a vitelline membrane on the surface of the yolk which is composed the fibers connected to the chalaziferous layer. During storage, the fibrous network disappears and the strength of the vitelline membrane decreases (Stadelman and Cotterill, 1995), which results in the yolk becoming flatter. Therefore, fresh eggs have a high yolk and unfresh eggs have a flatter yolk due to the hyperspectral imaging peak of lipid and protein being slightly different.

3.2. Establishment of the calibration model and prediction of HU

A minimum and maximum value of HU from the experiment in the calibration set covers the minimum and maximum value in the prediction set and indicates that the distribution of HU in the calibration set was suitable to build the calibration model for prediction. Each ROI of the image in each sample (50 × 90 pixels) contained absorbance spectra from hyperspectral imaging data in the wavelength over the range of 900–1700 nm and the spectra in each ROI were averaged and then used as a representative of each sample for analysis. The calibration set and the prediction set varied in similar ways in HU. This confirmed that the analysis of the performance of PLSR model was reliable (Table 1).

The SNV spectral pretreatment gave the best results (R^2 = 0.85 and RMSECV = 5.79) for the establishment of the calibration model for HU (Table 2). Therefore, the calibration model, using SNV spectral pretreatment was used for the prediction. The accuracy of

Table 3
Analysis of the results of PLSR model for prediction of HU in the calibration set and the prediction set.

Model	Spectral pretreatment	Calibration set				Prediction set				
		N	F	R^2	RMSEC	N	F	R^2	RMSEP	RPD
HU	SNV	58	6	0.91	4.58	33	6	0.85	6.29	3.07

N = number of samples.
F = factor (the number of principal component from partial least squares regression).
R^2 = coefficient of determination.
RMSEC = root mean square error of calibration.
RMSEP = root mean square error of prediction.
RPD = ratio of the SD to the RMSEP (ratio of prediction to deviation).

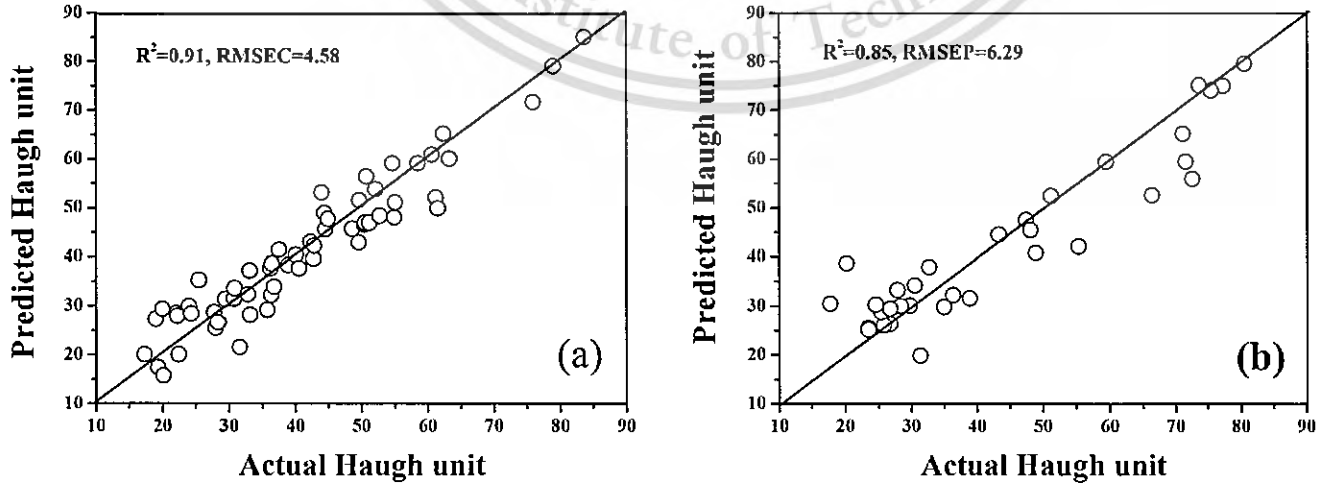

Fig. 4. Scattered plots of measured HU and predicted HU in the hyperspectral imaging measurement.
(a) calibration set.
(b) prediction set.

This material is reserved for educational use only, not allowed for commercial use.
Forbidden to modify the content, and cite the document when use

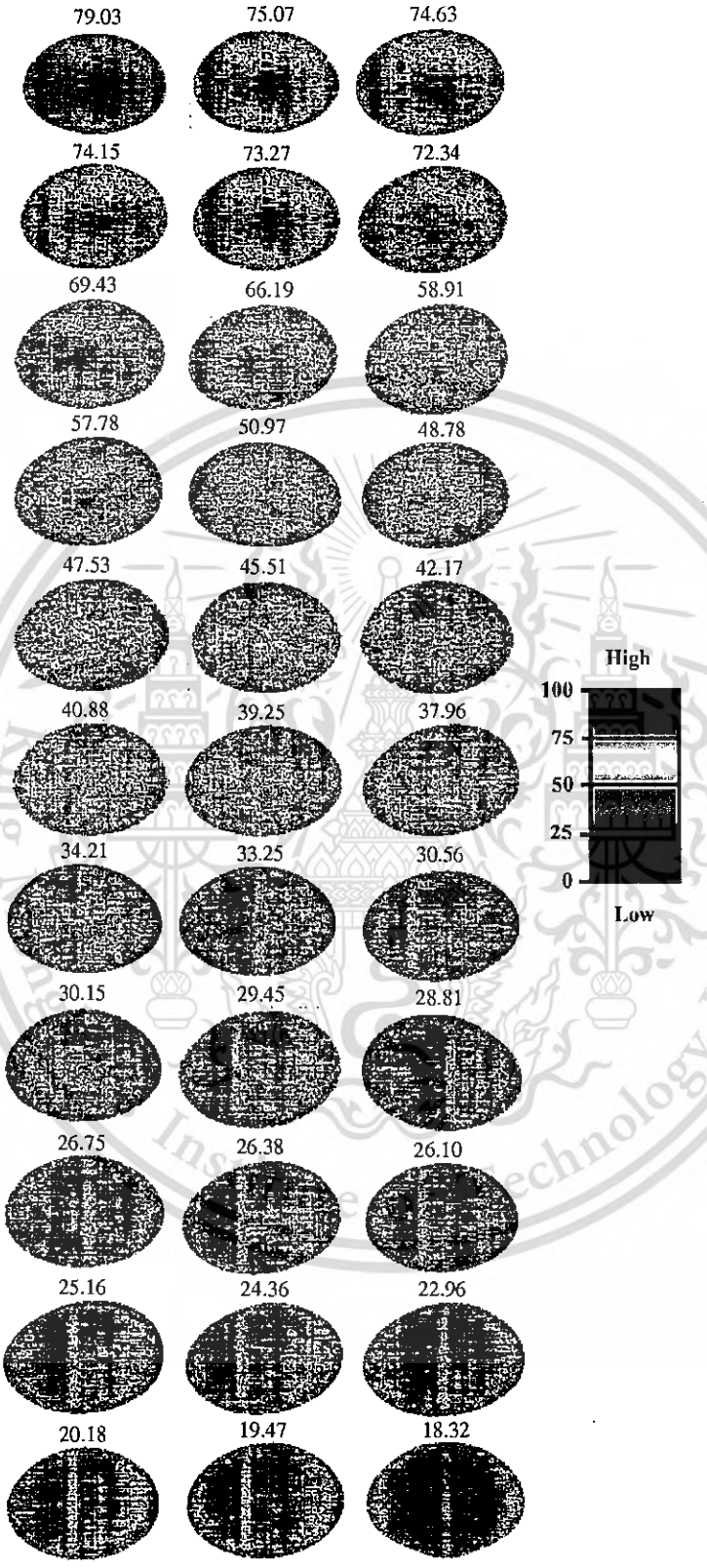

Fig. 5. Distribution maps of samples in the prediction set for HU.

This material is reserved for educational use only, not allowed for commercial use.
Forbidden to modify the content, and cite the document when use

the model for calibration and prediction are presented by the correlation coefficient, the root mean square error and the ratio of prediction to deviation (Table 3). The results of the prediction were plotted between actual values and predicted values in the calibration set (Fig. 4 a) and the prediction set (Fig. 4 b).

3.3. Distribution map of HU value

The calibration model from the SNV spectral pretreatment was used for determination of HU in every pixel of the images for prediction. The prediction of HU in all the pixels of each sample's image in the prediction set was the final step. The acquired image by prediction of HU, related to a linear color scale at all the pixels in each sample, was generated and called the distribution maps. The distribution maps explained the linear color scale which defined the difference in HU. The value of each HU was related to the linear color scale therefore HU in each pixel was predicted and transferred to color (Fig. 5). The highest values for predicted HU were represented by red and the lowest by blue. Other colors of predictive image in the linear color scale changed according to the level of predicted HU. The distribution map shows red, blue and other colors, which were spread throughout the image based on the predicted HU. The color in each image was different and related to HU of each sample. As a result of the light penetrated through albumen the acquired spectra contained information of albumen that related to HU in each pixel. The predicted image showed irregular colors in each part of each egg, which implied that the quality of albumen in each part of egg was non-homogeneous. However, overall colors of the images from different storage times between fresh and unfresh eggs were clearly different. Therefore the freshness of eggs could be predicted by observing the colors of the images. The fresh eggs contained more red while the unfresh eggs contained more blue.

4. Conclusion

Averaged spectra from ROI of hens' eggs by hyperspectral imaging were used to establish a calibration model for HU in order to predict their freshness. The standard normal variate transformation spectral pretreatment gave the optimum conditions for the model. The accuracy of the model was tested and showed R^2 of 0.85, RMSEP of 6.29 and RPD of 3.07, which implies that the model was excellent for prediction. The model was used to generate distribution maps for HU of hens' eggs. These acquired images can be simply used to classify the freshness of eggs by visual inspection of color specifically the level red color. However, this technique can also be used to predict HU without visualization by comparison with the cut-off HU value in order to classify groups of eggs into fresh and unfresh. It can therefore be concluded that hyperspectral imaging has a potential for use as a non-destructive, rapid online system to classify the freshness of hens' eggs.

Acknowledgement

This research was funded by Office of the National Research Council of Thailand (REF 2557A11802306). The authors acknowledge the permission to use the laboratory and equipment at the Faculty of Agro-Industry, King Mongkut's Institute of Technology Ladkrabang and Faculty of Engineering, Rajamangala University of Technology Isan, Khon Kaen Campus. We are grateful to Professor A K Thompson for proof reading the manuscript as well as Assoc. Prof. Panmanas Sirisomboon and Dr. Panuwat Supprung for technical help.

References

Burley, R.W., Vadehra, D.V., 1989. The albumen: chemistry. In: The Avian Egg (Ed.), Chemistry and Biology. Wiley, NewYork.

Cen, H., Lu, R., Zhu, Q., Mendoza, F., 2016. Nondestructive detection of chilling injury in cucumber fruit using hyperspectral imaging with feature selection and supervised classification. Postharvest Biol. Technol. 111, 352–361.

Dai, Q., Cheng, J.H., Sun, D.W., Pu, H., Zeng, X.A., Xiong, Z., 2015. Potential of visible/near-infrared hyperspectral imaging for rapid detection of freshness in unfrozen and frozen prawns. J. Food Eng. 149, 97–104.

Haugh, R.R., 1937. A new method for determining the quality of an egg. U. S. Egg Poult. 39, 27–49.

Hawthorne, J.R., 1950. The action of egg white lysozyme on ovomucoid and ovomucin. Biochim. Biophys. Acta 6, 28–35.

Karoui, R., Kemps, B.F., Bamelis, D., De Ketelaere, B., Decuypere, E., De Baerdemaeker, J., 2006. Method to evaluate egg freshness in research and industry: a review. Eur. Food Res. Technol. 222, 727–732.

Laghi, L., Cremonini, M.A., Placucci, G., Sykora, S., 2005. A proton NMR relaxation study of hen egg quality. Magn. Reson. Imaging 23, 501–510.

Leonardi, L., Burn, D.H., 1999. Quantitative *multiwavelength constituent* measurement using single-wavelength photo time-of-flight correction. Appl. Spectrosc. 53, 637–646.

Lee, W.H., Kim, M.S., Lee, H., Delwiche, S.R., Bae, H., Kim, D.Y., 2014. Hyperspectral near-infrared imaging for the detection of physical damages of pear. J. Food Eng. 130, 1–7.

Leiva-Valenzuela, G.A., Lu, R., Aguilera, J.M., 2013. Prediction of firmness and soluble solids content of blueberries using hyperspectral reflectance imaging. J. Food Eng. 115, 91–98.

Lin, H., Zhao, J., Sun, L., Chen, Q., Zhou, F., 2011. Freshness measurement of eggs using near infrared (NIR) spectroscopy and multivariate data analysis. Innov. Food Sci. Emerg. Technol. 12, 182–186.

Liu, Y., Ying, Y., Ouyang, A., Li, Y., 2007. Measurement of internal quality in chicken eggs using visible transmittance spectroscopy technology. Food contr. 18, 18–22.

Manley, M., Williams, P., Nilsson, D., Geladi, P., 2009. Near infrared hyperspectral imaging for the evaluation of endosperm texture in whole yellow maize (*Zea maize* L.) kernels. J. Agric. Food Chem. 57, 8761–8769.

Monira, K.N., Salahuddin, M., Miah, G., 2003. Effect of bread and holding period on egg quality characteristics of chicken. Int. J. Poult. Sci. 2 (4), 261–263.

National Bureau of Agricultral Commodity and Food Stadards (ACFS), 2010. Thai Agricultural Standard for Hen Egg. Ministry of Agriculture and Cooperatives, p. 12.

Osborne, B.G., Fearn, T., Hindle, P.H., 1993. Practical NIR Spectroscopy: with Applications in Food and Beverage Analysis. Longman Scientific & Technical.UK, Harlow.

Ortiz-Somovilla, V., España-España, F., Gaitán-Jurado, A.J., Pérez-Aparicio, J., De Pedro-Sanz, E.J., 2007. Proximate analysis of homogenized and minced mass of pork sausages by NIRS. Food Chem. 101 (3), 1031–1040.

Saeys, W., Mouazen, A.M., Ramon, H., 2005. Potential for onsite and online analysis of pig manure using visible and near infrared reflectance spectroscopy. Biosyst. Eng. 91 (4), 393–402.

Sim, J.S., 1998. Designer eggs and their nutritional and functional significance. In: Simopoulos, A.P. (Ed.), The Return of Omega-3 Fatty Acids into the Food Supply, 1. Land-based Animal Food Products and Their Health Effects, pp. 89–101. Basel, Switzerland.

Soltani, M., Omid, M., 2015. Detection of poultry egg freshness by dielectric spectroscopy and machine learning techniques. LWT-Food Sci. Technol. 62, 1034–1042.

Stadelman, W.J., Cotterill, O.J., 1995. Egg Science and Technology, fourth ed. Food Product Press, New York.

United States Department of Agriculture, 2000. Agricultural Marketing Service.-USDA Egg-grading Manual. Agricultural Handbook, Washington. No. 75.

Valous, N.A., Mendoza, F., Sun, D.-W., Allen, P., 2009. Colour calibration of a laboratory computer vision system for quality evaluation of pre-sliced hams. Meat Sci. 81 (1), 132–141.

Wang, W., Ni, X., Lawrence, K.C., Yoon, S.C., Heitschmidt, G.W., Feldner, P., 2015. Feasibility of detecting Aflatoxin B1 in single maize kernels using hyperspectral imaging. J. Food Eng. 166, 182–192.

Wu, D., Sun, D.W., 2013. Advanced applications of hyperspectral imaging technology for food quality and safety analysis and assessment: a review — Part I: fundamentals. Innov. Food Sci. Emerg. Technol. 19, 1–14.

Xiong, Z., Sun, D.W., Pu, H., Xie, A., Han, Z., Luo, M., 2015a. Non-destructive prediction of thiobarbituric acid reactive substances (TBARS) value for freshness

This material is reserved for educational use only, not allowed for commercial use.
Forbidden to modify the content, and cite the document when use

evaluation of chicken meat using hyperspectral imaging. Food Chem. 179, 175–181.
Xiong, Z., Sun, D.W., Xie, A., Pu, H., Han, Z., Luo, M., 2015b. Quantitative determination of total pigments in red meats using hyperspectral imaging and multivariate analysis. Food Chem. 178, 339–345.
Yang, Y.C., Sun, D.W., Pu, H., Wang, N.N., Zhu, Z., 2015. Rapid detection of anthocyanin content in lychee pericarp during storage using hyperspectral imaging coupled with model fusion. Postharvest Biol. Technol. 103, 55–65.
Yuceer, M., Caner, C., 2014. Antimicrobial lysozyme-chitosan coatings affect functional properties and shelf life of chicken eggs during storage. J. Sci. Food Agric. 94, 153–162.
Zhao, J., Lin, H., Chen, Q., Huang, X., Sun, Z., Zhou, F., 2010. Identification of egg's freshness using NIR and support vector data description. J. Food Eng. 98, 408–414.

King Mongkut's Institute of Technology Ladkrabang

This material is reserved for educational use only, not allowed for commercial use.
Forbidden to modify the content, and cite the document when use

Classification of sweet corn based on storage time after harvest using near infrared spectroscopy

S. Suktanarak[1], P. Supprung[2] and S. Teerachaichayut[1,a]
[1]Faculty of Agro-Industry, King Mongkut's Institute of Technology Ladkrabang, Thailand;
[2]Faculty of Engineering, Rajamangala University of Technology Isan Khon Kaen Campus, Thailand

Abstract

The freshness of sweet corns is important for production of canned sweet corn. The quality of sweet corns changes rapidly after harvest. Sweet corns should be processed through a production line as fast as possible after harvest. Therefore, some methods of classification of sweet corns based on storage time after harvest are needed. In this study, near infrared (NIR) spectroscopy operating in reflectance mode (1000-2500 nm) and interactance mode (588-1091) were investigated as methods of classification. Sweet corns both with and without husk were tested. Samples (N = 120) were scanned with an NIR spectrophotometer every 6 hours after harvest. They were then classified into two groups (0 and 1) with a 24-hour after harvest cut-off time between the two groups (<24 hr and ≥ 24 hr). Classification models were established and validated with a calibration set (N=80), and then the accuracies of the models were evaluated with a prediction set (N=40), using a partial least squares discriminant analysis (PLS-DA). It was found that second derivative spectral pretreatment gave the best results for NIR operating in reflectance mode. Regarding prediction accuracy, showed the best accuracies for both unhusked and husked sweet corns (100%), while it was found that mean center and second derivative spectral pretreatment gave the best results for NIR operating in interactance mode. The best accuracies for unhusked and husked sweet corns obtained 90% and 97.5%, respectively. All of the results demonstrated that NIR spectroscopy has a real potential for nondestructive classification of sweet corns based on storage time after harvest.

Keywords: sweet corn, storage time, near infrared, classification

INTRODUCTION

Sweet corn (*Zea mays* L. *saccharata*) is one of important cereal crops for human consumption. In addition, sweet corn plays a vital role in food industry. Sweet corn is largely processed into many corn products such as sweet corn kernel, corn milk and cream style corn. Quality of sweet corn is an important factor that affects the final product. Sugar content and water-soluble hydrocarbon in the kernels are key factors of consumption quality (Evensen and Boyer, 1986) in terms of taste and texture. The taste or sweetness of sweet corn depends on its storage time after harvest. Longer storage time causes corns to become hard and less sweet because the sugar in the corns turns into starch quickly after harvesting. Therefore, sweet corns should be transported and processed within 24 hours after harvest (National Food Institute, 2016). Appearances of sweet corns are important and consumers can inspect them before buying, but internal qualities that depend on storage time cannot be identified readily by visual inspection. Hence, it is necessary to use a nondestructive technique to detect these qualities in order to satisfy consumers.

[a] E-mail: ktsontis@kmitl.ac.th

This material is reserved for educational use only, not allowed for commercial use.
Forbidden to modify the content, and cite the document when use

Near infrared spectroscopy (NIRS) is one of the nondestructive detection techniques that are rapid, accurate and reliable. It has gained wide acceptance in determining the qualities of agricultural products (Teerachaichayut et al., 2011; Alfatni et al., 2013; Teerachaichayut et al., 2014; Srivichien et al., 2015). This technique utilizes the absorption of near infrared light by organic compounds which is related to vibrational energy of molecular bonds (O-H, C-H, C-O and N-H) (Cen and He, 2007). There have been several research studies that used NIRS to evaluate the qualities of corns products such as detection of fumonisins, B1 and B2 in corn meal (Gaspardo et al., 2012), evaluation of essential amino acids, lysine, crude protein, oil, and soluble sugar contents in maize (Tallada et al., 2009), detection of fumonisins content in maize (Giacomo and Stefania, 2013), prediction of proximates (moisture, ash, volatile matter, and fixed carbon) and lignocellulose components (cellulose, semi-cellulose, and lignin) of corn stover (Xue et al., 2015). Therefore, the main objective of this study was to use NIRS for nondestructive classification of sweet corns based on storage time after harvest.

MATERIALS AND METHODS

Sample preparation

Samples of sweet corns ('Insee 2' variety of hybrid sweet corn) were harvested from a farm in Nakhonratchasima province, Thailand. The samples (N=120) were selected to be of similar size, good appearance and without defect. They were carefully transported to the laboratory and stored at the ambient temperature. The samples were taken for measurement in every 20 samples at 6 hr, 12 hr, 18 hr, 24 hr, 30 hr and 36 hr after harvest. The samples were divided into 2 groups based on their storage time after harvest (60 samples for less than 24 hr and 60 samples for more than or equal to 24 hr).

Data acquisition

Spectra of all of the samples were determined with an FT-NIR spectrophotometer (NIRFlex N-500) operating in reflectance mode in the wavelength range of 1000-2500 nm and then determined again by an NIR spectrophotometer (FQA- NIR GUN) operating in interactance mode in the wavelength range of 588-1091 nm. Determinations were done in 2 parts. In the first part, each sweet corn with husk was scanned 3 times at its top, middle and bottom, and in the second part, each sweet corn without husk was scanned 3 times at the same positions.

Data analysis

Both reflectance mode and interactance mode were used to analyze samples with and without husk. Acquired NIR spectra from different positions of each sweet corn sample were averaged and used for analysis. All of the samples (N=120) were divided into 2 sets: a calibration set (N=80) and a prediction set (N=40). The calibration set, consisting of 40 samples stored for shorter time (<24 hr) and 40 samples stored for longer time (≥ 24 hr), was used for establishment of classification model, while the prediction set, consisting of 20 samples stored for shorter time (<24 hr) and 20 samples stored for longer time (≥ 24 hr), was used for accuracy evaluation. Spectral pretreatments such as first derivative, second derivative, multiplicative scatter correction (MSC) were used to reduce noise and scattering effect in order to find the best means to establish classification models. Partial least square discriminant analysis (PLS-DA) was used to develop classification models for sweet corns based on their storage time after harvest. Value of 0 was assigned for samples with shorter

This material is reserved for educational use only, not allowed for commercial use.
Forbidden to modify the content, and cite the document when use

storage time (<24 hr) and value of 1 was assigned for samples with longer storage time (≥ 24 hr). A cut-off value of 0.5 was used for accuracy evaluation–if the predicted value of a sample was less than 0.5, the sample was assigned to in the group with shorter storage time, while if the predicted value was more than 0.5, the sample was assigned to the group of with longer storage time. Statistical analysis was done with Unscrambler software version 10.1 (CAMO, Oslo, Norway).

RESULTS AND DISCUSSION

1. Classification model for sweet corns with husk based on storage time after harvest (<24 hr and ≥ 24 hr) using NIR operating in reflectance and interactance mode

Sweet corns with husk were classified based on storage time after harvest (<24 hr and ≥ 24 hr) by using reflectance and interactance NIRS. The average spectrum of 3 spectra of each sweet corn was calculated, and 120 average spectra of 120 corn samples were used for analysis (80 spectra for the calibration set and 40 for the prediction set). Several spectral pretreatments were performed on the spectra, then classification models were developed and cross-validated by PLS-DA on the calibration set as shown in Table 1. The cross-validation results showed that the second derivative and mean center pretreatments gave classification models of sweet corns with husk that were able to completely separate the corns into 2 groups when NIR was operating in reflectance mode (100%) and to separate them successfully at 98.75% when NIR was operating in the interactance mode, respectively.

Table 1. PLS-DA results from various spectral pretreatments for classification of sweet corns with husk by reflectance mode and interactance mode.

Spectral pretreatment	Reflectance mode				Interactance mode			
	N	F	correct	%Total accuracy	N	F	correct	%Total accuracy
original	80	18	77	96.25	80	12	75	93.75
Second derivative	80	7	80	100	80	14	76	95
Mean	80	15	75	93.75	80	12	79	98.75
MSC	80	13	77	96.25	80	11	76	95

N= number of samples, F = Factors, second derivative = Savitzky-Golay second derivative, Mean = mean center, and MSC = multiplicative scatter correction pretreatment

Hence, the second derivative spectral pretreatment was selected for establishing the classification model of sweet corns with husk in the reflectance mode and the mean center spectral pretreatment was selected for establishing the classification model of sweet corns with husk in the interactance mode. After the models were established, their accuracies were tested using the samples in the prediction set. The results of classification of samples in the calibration set and the prediction set with the models are shown in Table 2. The accuracies of classification of the calibration set and the prediction set by the reflectance mode were both excellent (100%), while the accuracies of classification of the calibration set and the prediction set by the interactance mode were 97.5% and 90% respectively.

This material is reserved for educational use only, not allowed for commercial use.
Forbidden to modify the content, and cite the document when use

Figure 1 showed plots of actual value versus predicted value with a cut off value of 0.5 used for accuracy evaluation of predictive discrimination between samples with shorter and longer storage times. Figure 1 (a) showed the actual value versus predicted value between groups with different storage times in the calibration set using the reflectance mode while Figure 1 (b) showed the actual value versus predicted value between groups with different storage times in the prediction set using the reflectance mode. The scattered plots between the actual value versus predicted value of groups with different storage times in the calibration set and the prediction set using the interactance mode are shown in figure 1(c) and 1(d), respectively. The results indicated that reflectance NIRS in the wavelength range of 1000-2500 nm had a better potential for classification of sweet corns with husk that had different storage times.

Table 2. Results of PLS-DA for sweet corns with husk at different storage times after harvest of the calibration and the prediction set (<24 hr and ≥ 24 hr) in reflectance mode and interactance mode.

Items		Reflectance mode		Interactance mode	
		The calibration set	The prediction set	The calibration set	The prediction set
number of samples		80	40	80	40
wavelength (nm)		1000-2500	1000-2500	588-1091	588-1091
spectral pretreatment		Second derivative	Second derivative	Mean	Mean
factor		9	9	12	12
< 24 hr after harvest	correct	40/40	20/20	40/40	17/20
	incorrect	0/40	0/20	0/40	3/20
≥ 24 hr after harvest	correct	40/40	20/20	38/40	19/20
	incorrect	0/40	0/20	0/40	1/20
%total accuracy		100	100	97.5	90

This material is reserved for educational use only, not allowed for commercial use.
Forbidden to modify the content, and cite the document when use

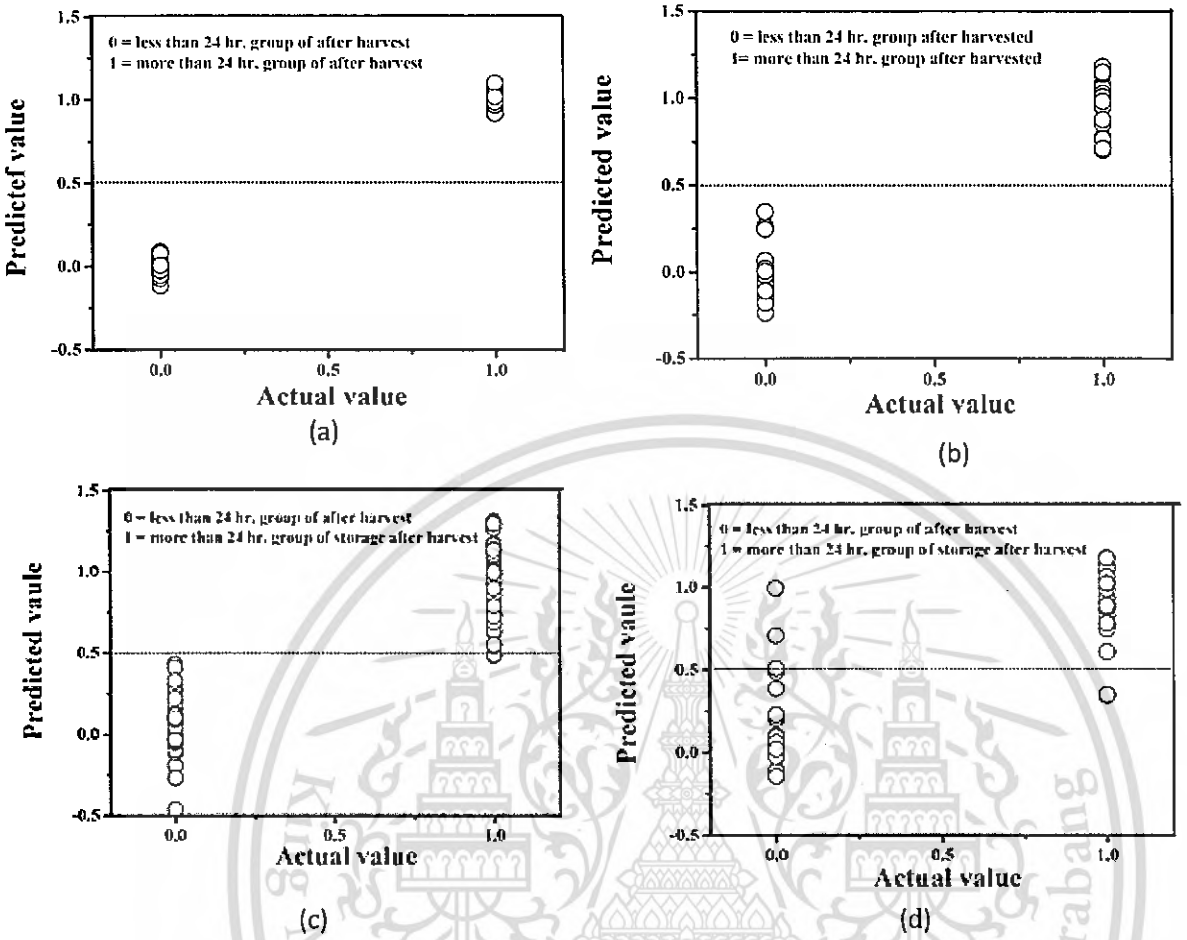

Figure 1. Scatter plots for classification of sweet corns with husk: (a) scattered plots of the calibration set in reflectance mode, (b) scattered plots of the prediction set in reflectance mode, (c) scattered plots of the calibration set in interactance mode and (d) scattered plots of the prediction set in interactance mode.

2. Classification model for sweet corns without husk based on storage time after harvest (<24 hr and ≥ 24 hr) using NIR operating in reflectance and interactance mode.

Similar to 1. above, sweet corns without husk were classified based on storage time after harvest (<24 hr and ≥ 24 hr) by using reflectance and interactance NIRS. The average spectrum of 3 spectra of each sweet corn was calculated, and 120 average spectra of 120 corn samples were used for analysis. Several spectral pretreatments were performed on the spectra, then classification models were developed and cross-validated by PLS-DA on the calibration set as shown in Table 3. The second derivative spectral pretreatment of the reflectance mode gave the best result (100% accuracy). For interactance mode, the second derivative spectral pretreatment also gave the best result (97.5% accuracy). Therefore, the classification models were established using the second derivative spectral pretreatment in both of the reflectance mode and the interactance mode.

This material is reserved for educational use only, not allowed for commercial use.
Forbidden to modify the content, and cite the document when use

Table 3. PLS-DA results from various spectral pretreatments for classification of sweet corns without husk in reflectance mode and interactance mode.

Spectral pretreatment	Reflectance mode				Interactance mode			
	N	F	correct	%Total accuracy	N	F	correct	%Total accuracy
original	80	16	72	90	80	12	77	96.3
2nd derivative	80	5	80	100	80	6	78	97.5
Mean	80	17	76	95	80	14	78	97.5
MSC	80	16	73	91.25	80	13	77	96.3

N= number of samples, F = Factors, Smoothing = Savitzky-Golay smoothing, second derivative = Savitzky-Golay second derivative, Mean = mean center and MSC = multiplicative scatter correction pretreatment.

Therefore, the second derivative spectral pretreatment was used and then the classification models of sweet corns without husk in the reflectance mode and the interactance mode were established. After that, the accuracies of the classification models were evaluated by using the samples in the prediction set. The results of classification of the samples in the calibration set and the prediction set with the models are shown in Table 4. The accuracies of classification of the calibration set and the prediction set by the reflectance mode were both excellent (100%), while the accuracies of classification of the calibration set and the prediction set by the interactance mode were 100% and 97.5% respectively. Figure 2 showed plots of actual value versus predicted value with a cut off value of 0.5 used for accuracy evaluation of predictive discrimination between samples with shorter and longer storage times. Figure 2(a) showed the actual value versus predicted value between groups with different storage times in the calibration set using the reflectance mode while Figure 2(b) showed the actual value versus predicted value between groups with different storage times in the prediction set using the reflectance mode. The scattered plots between the actual value versus predicted value of groups with different storage times in the calibration set and the prediction set using the interactance mode are shown in figure 2(c) and 2(d), respectively. The results indicated that reflectance NIRS in the wavelength range of 1000-2500 nm had a better potential for classification of sweet corns with husk that had different storage times.

This material is reserved for educational use only, not allowed for commercial use.
Forbidden to modify the content, and cite the document when use

Table 4. Results of PLS-DA for sweet corns without husk at different storage times after harvest of the calibration and the prediction set (<24 hr and ≥ 24 hr) in reflectance mode and interactance mode.

Items		Reflectance mode		Interactance mode	
		The Calibration set	The prediction set	The calibration set	The prediction set
number of samples		80	40	80	40
wavelength (nm)		1000-2500	1000-2500	588-1091	588-1091
spectral pretreatment		Second derivative	Second derivative	Mean	Mean
factor		5	5	6	6
< 24 hr after harvest	correct	40/40	20/20	40/40	19/20
	incorrect	0/40	0/20	0/40	1/20
≥ 24 hr after harvest	correct	40/40	20/20	40/40	19/20
	incorrect	0/40	0/20	0/40	1/20
%total accuracy		100	100	100	97.5

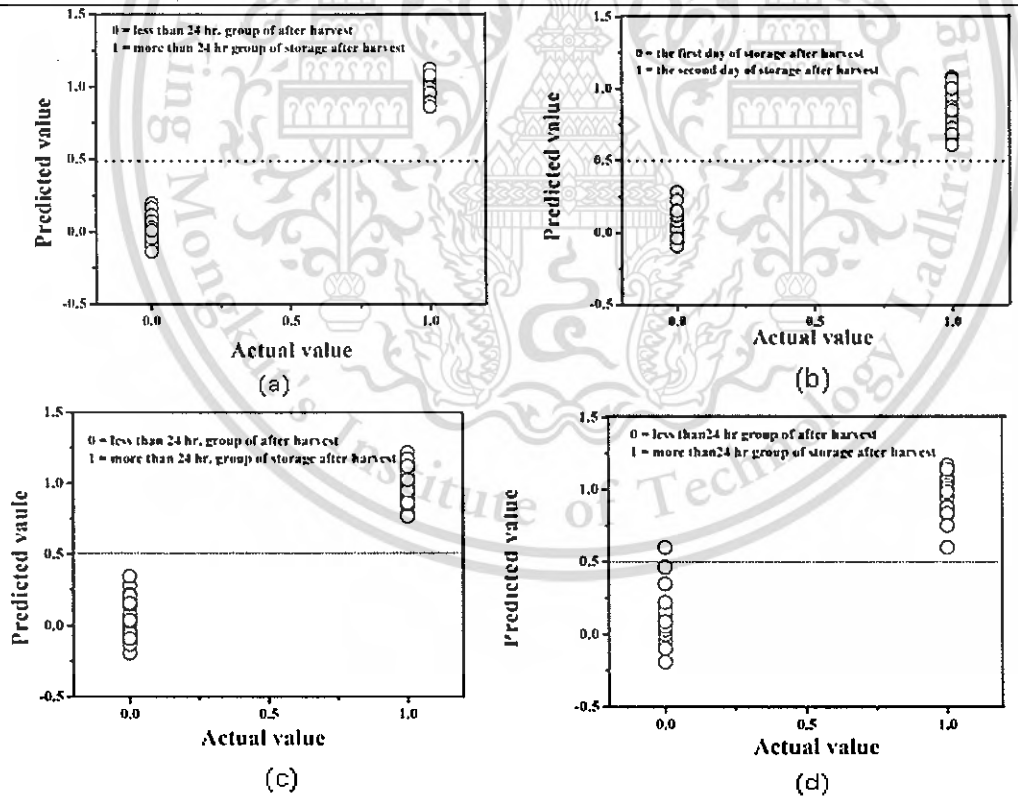

Figure 2. Scatter plots for classification of sweet corns without husk: (a) scattered plots of the calibration set in reflectance mode, (b) scattered plots of the prediction set in reflectance mode, (c) scattered plots of the calibration set in interactance mode and (d) scattered plots of the prediction set in interactance mode.

This material is reserved for educational use only, not allowed for commercial use.
Forbidden to modify the content, and cite the document when use

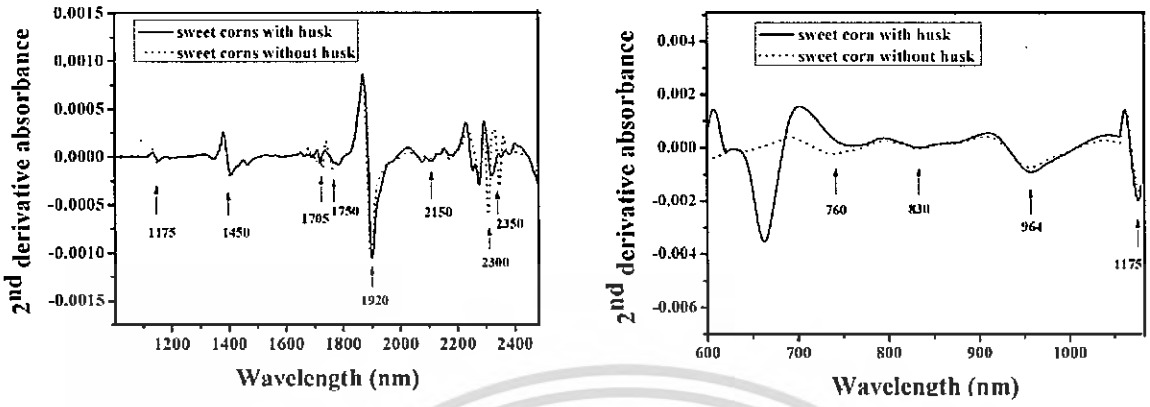

(a) (b)

Figure 3. Average 2nd derivative absorbance of sweet corns with and without husk: (a) in reflectance mode (b) in interactance mode

The results showed that the accuracies of the reflectance mode were better than those of the interactance mode for both cases of corn samples with and without husk. The accuracies of classification by the models using the reflectance mode were 100% for samples with and without husk, while the accuracy of classification by the model using the interactance mode for sweet corns without husk was better than that of sweet corns with husk. Figure 3 showed the average second derivative spectra of sweet corns obtained by using the reflectance mode (1000-2500 nm) and the interactance mode (588-1091 nm). In Figure 3(a), protein peaks in a N-H functional group were found at 1175 and 1705 nm; moisture peaks were at 1450 nm and 1920 nm; starch peak was found at 1750 nm; carbohydrate was found that 2150 nm; and oil peaks were found at 2300 and 2350 nm. Similarly, in Figure 3(b), moisture peaks were found at 760 and 830 nm; oil peak was found at 964 nm; and protein peak was found at 1175 nm (Osborne et al., 1993). The spectral features of sweet corns with husk and without husk were different in the range of the visible wavelength due to their having different colors.

CONCLUSIONS

Classification models for sweet corns at different storage times were developed. The reflectance mode in the wavelength range of 1000-2500 nm exhibited better accuracy than the interactance mode in the wavelength range of 588-1091 nm. In reflectance mode, the models treated with second derivative spectral pretreatment gave excellent accuracies for both sweet corns with and without husk. In interactance mode, the models treated with mean center and second derivative spectral pretreatment gave good predictive accuracies (90% and 97.5%) for sweet corns with and without husk. In conclusion, NIR spectroscopy has a real potential for classification of sweet corns with and without husk based on storage time after harvest.

ACKNOWLEDGEMENTS

This research was supported by the National Research Council of Thailand and the national research budget for fiscal year 2016. The authors acknowledged the permission to use the laboratory and equipment at the faculty of Agro-Industry, King Mongkut's Institute of Technology Ladkrabang and faculty of Engineering, Rajamangala University of Technology Isan Khon Kaen Campus.

This material is reserved for educational use only, not allowed for commercial use.
Forbidden to modify the content, and cite the document when use

Literature cited

Alfatni. M., Shariff, A., Abdullah, M., Abdullah, M., Marhaban, M. and Saaed, O. (2013). The application of internal grading system technologies for agricultural products-review. Journal of Food Engineering. 116: 3, 703–725

Evensen, K.B. and Boyer, C.D. (1986). Flavour qualities of frozen sweet corn are effected by genotype and blanching. Journal of American Society for Horticultural Science. 111(5): 734-738.

National Food Institute. Food intelligence center. [Online] resource http://www.nfi.or.th (7 February 2016).

Gaspardo, B., Del Zotto, S., Torelli, E., Cividino, S.R., Firrao, G., Della Riccia, G. and Stefanon, B. (2012). A rapid method for detection of fumonisins B1 and B2 in corn meal using Fourier transform near infrared (FT-NIR) spectroscopy implemented with integrating sphere. Journal of Food Chemistry. 135: 1608–1612.

Giacomo, D. R. and Stefania, D.Z. (2013). A multivariate regression model for detection of fumonisins content in Maize from near infrared spectra. Journal of Food Chemistry. 141: 4289–4294.

Cen, H. and He, Y. (2007). Theory and application of near infrared reflectance spectroscopy in determination of food quality. Trends in Food Science & Technology 18, 72-83.

Osborne, B.G., Fearn, T. and Hindle, P.H. (1993). Practical NIR spectroscopy with Application in Food and Beverage Analysis. Longman Scientific & Technical. 1-7.

Srivichien, S., Terdwongworakul, A. and Teerachaichayut, S. (2015). Quantitative prediction of nitrate level in intact pineapple using Vis–NIRS. Journal of Food Engineering 150: 29-34.

Tallada, J.G., Palacios-Rojas, N. and Armstrong, P.R. (2009). Prediction of maize seed attributes using a rapid single kernel near infrared instrument. Journal of Cereal Science. 50: 381–387.

Teerachaichayut, S., Terdwongworakul, A., Thanapase, W. and Kiji, K. (2011). Non-destructive prediction of hardening pericarp disorder in intact mangosteen by near infrared transmittance spectroscopy. Journal of Food Engineering. 106: 206-211.

Teerachaichayut, S., Suktanarak, S. and Kasemsumram, S. (2014). Non-destructive detection of internal mold infection in sweet tamarind using short wavelength near infrared spectroscopy. Acta Hort. (ISHS) 1053:113-119.

Xue, J. Yang, Z., Han, L., Liu, Y., Liu, Y. and Zhou, C. (2015). On-line measurement of proximates and lignocellulose components of corn stover using NIRS. Journal of Applied Energy. 137: 18-25.

This material is reserved for educational use only, not allowed for commercial use.
Forbidden to modify the content, and cite the document when use

Prediction of moisture content in sweet corn by reflectance NIR spectroscopy

Sineenart Suktanarak[1], Sontisuk Teerachaichayut[1] and Panuwat Supprung[2]
[1]Faculty of Agro-Industry, King Mongkut's Institute of Technology Ladkrabang, Thailand,
E-mail: sontisuk.te@kmitl.ac.th
[2]Faculty of Engineering, Rajamangala University of Technology Isan Khon Kaen Campus, Thailand

Abstract

The objective of this study was to use NIR spectroscopy to predict moisture content of husked and unhusked sweet corn. Moisture content (MC) is one of important indices that can be used to evaluate the freshness of sweet corn. Thai sweet corn ('Insee 2' variety of hybrid sweet corn) with and without husk was studied in this research. A set of 150 samples (105 samples in a calibration set and 45 samples in a prediction set) was scanned by a reflectance NIR spectrophotometer in the wavelength range of 588-1091 nm. Calibration models were established by using partial least squares regression (PLSR) to predict MC of husked and unhusked sweet corn. The calibration model for MC prediction of husked sweet corn was optimal when using the original spectra (R=0.80, RMSEP=0.52%), while the calibration model for MC prediction of unhusked sweet corn was optimal when using a smoothing (Savitsky–Golay) spectral pretreatment (R=0.71, RMSEP=0.72%). The results showed that the husk of sweet corn affected the accuracy of measurement. NIR spectroscopy in reflectance mode was found to have a true potential for rough screening of MC in sweet corn.
Keywords: sweet corn, moisture content, prediction.

Introduction

Moisture content (MC) of sweet corn is one of important parameters that indicate the degree of freshness of sweet corn. MC is reduced with storage time due to water being continuously evaporated from the surface of the corn after harvest. Near infrared spectroscopy (NIRS) is a nondestructive technique for determining the quality of agricultural products.[1] The aim of this research was to use NIRS for prediction of moisture content of sweet corn with/without husk.

Materials and Methods

Sweet corns ('Insee 2' variety of a hybrid sweet corn) were used in this study. All samples were kept at room temperature (25°C), and spectra and MC were determined at 6 hr, 12 hr, 18 hr, 24 hr, 30 hr and 36 hr after harvest. Reflectance NIR spectra were determined with a FOA-NIR GUN spectrophotometer (FANTEC inc., Japan) in the wavelength range of 588-1091 nm. The experiments in this research were separated into two parts. In the first part, each sweet corn with husk was scanned 3 times at the top, middle and bottom, whereas in the second part, each sweet corn without husk was scanned the same number of times and at the same positions. Subsequently, the moisture content of several kernels of each sweet corn was determined according to the method prescribed by AOAC.[2] Partial least squares regression (PLSR) was used for developing calibration models for prediction of MC of sweet corn with/without husk. Data were statistically analyzed with Unscrambler version 10.1 software (CAMO, Oslo, Norway).

Results and discussion

The original spectra of samples with/without husk can be compared; they are shown in Figure 1(a) and Figure 1(b), respectively. A water peak at 972 nm appears in the original absorbance spectra of both groups. A peak at 660 nm appeared clearly only in the original spectra of the samples with husk but did not appear in those of the samples without husk. This peak might be a chlorophyll peak at 680 nm because the husk was green and contained chlorophyll.[3] A smoothing savitsky–Golay (8-point fit) spectral pretreatment gave an optimal calibration model for MC of sweet corn with husk (R=0.77, RMSEC=0.57%). The model was tested with the prediction set. It gave an adequate prediction result (R=0.71, RMSEP=0.72%), shown in Table 1. The original spectra were used to establish a calibration model (R=0.87, RMSEC=0.45%) for sweet corns without husk from

This material is reserved for educational use only, not allowed for commercial use.
Forbidden to modify the content, and cite the document when use

the calibration set. The model was used to predict the MC in the prediction set and obtained a good prediction result (R=0.80, RMSEP=0.52%). Scatter plots of actual MC versus predicted MC of sweet corns with/without husk are shown in Figure 2(a) and Figure 2(b), respectively.

Conclusion

All of our results show that NIR spectroscopy can be adequately used to establish a model for predicting MC in sweet corn. Its prediction accuracy was better with sweet corns without husk than those with husk. The husk negatively affected the measurements and lowered the accuracy of prediction.

Acknowledgement

This research was supported by the National Research Council of Thailand (NRCT) and used a part of the national research budget for fiscal year 2016.

References

1. S. Teerachaichayut, A. Terdwongworakul, W. Thanapase and K. Kiji, "Non-destructive prediction of hardening pericarp disorder in intact mangosteen by near infrared transmittance spectroscopy", *J. Food Eng.* **106,** 206–211 (2011).

2. AOAC International, *Official Methods of Analysis of AOAC.* International. 17th ed. AOAC. International, Arlingtou, USA, (2000).

3. J.A. Abbott, R. Lu, B.L. Upchurch, R.L. Stroshine, "Technologies for nondestructive quality evaluation of fruits and vegetables" in *Horticultural Reviews –Technologies for Non-destructive Quality Evaluation of Fruits and Vegetables.* John Wiley & Sons, p. 1–120 (1997).

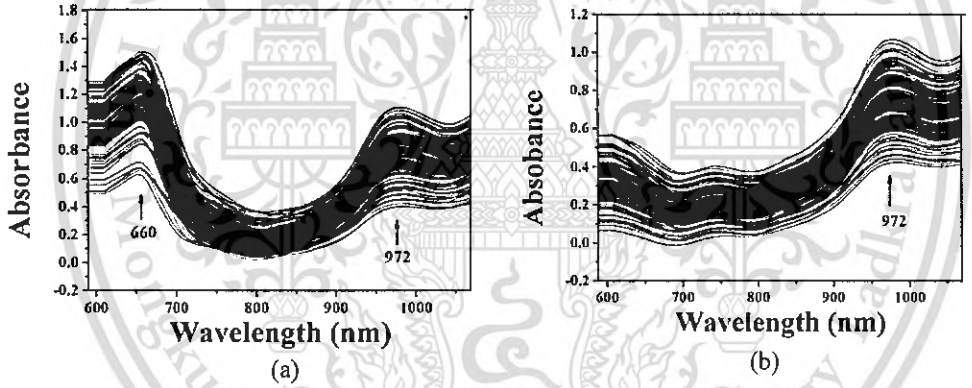

Figure 1. Original spectra of samples of (a) sweet corns with husk and (b) sweet corns without husk.

Table 1. PLSR results of the calibration model for MC of sweet corns with/without husk.

set	sweet corn with husk					sweet corn without husk				
	pretreatment	F	N	R	RMSEC(%)/ RMSEP(%)	Model	F	N	R	RMSEC (%)/ RMSEP (%)
calibration set	smoothing	8	105	0.77	0.57	original	8	105	0.87	0.45
prediction set	smoothing	8	45	0.71	0.72	original	8	45	0.80	0.52

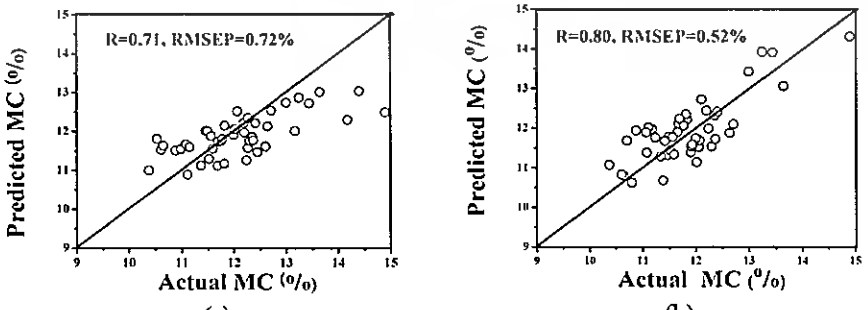

Figure 2. Scatter plots of actual moisture content versus predicted MC of the prediction set : (a) sweet corn with husk and (b) sweet corn without husk.

This material is reserved for educational use only, not allowed for commercial use.
Forbidden to modify the content, and cite the document when use

AUTHOR BIOGRAPHY

Name	Miss Sineenart Suktanarak
Dath of birth	December 4, 1987
Home address	67/5 Village No.2 Nongsumsak sub-district, Banbung district, Chonburi, 20170
Academic background	
2010-2013	M.Sc. (Food science) King Mongkut's Institute of Technology Ladkrabang.
2006-2010	B.Sc. (Agro-Industry Technology and Management) King Mongkut's University of Technology North Bangkok.
Work Experience	Lecturer, Faculty of Science and Technology, Valaya Alongkorn Rajabhat University under the Royal Patronage, Pathumthani
Publication	Teerachaichayut, S., Petcharaporn, K. and Suktanarak, S. 2012. Calibration model of soluble solids content for Intact Tomato by Transmittance SW-NIR Spectroscopy. Proceedings of the 3rd Asian Symposium on Near Infrared Spectroscopy, Thailand, 14-18 May. 120-121.
	Suktanarak, S and Teerachaichayut, S. 2012. Detection for Moisture Content of Sweet Tamarind flesh by Transmittance Short WavelengthNear Infrared Spectroscopy. International Conference on Nutrition and Food Sciences, July 23-24. IPCBEE vol.39 (2012) IACSIT Press, Singapore. 71-75.
	Suktanarak, S. and Teerachaichayut, S. 2013. Quantitative Analysis of Total Soluble Solids and Titratable Acidity of Sweet Tamarind by SW-NIRS. International Journal of Bioscience, Biochemistry and Bioinformatics, Vol. 3, No. 4, 328-331.
	Teerachaichayut, S., Suktanarak, S., and Kasemsumram, S. 2014. Non-destructive detection of internal mold infection in

This material is reserved for educational use only, not allowed for commercial use.
Forbidden to modify the content, and cite the document when use

sweet tamarind using short wavelength near infrared sectroscoy. Acta Hort. (ISHS) 1053:113-119.

Suktanarak, S, Teerachaichayut, S. and Supprung, P. 2016. Prediction of moisture content in sweet corn by reflectance NIR spectroscopy. Proceedings of the 5th Asian Near Infrared Symposium and the 32nd Japanease NIR Forum, Kagoshima, Japan, 30 Nov-3 Dec. 260-261.

Suktanarak, S., Supprung, P. and Teerachaichayut, S. 2017. Classification of sweet corn based on storage time after harvest using near infrared spectroscopy. Acta Hort. (ISHS) 1152:47-54.

Suktanarak, S. and Teerachaichayut, S. 2017. Non-destructive quality assessment of hens' eggs using hyperspectral images. Journal of Food Engineering 215: 97-103.

Teerachaichayut, S., Phonmakham, S. and Suktanarak, S. 2017. Grouping marian plums harvested at different times by transmittance near-infrared spectroscopy. Acta Hort. (ISHS) 1179:25-30.

This material is reserved for educational use only, not allowed for commercial use.
Forbidden to modify the content, and cite the document when use